SOME ASPECTS OF RAPID ANALYSIS OF COAL SLURRIES USING DIRECT CURRENT PLASMA EMISSION SPECTROMETRY

by

Terry Wade McCreary

Dissertation submitted to the Faculty of the
Virginia Polytechnic Institute and State University
in partial fulfillment of the requirements for the degree of

DOCTOR OF PHILOSOPHY

in

Chemistry

APPROVED:

Gary L. Long, Chairman

Harold M. Bell

John G. Mason

George Sanzone

Roe-Hoan Yoon

September 1988

Blacksburg, Virginia

SOME ASPECTS OF RAPID ANALYSIS OF COAL SLURRIES

USING DIRECT CURRENT PLASMA EMISSION SPECTROMETRY

by

Terry Wade McCreary

Committee Chairman: Gary L. Long

Chemistry

(ABSTRACT)

The direct current plasma is an excitation cell that should be well suited to rapid analysis of coal slurries by virtue of its tolerance for various sample matrices. Problems which are encountered in coal analysis by emission spectrometry include incomplete atomization of analyte by formation of metal oxides, lack of adequate methodology for sulfur analysis, and ineffective sample transport for coarse coal slurries.

Atomization of metal oxides can be improved by addition of small amounts of propane (ca 45 mL/min) to the nebulizing argon of the direct current plasma. However, the improved atomization is manifested above the normal viewing zone, and the enhancement effect of propane on analytical signals is offset by severe depression of emission signals caused by temperature reduction in the lower regions of the plasma.

Sulfur in coal can be determined by direct current plasma emission spectrometry. Emission lines accessible to the echelle grating of the DCP are not suitable for such analysis, so that the deep-UV lines from 180-183 nm must be utilized for such work. A relatively simple purge system with low argon consumption (5 L/min) is adequate for sulfur

analysis, and the beforementioned analytical lines provide detection limits that are adequate for sulfur determination in 1% slurries of coal. However, transport of the coal sample to the plasma is incomplete when compared to that of aqueous solutions, precluding the use of such solutions as calibration standards.

Transport of the coal can be improved by increasing the viscosity of sample and standards, which increases the droplet size from the nebulizer and hence the particle size transportable. The increased droplet size causes a decrease in sensitivity due to reduced desolvation/vaporization, but does permit the use of aqueous solutions as calibration standards for determination of sulfur, iron, aluminum, and silicon in coal.

ACKNOWLEDGEMENTS

So many people to thank, and so little space in which to do it. Thank you, , , , and , for the time and effort it took to serve on my committee. Your many useful suggestions made this task much easier. Special thanks to and the Department of Mining and Minerals Engineering, who were most helpful in providing coal samples and the accompanying data for them, as well as permitting the use of their Spectraspan IV DCP while I was on the "learning curve". Of course, I have to tell the "Plasmen" to take a bow; , , and . Numerous "discussions", punctuated occasionally by yelling and red faces, provided many fruitful ideas and were a lot of fun even when no ideas were forthcoming.

I wish to acknowledge two organizations for their financial support. The Department of Energy, Pittsburgh Energy and Technology Center provided my assistantship for my last two years at Virginia Tech, which made my work much easier. The provision of a direct current plasma instrument by Phillips Petroleum saved us money and saved me a great deal of time (that would have been required to construct one); thanks to for arranging that donation.

Very special thanks go to Gary Long. Before I came to VPI & SU, I did research because I had to. Now I'll be doing research because I

want to. Your guidance, your humor, your support, and most importantly your patience got me through the last three years and helped me get to where I am now.

To my new daughter, . Without your precipitous arrival at a most inopportune time (right in the middle of interviews and dissertation writing), this document and the accompanying degree would have been procured a great deal sooner. And I wouldn't have wanted it any other way! Someday you'll read this and know how necessary you were and are to me.

Finally, to my wife, "Thank you" sounds so trivial for what you have done and what you have endured during this "experience". Without you I would never have had the fortitude to attempt the Ph.D. During our three years in Blacksburg, you supported me financially and emotionally; you were always there, and you knew when to say and do just the right thing to keep me going. The diploma I receive will be as much yours as it is mine.

TABLE OF CONTENTS

LIST OF FIGURES

LIST OF TABLES

CHAPTER 1

INTRODUCTION

Over the last two decades, the quality of coal that is used as an energy source has become an increasingly important matter to environmentalists, coal scientists, and combustion engineers. The elements present in coal can have a serious impact on the environment and on the system or device used to burn the coal. Sulfur is an element of major interest because of its significant role in the formation of acid rain and because of its potential effect on the combustions chamber. The major ash-forming metals in coal (aluminum and silicon) and the corrosive or slagging metals (iron and several others) are also of importance in terms of their potential for generation of fly ash and in terms of their impact on the combustion chamber used for the coal. Currently, there is no atomic spectrometric method that is suitable for rapid simultaneous determination of sulfur and the ash-forming elements in coal. It is the purpose of this study to investigate the use of direct current plasma (DCP) emission spectrometry in conjunction with slurry injection for rapid simultaneous multielement analysis of coal slurries.

To establish the applicability of DCP emission spectrometry to this analysis, it is appropriate first to review several topics, including: pertinent characteristics of coal and requirements for

analysis; current methods of coal analysis; and aspects of the direct current plasma and its sample introduction system.

CHARACTERISTICS OF COAL

As stated earlier, the sulfur content of coal is of considerable importance. Sulfur is an undesirable component of all coals, and may be present at levels as high as 4-6%. Upon combustion of coal, sulfur dioxide (and to a lesser extent sulfur trioxide) may be formed. The sulfur dioxide can cause serious corrosion of parts of a boiler plant, so that combustion of very-high-sulfur coals is economically undesirable [1]. An important aspect of sulfur in coal with respect to the environment involves the production of acid rain. The sulfur dioxide which is formed on combustion can dissolve in precipitation to form sulfurous acid. A relatively small amount of sulfurous acid can cause a considerable decrease in the pH of precipitation.

The abundance of the ash metals (in the form of their oxides) has a bearing on the characteristics of the combustion chamber used to harness the energy of the coal. For example, a coal which is high in silicon and aluminum and low in the slagging metals will produce a refractory ash; such a coal would be best utilized in a dry bottom furnace [2]. A high-iron coal would produce a slag-type ash, which would be better utilized in a wet-bottom furnace specifically designed for slagging coals. Other characteristics of coal which are of interest and which are defined by the composition and content of the ash include [3]:

1. Fusibility temperature of the ash, which is characteristic of the base/acid ratio. The latter is defined as $(Fe_2O_3 + CaO + MgO + Na_2O + K_2O)/(SiO_2 + TiO_2 + Al_2O_3)$.
2. Foulibility, which is a function of the sodium and potassium content of the ash.
3. Organic/pyritic sulfur ratio, which can be described by [S(total) - Fe]/S

It is clear that the metal and sulfur content of coal must be monitored to maximize efficiency of the combustion system and to minimize pollution. Monitoring can be performed either before or after combustion of the coal. Elemental determination after combustion can be performed gravimetrically or titrimetrically, using the combustion products as the sample [4]. Since the elements emitted into the environment will be diluted by the atmosphere/water in that environment, such determinations are somewhat limited in scope. A more practical method of monitoring these elements is that of pre-combustion analysis. Analysis prior to combustion is particularly effacious for those elements that are present at lower concentrations. Also, the a priori information on metals/sulfur content can allow the operator of the combustion chamber to adjust either the conditions of combustion or the quality of the fuel via mixing of several coals, to improve the situation.

Pre-combustion analysis that can permit changing of either the combustion chamber characteristics or the fuel quality as required during the combustion process, implies an on-line technique. Some desirable characteristics of on-line techniques include:

1. A minimum of sample preparation, for reason of speed (if the information is to be used to adjust the combustion conditions on-line) and to minimize the risk of sample contamination.
2. Simultaneous multielement capability. Specifically, the technique should be capable of determining all the elements of interest simultanously, with minimal adjustment of instrument/sample conditions. Again, a simultaneous technique is required for speed of analysis. All other parameters being equal, a sequential analysis will take at least n times as long to perform as a simultaneous analysis, where n is the number of components being determined.
3. Sufficient sensitivity for determination of all the desired elements at levels that are typically found in the sample. Typical levels of ash elements in coal are noted in Table 1 [5].
4. Insensitivity to sample morphology and matrix. Samples may vary widely in character and composition, and the instrument should not respond to these variations.
5. Sufficiently rugged to withstand the environment of the processing facility.
6. Little technical assistance should be required for operation, as the operator may not be a technician.
7. The technique should be cost effective.

Table 1: Typical Levels of Elements in Coal Ash

Element	Reported as	Percentage of moisture-free ash, range
Si	SiO_2	10-60
Fe	Fe_2O_3	5-50
Al	Al_2O_3	5-30
Ca	CaO	1-15
Mg	MgO	0.3-10
Na	Na_2O	0.1-10
K	K_2O	0.3-3
Ti	TiO_2	0.5-2
Mn	MnO_2	< 0.2

CURRENT METHODS OF COAL ANALYSIS

The American Standard Testing Materials Commission lists atomic absorption spectrometry (AAS) as an acceptable method for the determination of metals in ultimate analysis of coal [5]. The procedure for this analysis consists of the following general steps: a) a weighed quantity of the coal is ashed in the presence of oxygen in a furnace; b) a weighed quantity of the ash is fused with lithium tetraborate; c) the melt is dissolved in acid; d) various interference suppressors are added to portions of the solution, depending on the elements being determined; e) the concentration of each metal is directly determined by AAS.

There are several acceptable ASTM procedures for determination of sulfur in coal. In the Eschka Method, the coal sample is ignited in contact with the "Eschka Mixture", a 2:1 mixture of $MgO:Na_2CO_3$. The soluble sulfur compounds are leached out and oxidized to sulfate by bromine, followed by gravimetric determination of the sulfate as $BaSO_4$. In the Bomb Washing Method, the sulfate-containing residue from oxygen bomb calorimetry is collected and the sulfur gravimetrically determined as $BaSO_4$. In the High-Temperature Combustion Method, the coal is burned in the presence of oxygen, followed by absorption of the sulfur dioxide by hydrogen peroxide. The resultant sulfuric acid is titrated volumetrically or coulometrically [6].

These methods of analysis for sulfur and metals in coal are far too slow to be suited to on-line analysis. However, AAS does meet several of the criteria for on-line determinations. It is not

extremely sensitive to minor differences in similar matrices, the instrument is fairly simple to operate, and the technique is inexpensive to implement. AAS falls short of the on-line criteria in that extensive sample preparation is usually required. Also, although AAS is capable of determining most metals, it is an inherently sequential method, in which setup time for each element is rather long when compared to the actual analysis time. Furthermore, the linear dynamic range for absorption spectrometry is limited by photometric error to 2-3 orders of magnitude. Finally, determination of sulfur by AAS is inconvenient at best. Atomic sulfur absorbs most strongly in the vacuum UV region of the spectrum (<190 nm), which region of the spectrum cannot be used with most flames. The method developed for sulfur analysis via AAS is an indirect one, again based on conversion of sulfur to sulfate, precipitation of $BaSO_4$, and AAS determination of the excess barium [7].

Other methods have been suggested for on-line analysis of coal. X-ray fluorescence (XRF) is suitable in some respects, but it is somewhat limited in terms of sensitivity and multielement analysis. XRF is best suited for major elements, and it is difficult to detect species which are present at concenrations of less than 100 ppm by XRF [8]. More significant is the fact that XRF is an inconvenient method for elements of atomic number below 21, requiring an evacuated operating system for these elements; even so, transmission is severly attenuated for many of these elements, which include sulfur and the two most important ash elements, silicon and aluminum [8]. In addition, empirical corrections must be made or grinding performed for coals of

varying particle sizes [9]. Finally, the cost of an XRF spectrometer is rather high.

Neutron activation analysis has a number of advantages for on-line analysis of coal. It is rapid, accurate, and precise; detection limits are <1 mg/kg for most elements in coal. NAA is in fact used in some coal processing plants for assessment of coal quality. It is, however, an exceedingly expensive technique; typical instrument cost is on the order of $500,000 [10].

Because of the limitations of X-ray and activation methods, work has been directed toward the development of atomic spectrometric methods for rapid coal analysis. One of the first studies was performed by Hicks and O'Reilly, who reported on elemental determinations in coal by AAS [11]. Their method of sample preparation consisted of grinding the coal to a small particle size. The resulting coal slurry was then delivered directly to the flame for analysis.

Three major problems with this method of analysis were observed. First, absorption methods are sensitive to scatter of the incident radiation, and unvaporized coal particles contributed to the scatter interference. Second, the flame was apparently not hot enough to completely vaporize the sample and convert it to its component atoms. The signal recovery (ratio of signal from the coal slurry to signal from an aqueous solution of equivalent concentration) varied somewhat from sample to sample, but was typically on the order of 50%. An empirical correction factor was required to determine the analyte content. Finally, the nebulizer had some tendency to clog, as the slurry had to pass through a small orifice.

It is clear from the work of Hicks and O'Reilly that AAS is not totally suited as an analytical technique for the rapid analysis of coal. However, two other atomic spectrometric techniques have considerable potential for this analysis. Plasma atomic emission spectrometry (AES) and plasma atomic fluorescence spectrometry (AFS) can overcome some of the limitations of AAS while retaining most of the advantages [12]. Detection limits of plasma AES and AFS are two to four orders of magnitude better than those of AAS. Linear dynamic ranges for AES and AFS are typically 4-7 orders of magnitude, as compared to 2-3 orders of magnitude for AAS. Both AES and AFS are readily adapted to simultaneous or rapid sequential multielement analyses. Also, the high plasma temperature should be conducive to more complete vaporization of the sample.

The major limitation of fluorescence measurements is that they are prone to scatter interference, even more so than are absorption measurements; emission measurements suffer but slightly from this interference. Since coal slurries would provide a large particulate population in the plasma prior to complete vaporization, it would appear that plasma AES would be more suited to on-line analysis of coal slurries by direct injection of the coal slurry (with dilution if necessary) into the plasma than would plasma AFS.

Several aspects of plasma AES would have to be addressed in the application of this technique to coal analysis. First, the plasma selected for the work would have to be appropriate to the sample in all its aspects. Second, a nebulizer that is suited to slurry samples would have to be used. Third, the effect of the coal matrix on the

plasma would need to be investigated, since plasma spectrometry can be subject to matrix interference. Fourth, an analytical method for sulfur determination using the plasma would have to be developed and characterized, as such methods are not yet available. Finally, the overall suitability of the technique for coal analysis would have to be shown.

THE DIRECT CURRENT PLASMA

The direct current plasma (DCP) provides what is arguably the most universal atom cell for emission spectrometry. It can be used for determination of over sixty elements, including both metals and nonmetals. Most of these elements can be determined at sub-parts-per-million levels, and most have linear dynamic ranges of four or more orders of magnitude. The DCP is normally coupled with an echelle grating monochromator, which allows rapid simultaneous multielement analysis. Most important with respect to on-line analysis is the fact that the DCP can readily accept a wide variety of sample matrices, including organic solvents as well as samples with high levels (up to 50%) of dissolved and/or suspended solids. In contrast, the inductively coupled plasma (ICP) cannot normally accept samples containing more than approximately 5% organic material or solids.

The first direct current "plasma jet" was developed independently by Margoshes and Scribner [13] and by Korolev and Vainshtein [14] in 1959. Subsequently, many workers modified the plasma jet for improved performance for spectrochemical excitation [15-20]. Only one company,

Spectrametrics Inc., pursued commercial development of the DCP. In 1971, Elliot [21] described a device which was later offered by Spectrametrics as the SpectraJet (Figure 1). An improved version, called the SpectraJet II (Figure 2) followed in 1975.

The SpectraJet III, developed in 1979 (Figure 3), is the state of the art in direct current plasma sources [22]. In this configuration the DCP consists of two graphite anodes and a tungsten cathode. The inverted-Y configuration of the SpectraJet III has been shown to be significantly more stable, upon introduction of the nebulizing gas, than the two-electrode configuration of the SpectraJet II [23]. Argon passes over the anodes at about 1 L/min, and over the cathode at about 1.5 L/min. The electrodes are held in pneumatically controlled sleeves, and the plasma is initiated by touching the three electrodes together, then returning them to their working positions. The SpectraJet III operates on two independent anode power supplies, each providing approximately 7 A at 40-60 V with respect to the cathode. The sample is introduced as an argon aerosol, below the inverted-Y, using a special ceramic nebulizer that is optimized for the high nebulizer argon flow rate (3-6 L/min). The aerosol droplets are desolvated, vaporized, converted to their component atoms, and are excited in a relatively small region below the apex of the plasma.

The difference between the direct current plasma and the direct currennt arc lies in the region of sample residence. In arcs and sparks, the sample is contained in the electrode or is introduced into it. When the arc/spark is ignited, the sample matrix helps support the discharge. This means that characteristics of the arc/spark will

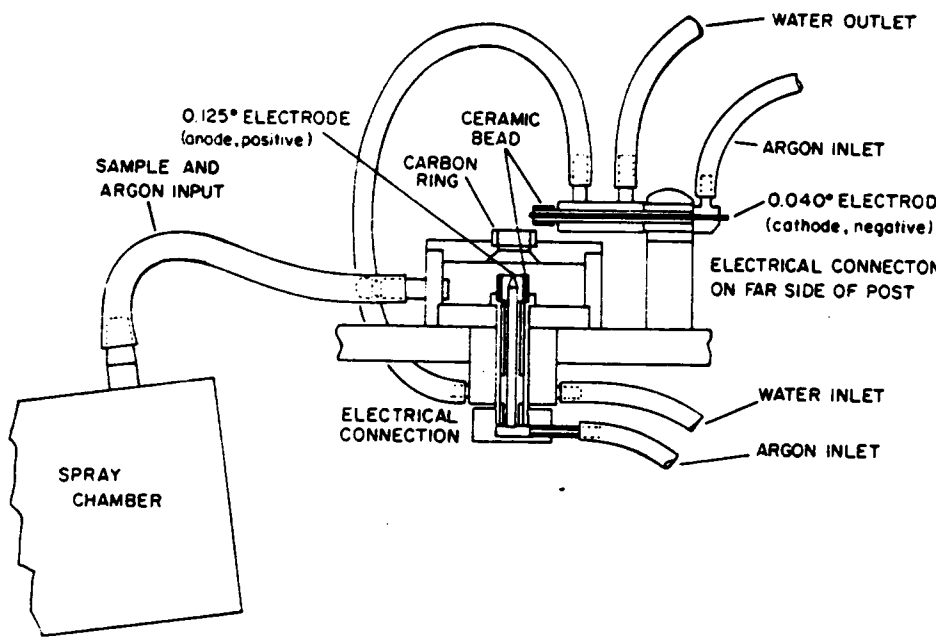

Figure 1: Original SpectraJet direct current plasma

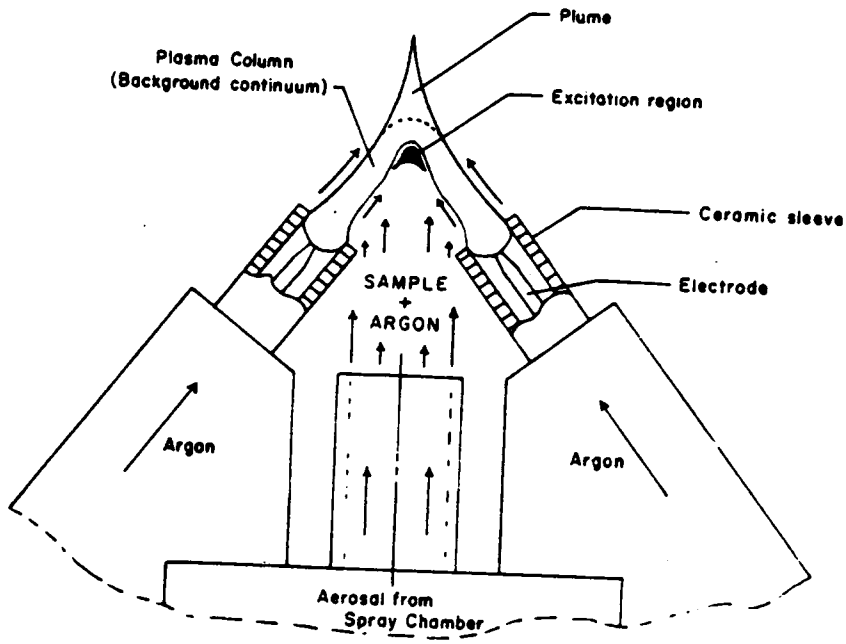

Figure 2: SpectraJet II direct current plasma

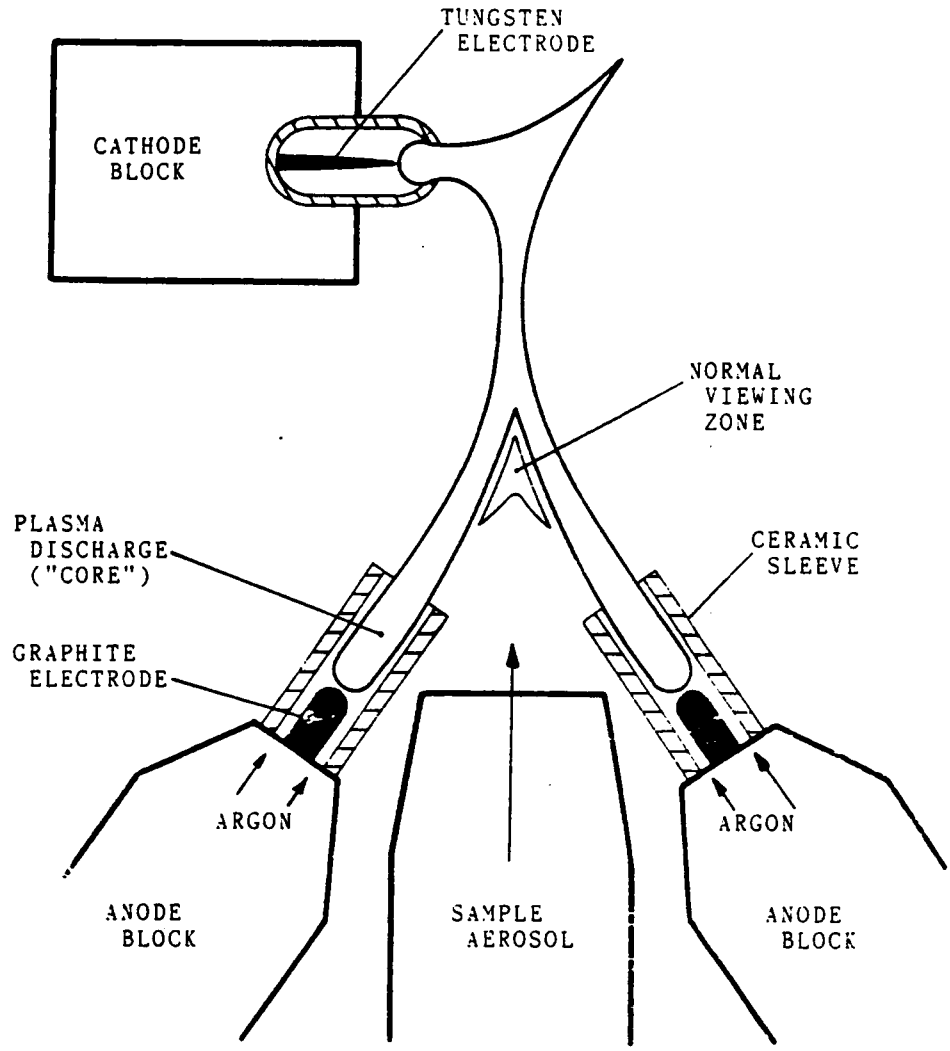

Figure 3: SpectraJet III three-electrode direct current plasma

depend to a great extent on the nature of the sample. In the direct current plasma, the arc is supported entirely by argon; sample does not penetrate to the discharge core, but resides on the outside of this discharge [24,25]. The plasma is considerably less affected by sample characteristics than is an arc or spark, resulting in lower noise as well as reduced matrix effects. Also, since this normal viewing zone or NVZ of the plasma is outside the discharge, background continuum emission is relatively low, providing a high signal-to-background ratio for excellent sensitivity.

Commercially, the SpectraJet III is coupled with an echelle grating monochromator as shown in Figure 4. This monochromator uses a 30^{o} prism in the Littrow configuration in conjunction with a coarse echelle grating [26]. Radiation is dispersed by the grating according to wavelength, and by the prism according to order, as shown in Figure 5. The result is a compact dispersive system (approximately 120 x 40 x 30 cm) with a focal length of 0.75 m and with resolution of better than 0.001 nm (at 200 nm wavelength). The entrance aperture is adjustable in width from 30-100 um, and in height from 50-500 um, which is well-suited to the size of the NVZ of the DCP. The spectrum from 190-800 nm is accessible to the echelle, and the resulting focal plane contains all the spectral information in an area about 8x10 cm. The spectrum can be focused on ordinary photographic film for recording *in toto*. Alternatively, a twenty element cassette can be inserted at the focal plane, whereby selected spectral lines are directed to a battery of photomultiplier tubes. The DCP-echelle combination thus has the ability to simultaneously determine up to twenty elements in about one

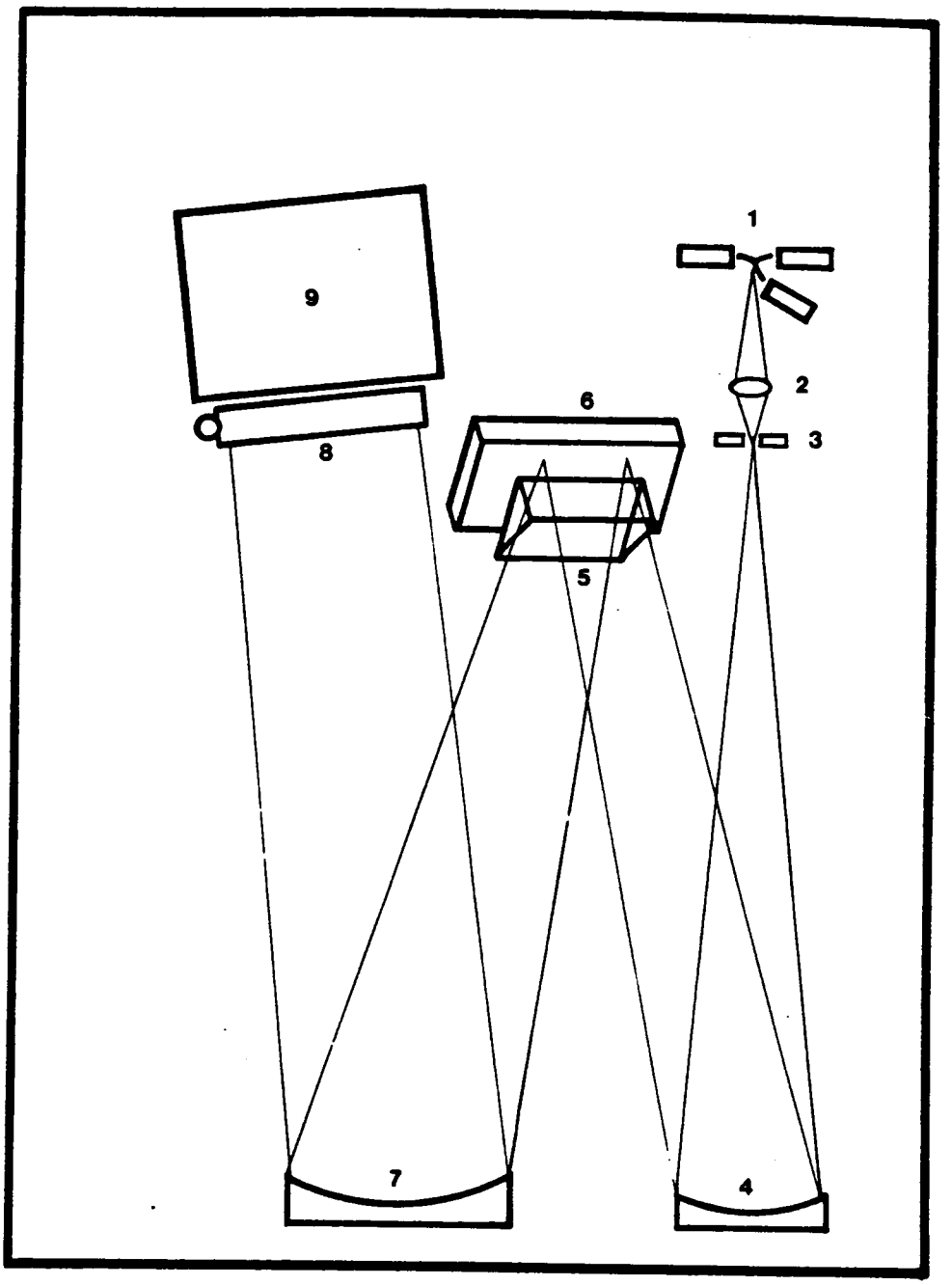

ECHELLE GRATING SPECTROMETER

1.) PLASMA JET	4.) COLLIMATING MIRROR	7.) FOCUS MIRROR
2.) LENS	5.) PRISM	8.) CASSETTE
3.) ENTRANCE APERTURE	6.) ECHELLE GRATING	9.) DETECTOR

Figure 4: Optical Train for the Spectraspan III direct current plasma emission spectrometer

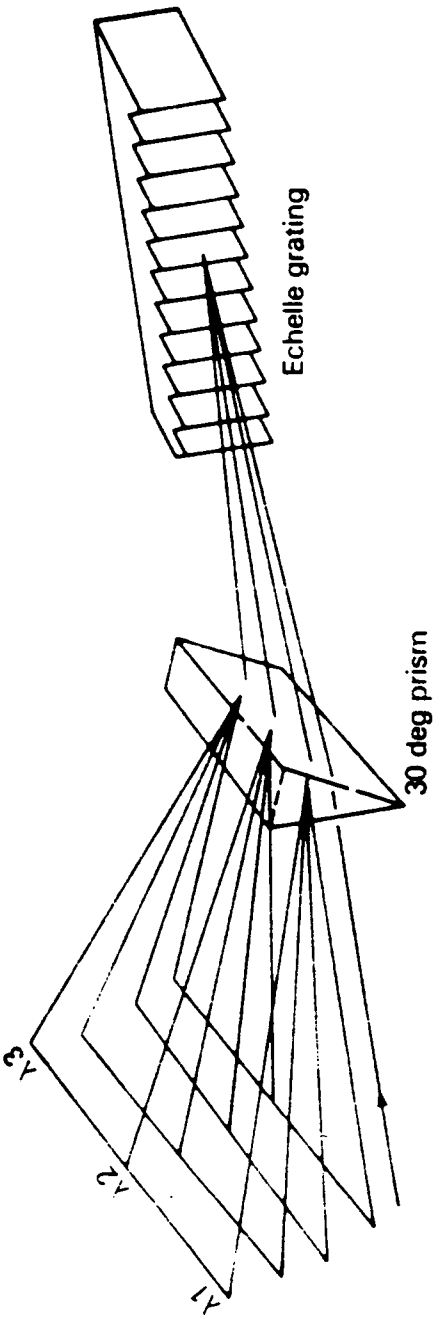

Figure 5: Dispersion of light by an Echelle grating

minute, with a linear dynamic range from sub-ppm to 1000 ppm for most elements. This system would appear to be well suited to on-line analysis of coal slurries.

THE BABINGTON NEBULIZER

A nebulizer is a device which produces the sample aerosol required for atomic spectrometric analysis. Most atomic absorption and ICP spectrometers use a type of pneumatic nebulizer, in which support gas (air or argon) is passed through a narrow tube. The reduced pressure causes the (liquid) sample to be drawn up a smaller tube concentric with or at right angles to the gas tube [27]. A number of variations on this device have been designed, including the Meinhard concentric nebulizer [28] and the MAK high-pressure nebulizer [29]. A variation on the ordinary pneumatic nebulizer is used in the commercial DCP. This nebulizer is constructed of ceramic to maximize wetting, has a wide orifice to accomodate the higher argon flow of the DCP (3-6 L/min as opposed to 1-2 L/min for most other pneumatic nebulizers), and is supplied with sample from a peristaltic pump to minimize variations in sample uptake. The nebulizer and spray chamber assembly are shown in Figure 6.

Although the ceramic nebulizer is excellent for solutions, being capable of 5-10% efficiency in production of analytically useful droplets, its utility for slurries is rather limited. As can be seen in Figure 6(B), the sample must pass through a relatively small orifice; slurries tend to clog this orifice. To avoid this problem,

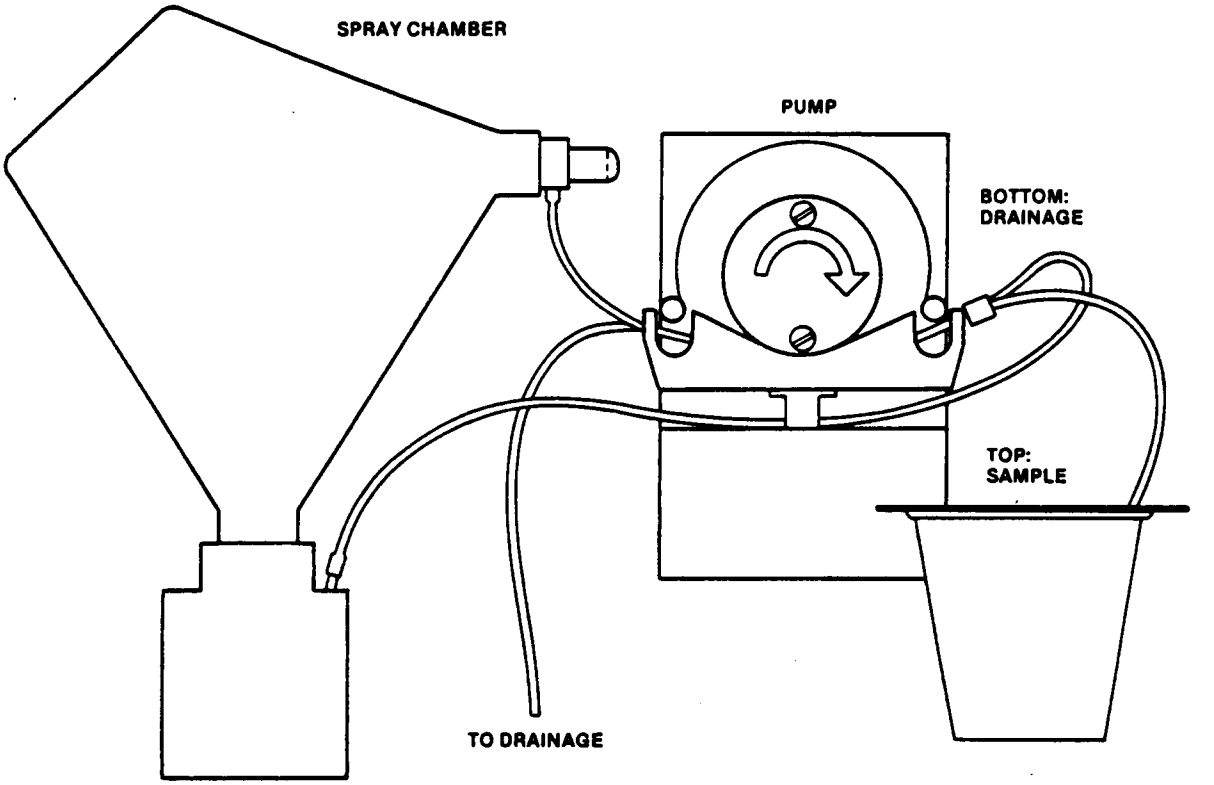

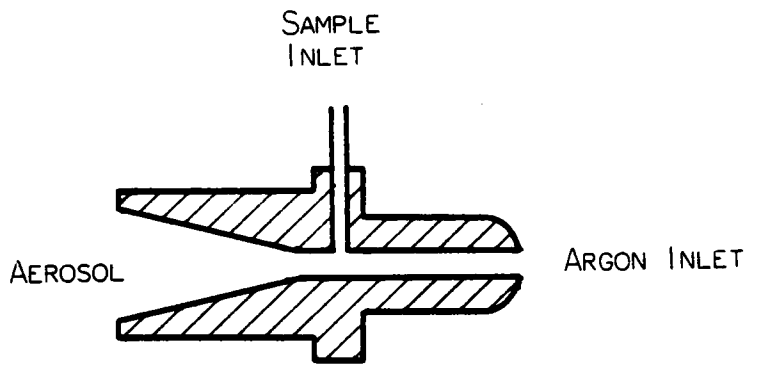

Figure 6: (A) Spray chamber, nebulizer, and sample delivery system for the Spectraspan III
(B) Close-up of ceramic nebulizer

Babington and coworkers devised a non-clogging nebulizer [30]. In the original configuration shown in Figure 7, the sample is pumped over a hollow bulb which has a tiny orifice. The nebulizing gas is passed through this orifice, which creates an aerosol by impact of the gas stream with the flowing liquid. Since the sample does not pass through the orifice, clogging of the nebulizer is greatly reduced.

The original Babington nebulizer was designed for argon flow rates of 1-2 L/min, and was made entirely of glass, thus being somewhat difficult to construct and adjust. A variation on this nebulizer, designed specifically for the DCP, was constructed and characterized by Fry and coworkers [31]. This design is shown in Figure 8. The argon orifice is in the center of a groove over which the sample is pumped. The groove directs the sample to the orifice to minimize sample waste. Argon flow rate can be varied by using different orifice diameters, and the sample delivery tube distance can readily be adjusted by sliding the tube nearer to or farther from the orifice. This nebulizer is well suited to creation of aerosols from slurries and from solutions.

From the preceding discussion, it is hypothesized that the direct current plasma, in conjunction with a Babington nebulizer for sample delivery, should be a suitable vehicle for on-line analysis of coal slurries for metals and nonmetals. The DCP is capable of simultaneous determination of up to twenty elements, at concentrations of ca 1 ppm or better for most elements; it is much less sensitive to most interferences, to sample morphology and matrix effects than is AAS; it is more rugged than the ICP; it is as simple to operate as is an AA; and the DCP is, in its simultaneous multielement configuration,

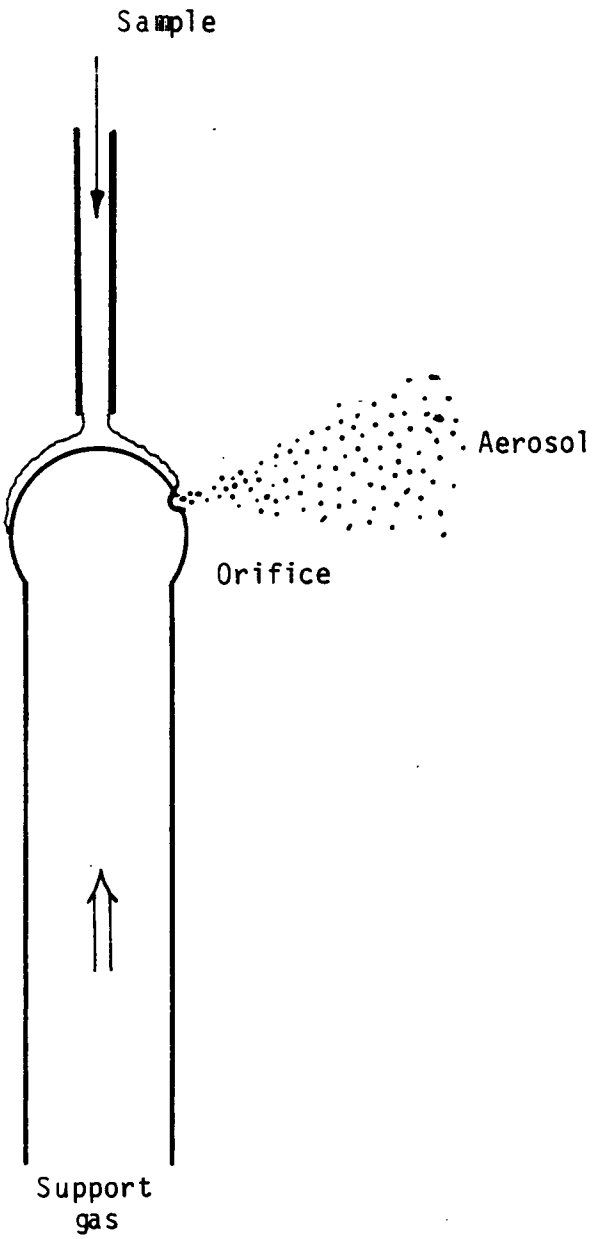

Figure 7: Babington nebulizer

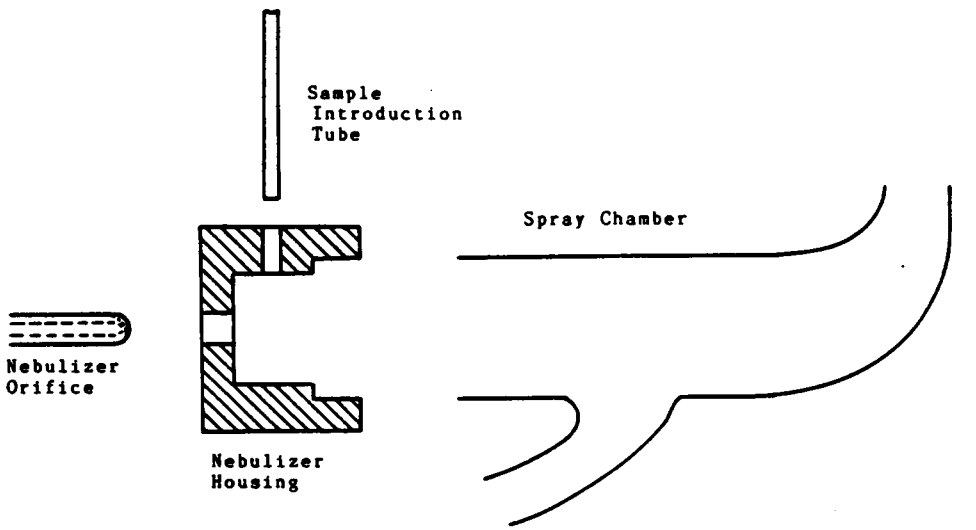

Figure 8: Babington-type (V-groove) nebulizer designed by R. Fry for the direct current plasma

considerably less expensive than an ICP, and in fact is not much more expensive than an AA.

The characteristics and aspects of the DCP which will be explored in this dissertation for the use of this technique as an on-line multielement analyzer for coal slurries include:

1. Determination of the effect of gaseous carbon (presumably from vaporization of the coal sample) on the direct current plasma. The major component of coal is carbon, hence the major potential matrix interference should involve carbon. Also, carbon-containing gases have been found to affect atomic spectrometric signals in the ICP via molecular interactions [32,33], and could presumably affect DCP signals by a similar mechanism.
2. Establishment of the use of the direct current plasma for analysis of sulfur in coal. A methodology for sulfur determination using DCP-OES has yet to be described, primarily because the strongest emission lines of sulfur (and most other nonmetals) lie below 190 nm, in the vacuum UV region of the spectrum. A non-intrusive interface between the atmospheric-pressure plasma and the evacuated or purged monochromator must be developed.
3. Determination of the utility of the direct current plasma for determination of iron, aluminum, and silicon in coal. These are the major ash elements; although methods and figures of merit have been established for these elements in aqueous solution via DCP-OES [34], the use of this technique for

determination of these elements in coal slurries has yet to be explored.

4. Investigation of technique(s) for improving the recovery of elemental emission signals from slurries. Sample transport is a problem with direct slurry injection in atomic spectrometry, in that the solid particles are not transported with the same efficiency as are aqueous solutions. This difficulty could be minimized by using coal slurries as standard "solutions"; however, this approach is undesirable for two reasons: the cost of standard coals, and the variance of coal characteristics from one sample to another. It is preferable to use aqueous solutions for standardization when possible. The problem of poor recovery has been reduced by grinding the coal to reduce the slurry particle size [35,36]. For on-line analysis of coal, an approach to improved recovery relative to aqueous standards, that would be less time-consuming than grinding, would be preferable.

CHAPTER 2

EXPERIMENTAL

In this chapter, the various reagents, samples, equipment, and data collection routines will be discussed.

Reagents and Solutions

All chemicals used were analytical reagent grade except as noted otherwise. Water was distilled and deionized. Elemental stock solutions of 1000 and 10000 mg/L were either purchased (Buck Scientific, Sargent-Welch) or prepared according to methods accepted for atomic absorption standards [37]. These stock solutions were diluted as required for all work involving standard solutions.

Stock solutions of poly(ethylene oxide) (PEO) were difficult to prepare because of the low rate of solution of the solid and the high viscosity of the resulting solution. The stock solutions were prepared by weighing the appropriate amount of the solid and adding about 300 mL of water. This mixture was stirred on a magnetic stirrer overnight, resulting in a viscous solution which was saturated with PEO, and a gel-like layer. The solution was poured into a volumetric flask, and another 100-200 mL of water was added to the remaining gel. This mixture was stirred again, and the process repeated until the gel had been completely solubilized; the resulting mixture was then diluted to

volume with water.

Grade 4.8 argon (Airco, Inc.) was used for operation of the plasma. Argon flows to the two anodes, the cathode, and the nebulizer were separately metered using Air Products flowmeters (Model 150MM2 for the electrodes and 150MM3 for the nebulizer). Propane for the study described in Chapter 3 was from a 14 oz. disposable cylinder, and was metered via a 150MM1 flowmeter.

Coal Slurries

Coal slurries were prepared by first sieving the powdered coal through a 200 mesh (75 micron) screen to remove large particles and aggregations. The fine powder was accurately weighed and transferred to a volumetric flask, and a small amount of water was added, to which TRITON X-100 had been added (such that the final concentration of the TRITON would be 0.2%). The mixture was stirred (usually overnight) to break down any remaining aggregates. At this point, PEO stock solution was added for those experiments requiring its use, and the slurry was then diluted to volume with water. Most of the work done with coal slurries utilized a 1% concentration of coal as being an appropriate and convenient concentration for analysis.

Plasma Source and Instrumentation

A Beckman Spectraspan IIIB direct current plasma emission spectrometer was used for this work. Detailed specifications for this instrument can be found in Table 2. The instrument was used with a single-element cassette for all studies.

TABLE 2: Specifications for the Spectraspan IIIB Direct Current Plasma [22]

Excitation Source	SpectraJet III three-electrode dc argon plasma, formed by a tungsten cathode and two carbon anodes in an inverted-Y configuration
Jet Power Supply	7 amps constant current output at low voltage (approx. 40 V after plasma is established)
Recommended Pressures:	Sleeve 50 psig Nebulizer 10-30 psig
Nebulizer	Pneumatic ceramic type with polyethylene spray chamber 2 mL sample/min
Optical Design	Modified Czerny-Turner using an echelle grating with 30^{o} prism for order separation
Optical Parameters	Focal length 750 mm Focal ratio f/13 Grating 9.6 x 4.6 cm high 79 grooves/mm
Dispersion	0.061 nm/mm at 200 nm 0.122 nm/mm at 400 nm 0.244 nm/mm at 800 nm
Slit widths	25, 50, 100, 200, and 500 microns
Detector	Twenty-element photomultiplier battery (Hamamatsu R292 or equivalent). Each PMT has voltage adjustable in 50 V steps from 550-1000 V

For slurries and solutions that were to be compared to slurries, a Babington-type nebulizer, specifically designed and constructed for the DCP by R. Fry, was used in conjunction with a Rainin Rabbit ten-roller peristaltic pump (the latter was required for reduced pulsation of sample delivery. Sample uptake rate for this nebulizer was 9.5 mL/min.

The echelle grating was not suitable for work that required the scanning of a spectral region (H_β line widths or qualitative searches for emission lines), as scanning with this grating requires careful manipulation of both the order and wavelength controls in tandem. It is also unsuited to studies below 190 nm, in which region the echelle is not calibrated. For such work, an auxiliary monochromator was used. The auxiliary monochromator that was chosen for this work was a Czerny-Turner 0.35 m focal length, f/6.7 (Heath, Inc.) with a dispersion of 2 nm/mm. The entrance slit of the monochromator was adjusted to 0.05 mm width and was vignetted with a 0.5 mm circular aperture to restrict the area of the plasma being observed.

In order to use the sulfur lines below 190 nm, the monochromator and optical path must either be evacuated or purged with an inert gas. Two laboratory-designed and -constructed purge systems are shown in Figures 9 and 10. Basically, these systems consist of aluminum and plastic tubing connected to the monochromator, with a brass exit sleeve in near-contact with the plasma. Argon passing through the tube purges the optical path (the latter consists of one or two lenses for imaging of the plasma on the entrance slit of the monochromator). A more detailed discussion of the design and operation of the purge system will be found in Chapter 4.

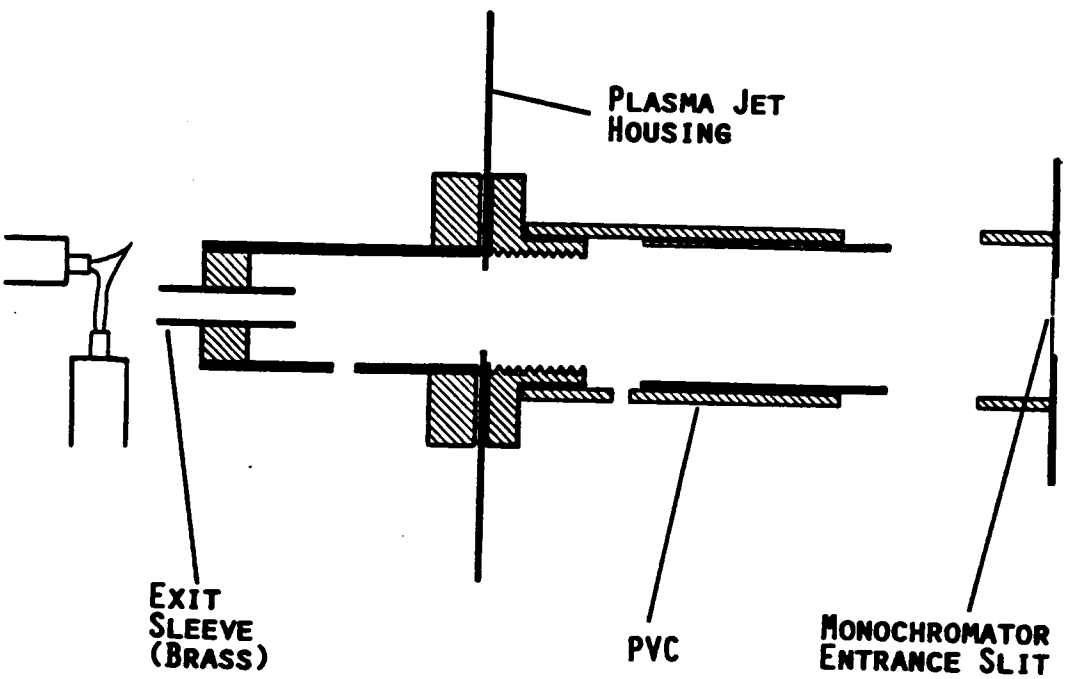

Figure 9: Purge system for the Spectraspan III direct current plasma. SpectraJet is used in place on the instrument with this purge system

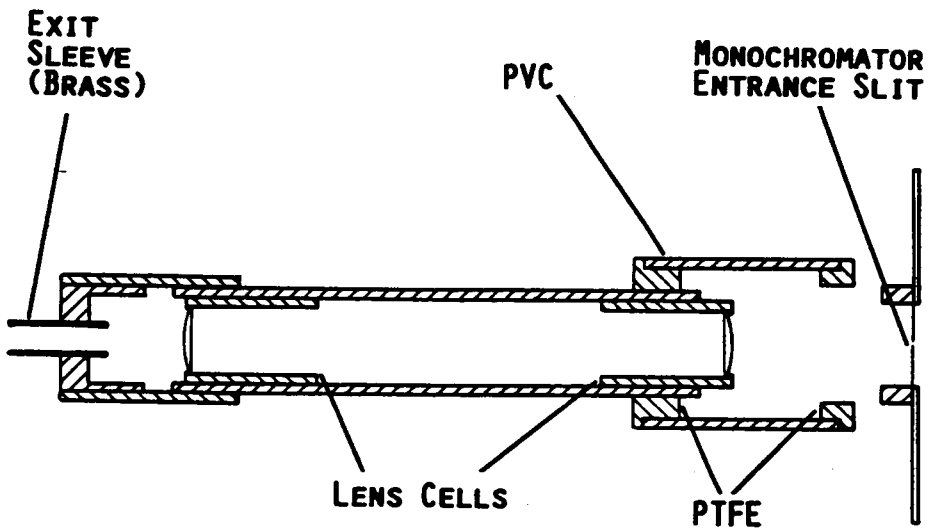

Figure 10: Purge system for the Spectraspan III direct current plasma. SpectraJet is demounted onto a separate optical bench with this purge system

Data Acquisition and Reduction

Data acquisition from the echelle grating spectrometer was performed by connecting the recorder output (0-10 V) of the #1 photomultiplier tube to the 12-bit analog-to-digital converter (ADC) of an ADALAB card (Interactive Microware, Inc.) installed in an Apple IIe computer. A laboratory-constructed resistive attenuation circuit (Figure 11) was used to reduce the signal from the recorder output to a level acceptable to the ADALAB card (2 V).

In use, the gain of the Spectraspan III computer/readout module was adjusted such that the maximum signal expected was well under the 10 V maximum of the recorder output. The attenuation circuit was then adjusted as necessary to bring the signal to a level that was manageable by the ADALAB card, and the computer/readout module was then set for "Diagnostic" and "Continuous" modes, in which the module acted simply as a current-to-voltage converter which continuously updated the recorder output.

The ADC of the ADALAB card is an Intersil 7109 integrating ADC with a maximum data acquisition rate of about 40 Hz, and can thus be programmed in BASIC without excessive software overhead. The QUICK I/O software provided with the ADALAB card was used for programming. BASIC routines that were written for various types of data acquisition in this study are listed in Appendix A.

Data acquisition from the auxiliary monochromator was performed by connecting the output of the photomultiplier tube to a current amplifier (Model 5002, EG&G PAR). For H_β line width measurements, the

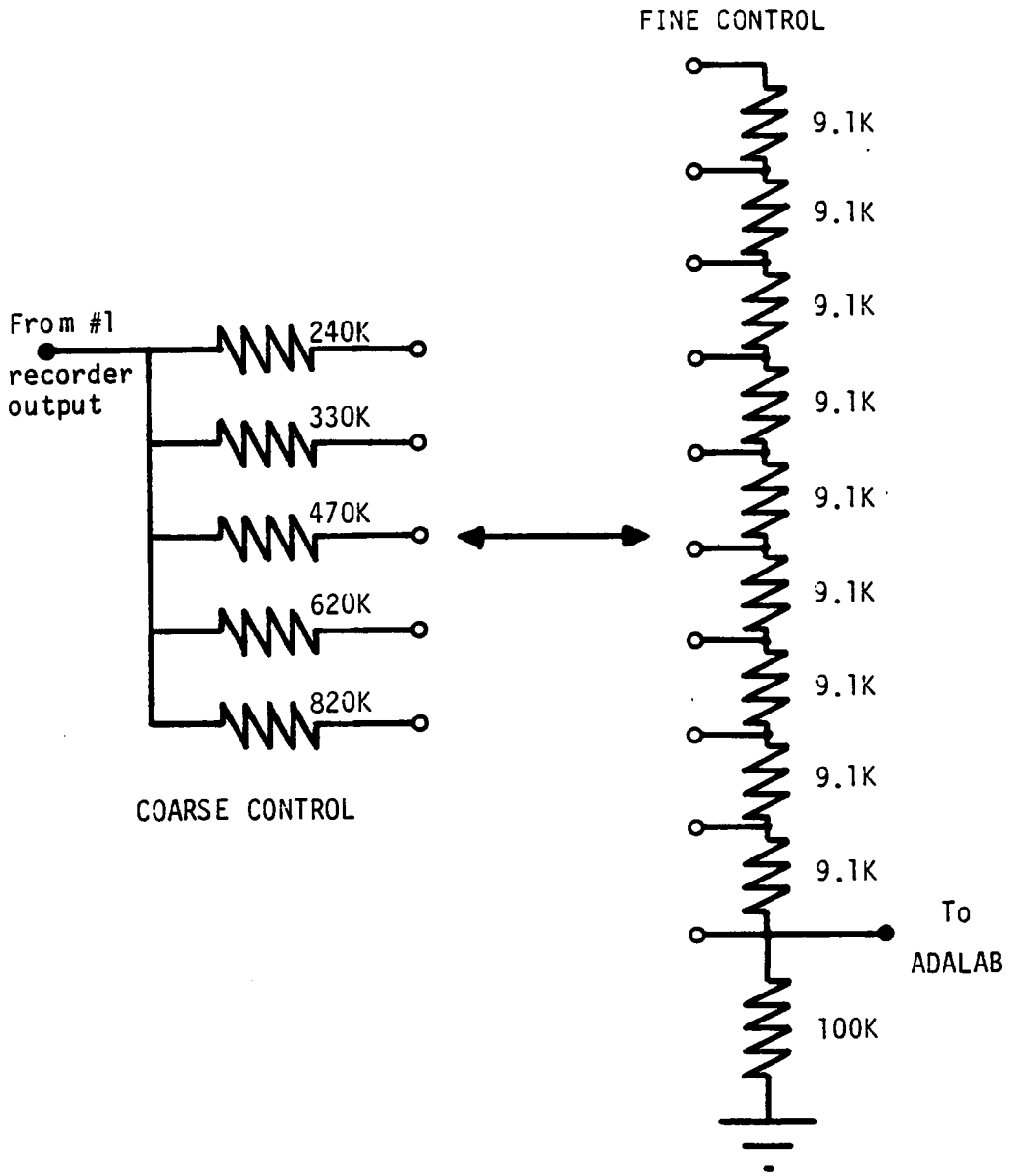

Figure 11: Resistive attenuator circuit for signals from the Spectraspan III DCP

output of this amplifier was connected to a PAR Model 5104 lock-in amplifier, and the optical path was modulated with a PAR Model 125A rotating light chopper. Spectra were recorded by connecting the output of the lock-in amplifier or the current amplifier to a Houston Model 100 X-Y recorder, which was operated in the Y-T mode wherein the time base was generated from the digital-to-analog converter of the ADALAB card. For data collection, the output of the current amplifier was connected to the ADC of the ADALAB card as described above.

Detection limits were determined using the c_L (k=3) convention:

$$c_L = \frac{3\sigma}{m}$$

where c_L is the limit of detection, σ is the standard deviation of the blank readings, and m is the slope of the working curve [38].

CHAPTER 3

THE EFFECT OF PROPANE ON THE DIRECT CURRENT PLASMA

One of the most significant advantages of the direct current plasma (DCP) over the inductively coupled plasma (ICP) is the tolerance of the DCP to a wide variety of sample matrices. Large quantities of suspended or dissolved solids, as well as nonaqueous solvents, can be aspirated directly, which makes the DCP more suitable for analysis of coal slurries than is the ICP.

The effect of the coal matrix on the DCP may be of some consequence. In the DCP, the solid coal will vaporize, the major products being carbon, hydrogen, oxygen, and nitrogen. The latter three are present in the plasma from water and from entrained air. Thus, it is important that the effect of carbon on the DCP be determined.

In the ICP, it has been found that the addition of carbon to the plasma in the form of propane has a beneficial effect. Winefordner and Long [32], Demers [33], and Greenfield and Thomsen [39] found that atomic fluorescence signals for several elements increased upon addition of small amounts of propane. These enhancements are thought to result in part from the reduction of metal oxides to metal atoms in the plasma:

$$MO + C \rightleftharpoons CO + M \qquad (1)$$

In this work, the effect of propane on the DCP is examined, with emphasis on the feasibility of harnessing Reaction 1 to enhance DCP spectrometric signals. Carbon is added to the plasma by metering propane into the argon nebulizing gas. Using this gas, the effect of carbon on the atomic spectrometric signals of several elements, as solutions and as oxide slurries, is evaluated. The effect of propane on the excitation temperature, electron number density, and argon metastable population is determined.

EXPERIMENTAL

Reagents, instrumentation, and data processing were as described in Chapter 2. Slurries of metal oxides were prepared from the oxide powders (Aldrich Chemical Company) of <10 um particle size. The propane (metered with a 150MM1 flowmeter) was held at the same pressure as the nebulizing argon to reduce potential mass transport effects. The nebulizer argon flow was reduced when propane was used, to maintain a constant total nebulizer flow of 3.9 L/min.

Vertical one-dimensional background corrected emission profiles were obtained by focusing the image of the plasma on the entrance slit, then manually moving the plasma upward (plasma image downward) using the vertical plasma positioning screw, in 0.5 mm or 1 mm increments. A complete background emission profile was first obtained for a given set of conditions, after which a complete signal profile was taken, and the

former subtracted from the latter.

Data acquisition was performed using the ADALAB card and Apple IIe computer as described in Chapter 2. The program used for data collection is "DCP", listed in Appendix A. The average of at least fifty A/D conversions was used for each background and each signal measurement, and at least three completed profiles were averaged to obtain a composite profile for a given element at a given wavelength.

The data obtained were collected under nearly identical experimental conditions. Gain and PMT voltage were adjusted in each experiment as necessary. Thus, only relative correlations between different plots is intended. Data was plotted as background corrected relative emission intensity, on a scale of 0-100 arbitrary units, as a function of distance from the apex of the plasma as shown in Figure 12.

RESULTS AND DISCUSSION

Effect of Propane on Plasma Appearance

Upon addition of propane to the nebulizing argon, the plasma assumed a radically different appearance, as shown in Figure 13. The sharply defined, bright, current-carrying core became surrounded by a diffuse violet layer, which layer became more prominent as the propane flow rate increased. The core itself became somewhat thinner and tapered, almost disappearing near the junction of the anode discharges. However, the plasma geometry was unaffected by flow rates of less than about 50-75 mL propane/min; i.e., the physical position of the core was unaffected. This is in direct contrast to the work done with organic

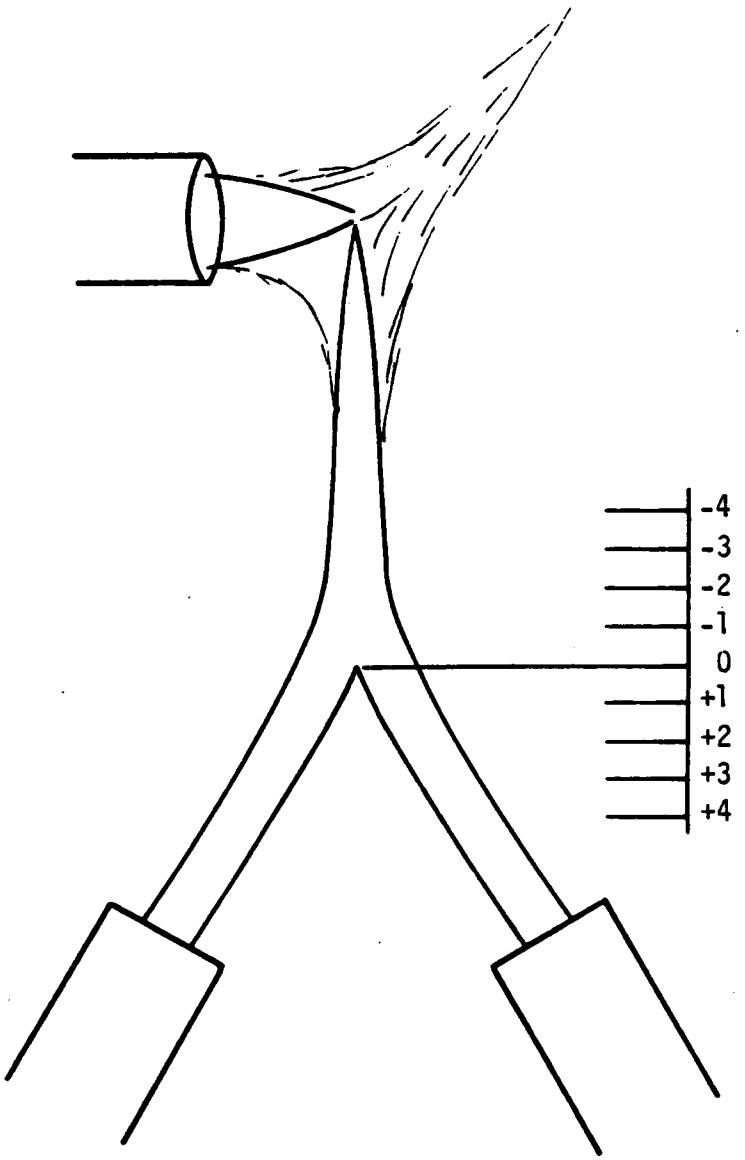

Figure 12: Appearance of normal direct current plasma jet

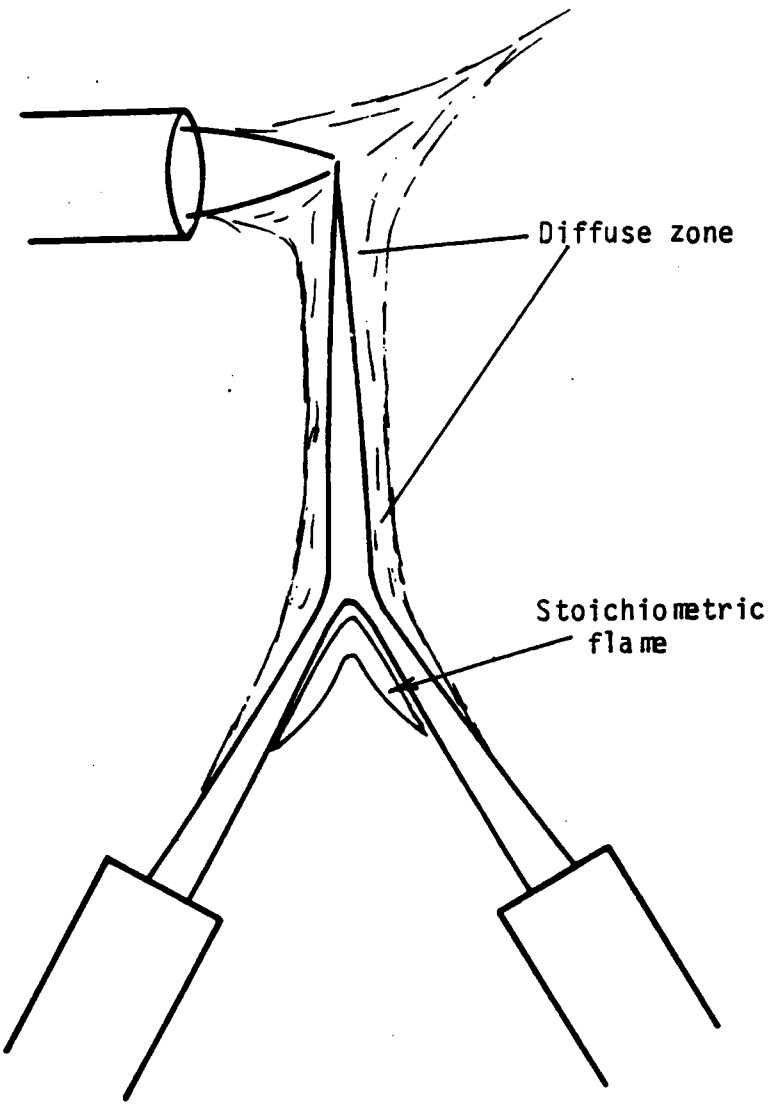

Figure 13: Appearance of direct current plasma jet with stoichiometric amount of propane added

solvents and gases by Gilbert and Penney [40]. These authors reported the appearance of a continuum emission below the plasma, and distortion of the plasma itself, upon addition of 200 mL/min of butane. The discrepancy can readily be explained by noting the much smaller quantity of propane used in these studies. When more than 50 mL/min was added to the nebulizing argon, the plasma assumed the appearance shown in Figure 14, which is similar to that described by Gilbert and Penney.

It is theorized here that the propane dissociates largely into its component atoms upon entering the plasma. The atmosphere around the plasma core is thus rich in carbon and hydrogen. Ionization of the carbon and hydrogen (ionization potentials of 11.3 and 13.6 eV, respectively) causes a current-carrying layer of carbon and hydrogen ions to appear around the core. The ionization potential of argon is 15.8 eV, so that the more easily ionized carbon-hydrogen layer becomes a significant current carrier in the plasma. Thus, a diffuse layer appears about the core of the plasma, and the core is less energetic and thinner as a result.

In the normal viewing zone, blue-green emission was observed similar to that seen in a stoichiometric Bunsen burner flame, corresponding to CH molecular emission. Upon increasing the flow rate of propane to above 46 mL/min, a yellow continuum appeared below the green region; this yellow flame skirted the plasma in approximately the path traveled by analyte. This yellow flame also appeared at flow rates above 10 mL/min of propane, if no aqueous sample was aspirated. Upon aspiration of aqueous samples at low propane flow rates, the

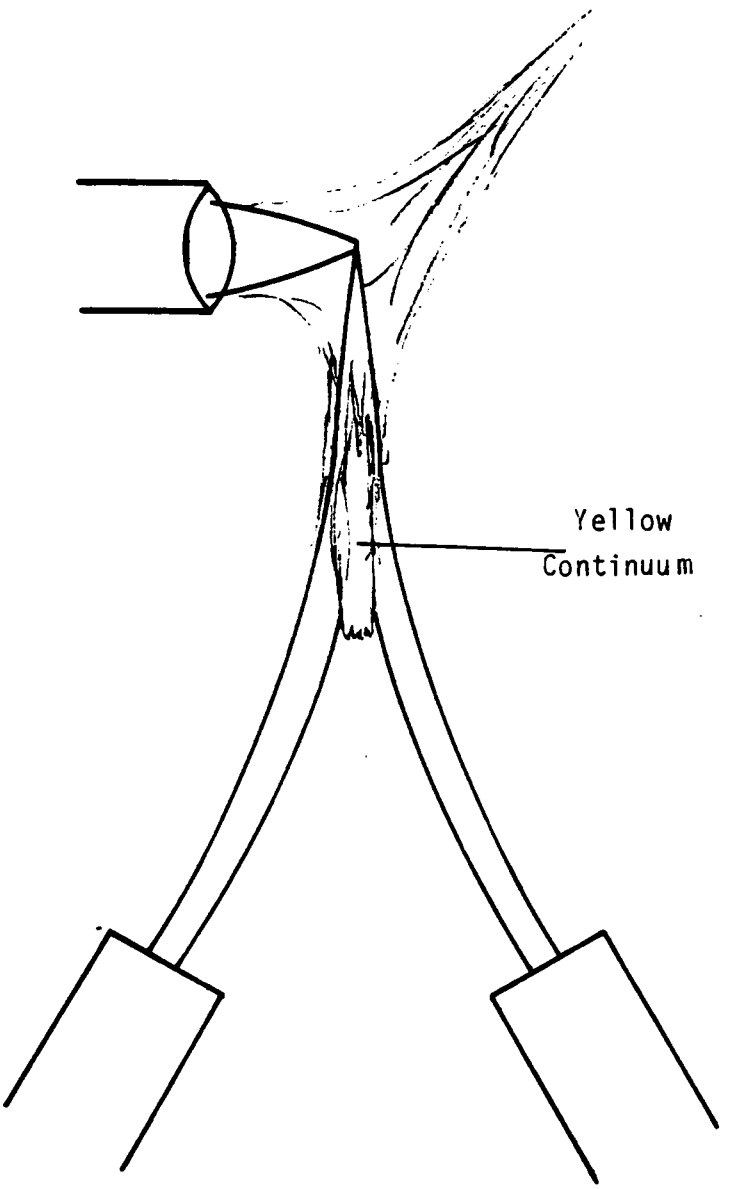

Figure 14: Appearance of direct current plasma jet with excess propane added

yellow flame would disappear. This is clear evidence of a reaction between propane and water, or between species derived from propane and water.

The flow rate of 46 mL/min of propane will be referred to as the "stoichiometric" flow rate. At greater flow rates than this, the yellow flame appeared, indicating stoichiometry between propane and the sample. At a flow rate of 46 mL/min, approximately 6.1×10^{-3} moles of elemental carbon/min enter the plasma, assuming 100% transport efficiency and complete dissociation. If the sample is introduced into the nebulizer at 2 mL/min, and the spray chamber operates at typical efficiency (5%), approximately 5.6×10^{-3} moles/min of elemental oxygen is added to the plasma. Hence, the observation of a stoichiometric "flame" in the normal viewing region is consistent with the amounts of carbon and oxygen introduced into the plasma.

Excitation Temperature

Excitation temperature is a measure of the energy available for excitation of analyte species. Thus, it is a factor which describes the suitability of a plasma or flame for emission spectrometry. Excitation temperature can be determined by the slope method [41], in which the relative emission intensities of two or more lines of a given element are determined. By assuming a Boltzmann distribution of excited states, the following equation can be applied:

$$\ln (I\lambda / g_k A_{ki}) = E_k/kT_e$$

where I = relative intensity of emission from the lines

λ = wavelength

g_k = statistical factor of the upper state

A_{ki} = transition probability

E_k = energy difference between the two states

k = Boltzmann constant

T_e = excitation temperature

A plot of $\ln (I\lambda / g_k A_{ki})$ vs. E_k will yield a straight line with a slope of $1/kT_e$. The use of multiple lines is most favored when a multi-wavelength detector is available and when the excitation cell is spatially stable; the use of two lines was deemed preferable for this work. A number of sets of lines have been noted in the literature as being suitable for determination of excitation temperature in plasmas [42].

Two assumptions are made in the use of this method. First, LTE is assumed; i.e., the populations of the states are assumed to be Boltzmann controlled. It has been determined by Miller, Eastwood, and Hendrick that the analytical region of the DCP is not in LTE [43]. Still, the excitation temperature has been found to be a useful guide in the DCP.

Second, the emission measured for each state is assumed to be proportional to the number of species in that state, in the region of the plasma being observed. Unfortunately, in most excitation cells, a significant amount of self-absorption can occur; the emitting region of the plasma is surrounded by an indeterminate population of ground state atoms, which can absorb the emitted radiation. Most workers have

suggested that, since the self-absorption should be nearly the same for most emitted lines, the effect of self-absorption on the net signal should be negligible. However, Boss has reported that, in the DCP, self-absorption can be a significant factor in the nonlinearity of working curves [44]. The answer to this dilemma would be the use of a method that would spatially resolve the atom population in an atom cell. Although this is possible with the saturated absorption method [45], the latter is limited to the determination of ground state species rather than excited state populations.

With these limitations in mind, the excitation temperature was determined with and without propane, using the two-line method with iron as the analyte (373.71 nm and 373.49 nm). As can be seen in Figure 15, the excitation temperature decreased greatly in and below the normal analytical zone, with a 1400 K drop in the normal analytical zone. At the center of the plasma, a slight temperature increase is apparent; above the apex, the excitation temperature is not significantly affected by propane.

Based on bond dissociation energies, it can be calculated that approximately 150 W of power are needed to atomize 46 mL of propane/min. The DCP normally operates at 500-750 W [46], so that this represents a decrease in power of approximately 20%. This corresponds roughly to the relative decrease in temperature, so that it was concluded that the temperature decrease results from the consumption of energy required to dissociate the propane. The temperature increase directly above the normal analytical zone is thought to be a result of the temperature decrease in the normal analytical zone. This decrease

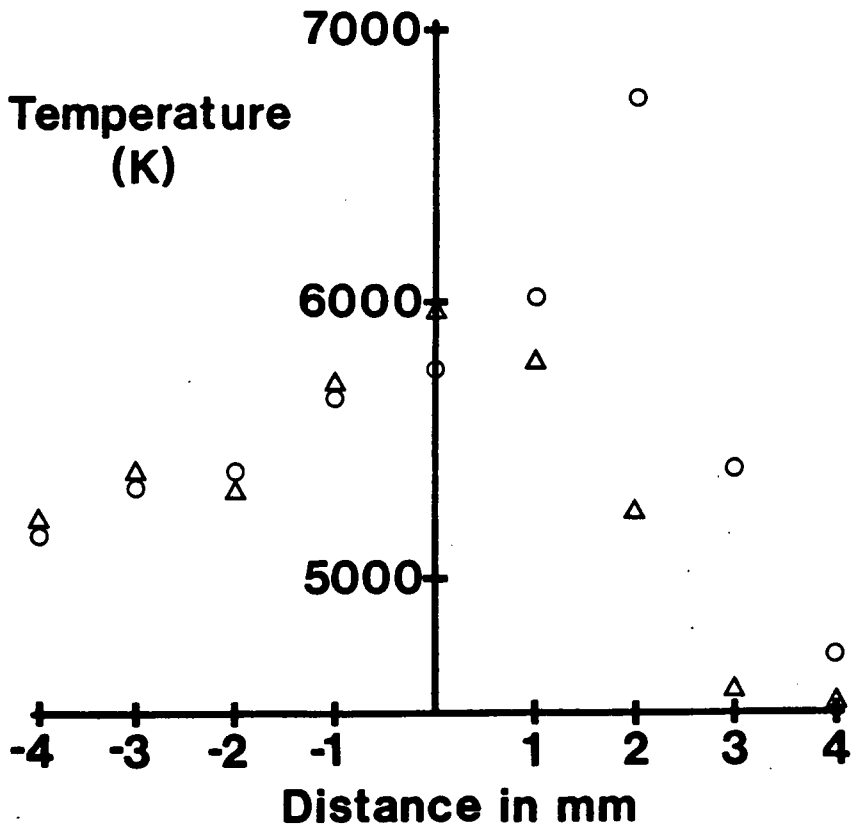

Figure 15: Vertical profile of iron excitation temperature in the direct current plasma, with (Δ) and without (o) stoichiometric propane added

results in a reduced temperature gradient in this region of the plasma. Since the thermal gradient directly controls the degree of penetration of analyte into the plasma [47], the sample does in fact penetrate more deeply, into a region where the analyte is exposed to a slightly higher excitation temperature.

One would expect that the temperature of the plasma above the apex would be much greater than that of the normal analytical zone, since this higher region corresponds to the plasma core. It was stated earlier that the analyte skirts around the plasma, so that the temperature given for regions "above" the plasma actually corresponds to a region above the apex and out of the plane of the plasma, as shown in Figure 16.

Electron Number Density

Electron number density (n_{e-}) is the mean number of free electrons per unit volume (cm^{-3}). Since a plasma is a mixture of free anions and free electrons, n_{e-} provides a measure of the electron temperature, and hence the energy, of the plasma. Electron number density was determined using the H_β line width method as described by Griem [48]. Although this method has drawbacks for determination of absolute n_{e-} in plasmas, it was considered adequate for assessing changes in n_{e-} in a given region of the plasma. A profile of n_{e-} was not obtained due to interfering line emission in most regions of the plasma, and due to high argon background emission in the upper regions of the plasma. For the same reason, n_{e-} was not determined at the stoichiometric flow rate of propane: the H_β line was partially obscured by two background

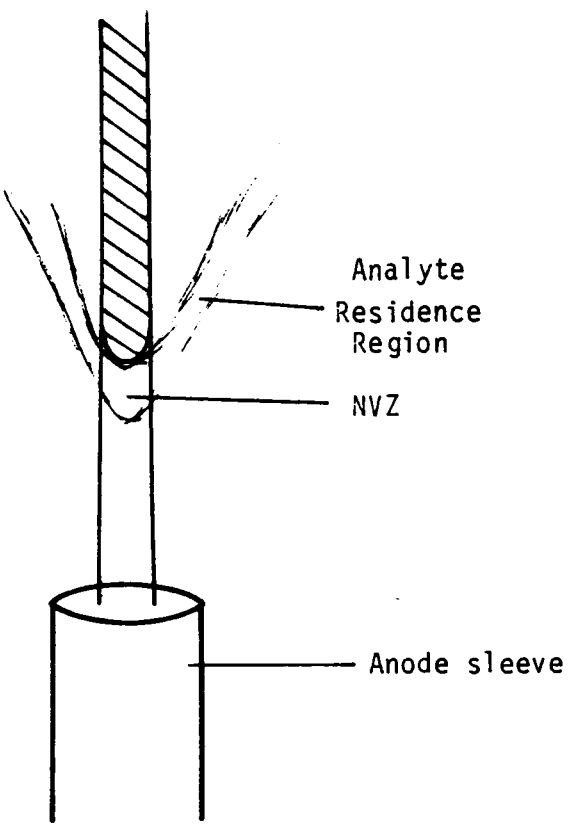

Figure 16: Side view of direct current plasma jet depicting residence area for analyte

emission lines. However, in the NVZ and at 36 mL/min of propane, n_{e-} was found to be 1.6 x $10^{15}cm^{-3}$. In the same zone with no propane, n_{e-} was also found to be 1.6 x 10^{15}. These values are in agreement with those reported by others for this region of the DCP [49,50].

Since the NVZ exhibited the greatest change in excitation temperature upon addition of propane, it should also be expected that the NVZ would exhibit the greatest change in n_{e-}. Since there was no significant change in n_{e-} in the NVZ, it is expected that there is no significant change in n_{e-} in other regions of the plasma upon addition of propane.

Argon Metastable Population

It has been suggested that argon metastables (Ar_m) act as an energy reservoir in the DCP [51] and may be partially responsible for the excitation process [52]. Profiles of Ar_m with and without propane are shown in Figure 17. In the NVZ and up to 2 mm above the center of the plasma, propane causes a reduction in Ar_m of about an order of magnitude. Higher in the plasma, the reduction in Ar_m is rather less, about 50-75%.

It should be remembered that above the NVZ, the Ar_m measured by emission is characteristic of the plasma core, since the core is optically aligned with thhe entrance slit and does contain argon. Analyte emission above the NVZ is not characteristic of the core because analyte does not penetrate to the core [53]. Below the plasma, the Ar_m emission is characteristic of the zone measured. Three conclusions can be drawn from this observation. First, the Ar_m of the

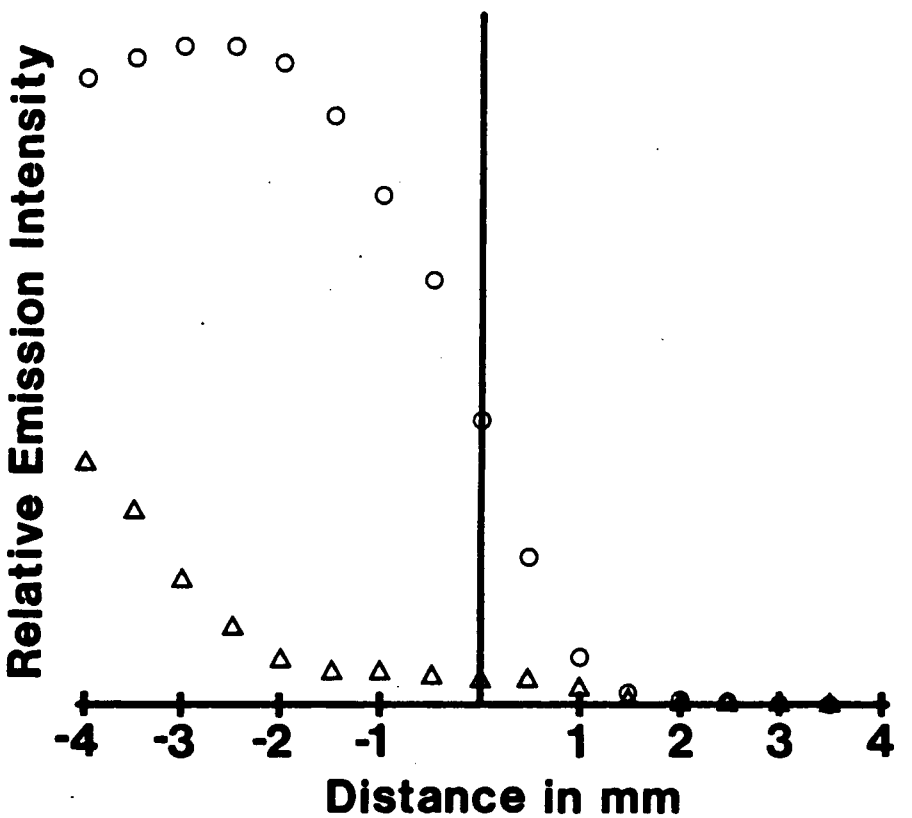

Figure 17: Vertical profile of argon metastable emission in the direct current plasma, with (△) and without (○) stoichiometric propane added

core is affected less that that of the surrounding regions. Second, propane does cause penetration of nebulizer gas (and presumably, analyte) deeper into the plasma, since the NVZ and the region slightly above it are affected to roughly the same degree, unlike the core region. Third, the plasma is overall less energetic as a result of the addition of propane.

Based on these diagnostic studies of the plasma, it would be expected that propane would cause a considerable decrease in analyte and background continuum emission in and below the NVZ (based on temperature); the decrease could be estimated for a particular species and emission line. Background line emission from carbon and hydrogen would be expected to increase, of course, since both these species are being added to the plasma. Although the temperature and presumably the electron number density do not change above the apex of the plasma, the Ar_m population does decrease, so that a decrease in emission above the NVZ would also be expected.

Background and Analyte Emission

Continuum background emission intensity decreased in most regions of the plasma, as shown in Figure 18 (this continuum emission decrease is true of all wavelengths observed, although only one wavelength is shown in this figure). However, below the plasma, the continuum emission increases. This is probably a result of the molecular population below the NVZ (this is observed in the form of the stoichiometric "flame"). Structured background also increased for carbon, although hydrogen emission decreased in intensity; a large

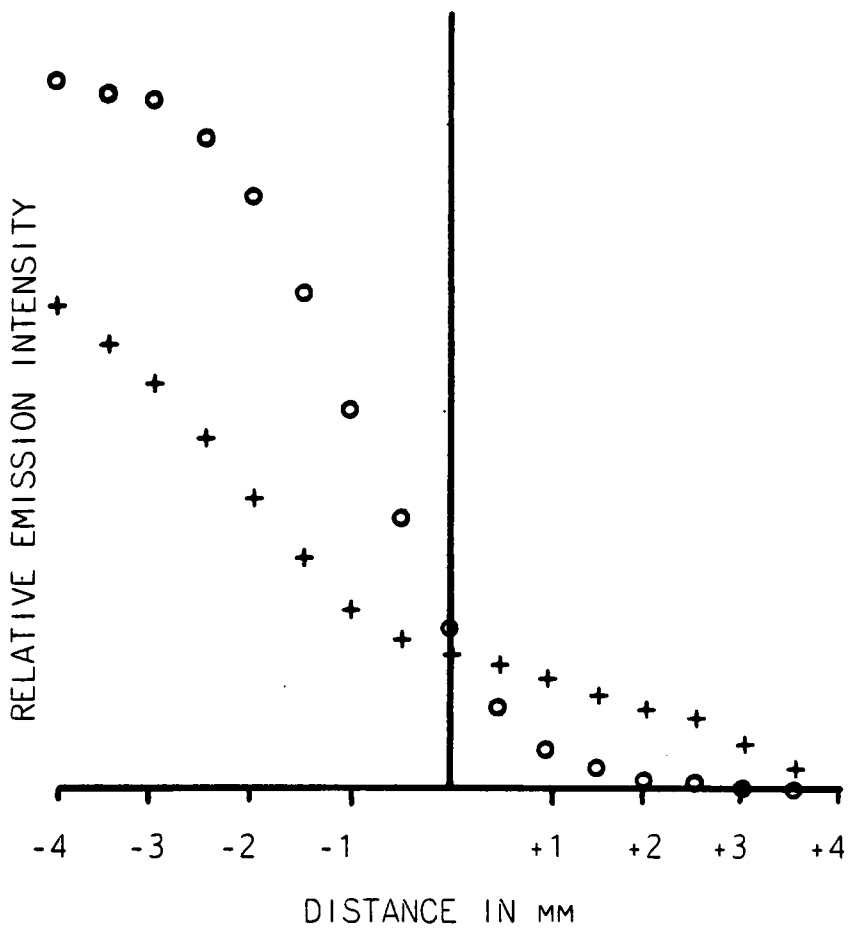

Figure 18: Vertical profile of background emission intensity in the direct current plasma, with (+) and without (O) stoichiometric propane added

hydrogen population already exists in the plasma from dissociation of water.

Figures 19 through 22 show atomic emission profiles for magnesium, titanium, silicon, and tungsten, with and without propane. As expected, a reduction in emission intensity occurs in and below the NVZ, due to the temperature decrease. Also as expected, the relative reduction in emission varies with the element. However, the reduction is not nearly that which would be predicted by the Boltzmann equation. Table 3 compares the decrease in emission intensity that was calculated for several zones of the plasma, based on temperature considerations, to the observed decreases. It is clear that the decrease in emission is not as great as would be expected in any zone of the plasma. Also, according to this table, the emission lines observed for silicon and magnesium should be nearly equally affected by the temperature change. In fact, the observed difference in reduction is over fourfold. Moreover, an increase in emission is observed for three of the elements above the apex of the plasma.

These observations argue for the existence of a process that increases the atomic population. Such a process cannot involve excitation temperature, n_{e-}, or Ar_m, since all these parameters either decreased or remained the same upon addition of propane (except for an increase in temperature at the apex of the plasma, where an increase in emission intensity was observed for each element). It is theorized here that the suggested process is chemical in nature, and is similar to the processes seen in the ICP upon addition of propane, namely, that of carbon reduction of metal oxides.

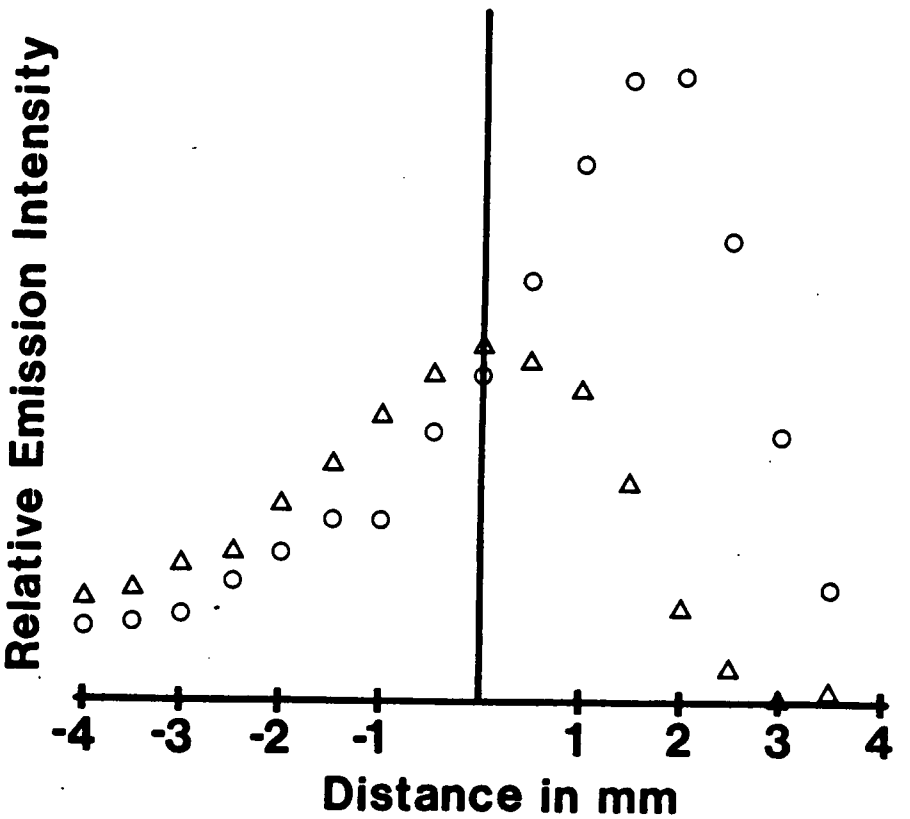

Figure 19: Vertical profile of emission from magnesium solution, with (Δ) and without (o) propane

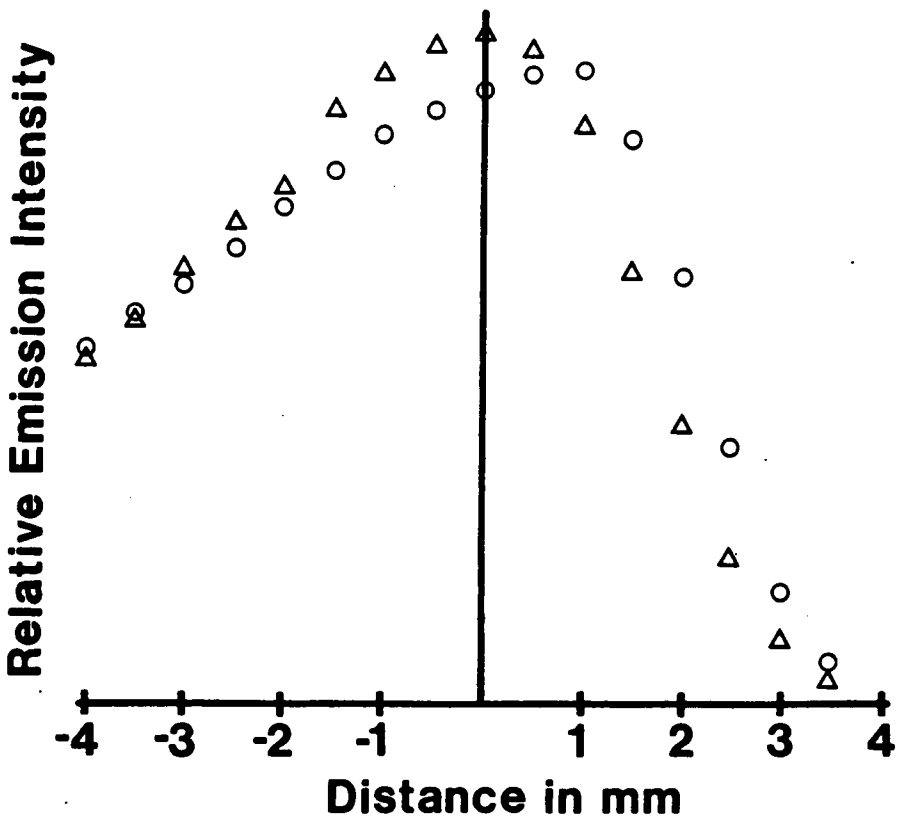

Figure 20: Vertical profile of emission from silicon solution, with (Δ) and without (O) propane

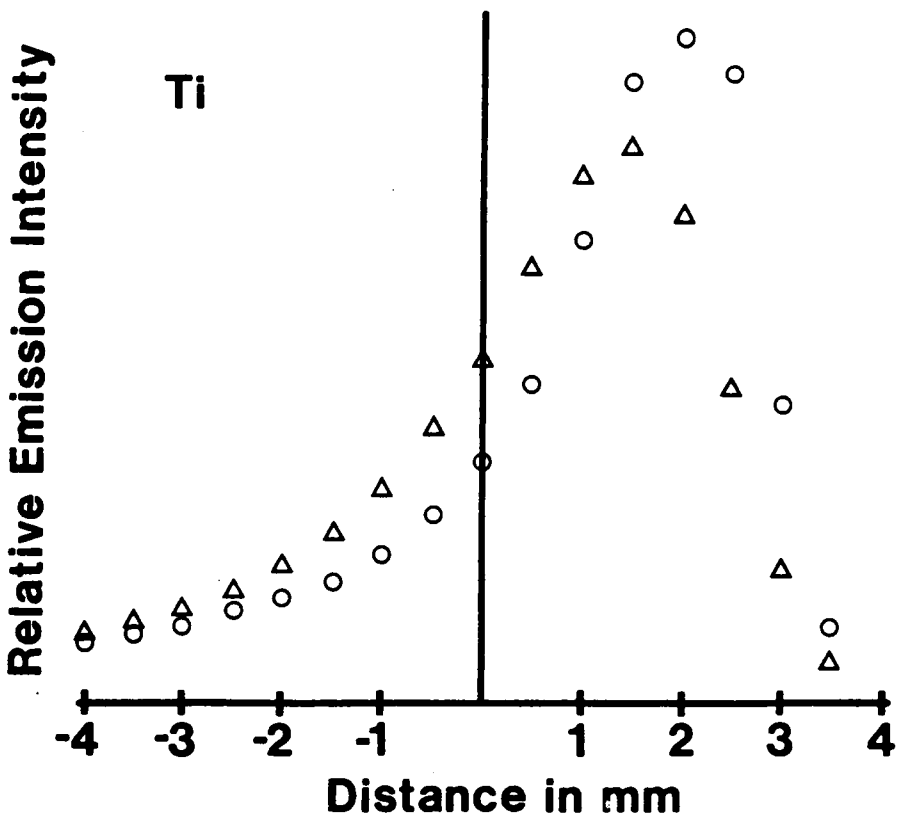

Figure 21: Vertical profile of emission from titanium solution, with (Δ) and without (o) propane

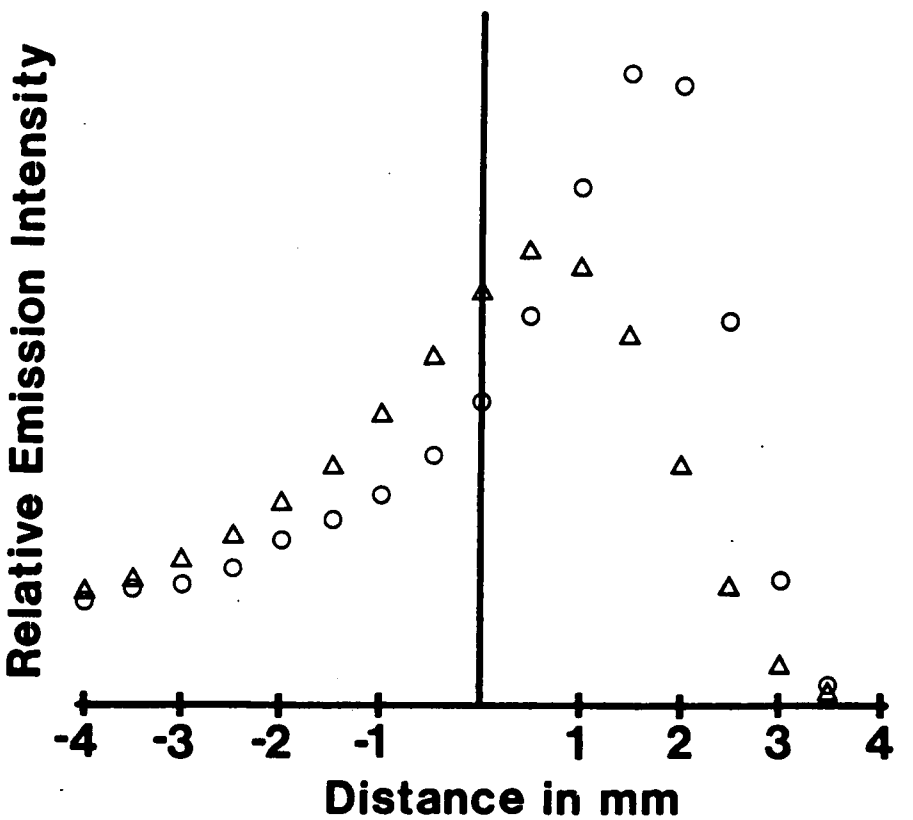

Figure 22: Vertical profile of emission from tungsten solution, with (△) and without (○) propane

Table 3: Ratio of emission intensity without propane to emission intensity with propane

	Calculated	Observed
Si	9.8	1.5
Ti	4.3	1.4
Mg	10.4	6.5

Carbon Species in the Plasma

The relative abundances of different carbon species in the plasma should provide some insight into the effect of propane on the plasma. In Figure 23, emission profiles are shown for atomic carbon and for molecular C_2 and CH. Since propane does affect the plasma, these profiles could not be obtained by merely comparing emission with propane to that without propane. To obtain a true measure of these species near the stoichiometric propane flow, these profiles were obtained by subtracting the emission observed at 40 mL propane/min from that observed at 46 mL/min. The small change in propane flow was assumed not to change the plasma appreciably.

Emission from C_2 shows a maximum well below the plasma, as would be expected for undissociated propane. The emission drops off rapidly above this point, indicating that dissociation of the C-C is nearly complete. Molecular CH shows a maximum in the NVZ, and a decrease in emission below and above this region. The emission from atomic carbon reaches a minimum at the plasma apex, indicating that it is depleted. This supports the theory that a reaction occurs between oxygen and atomic carbon, and that the reaction is nearly complete at the stoichiometric point. Above the apex, the population of atomic carbon increases rapidly. Since the region above the apex shows a lower temperature than the region below the apex, we can conclude that the population of atomic carbon is increasing above the apex even more rapidly that is indicated by the emission profile.

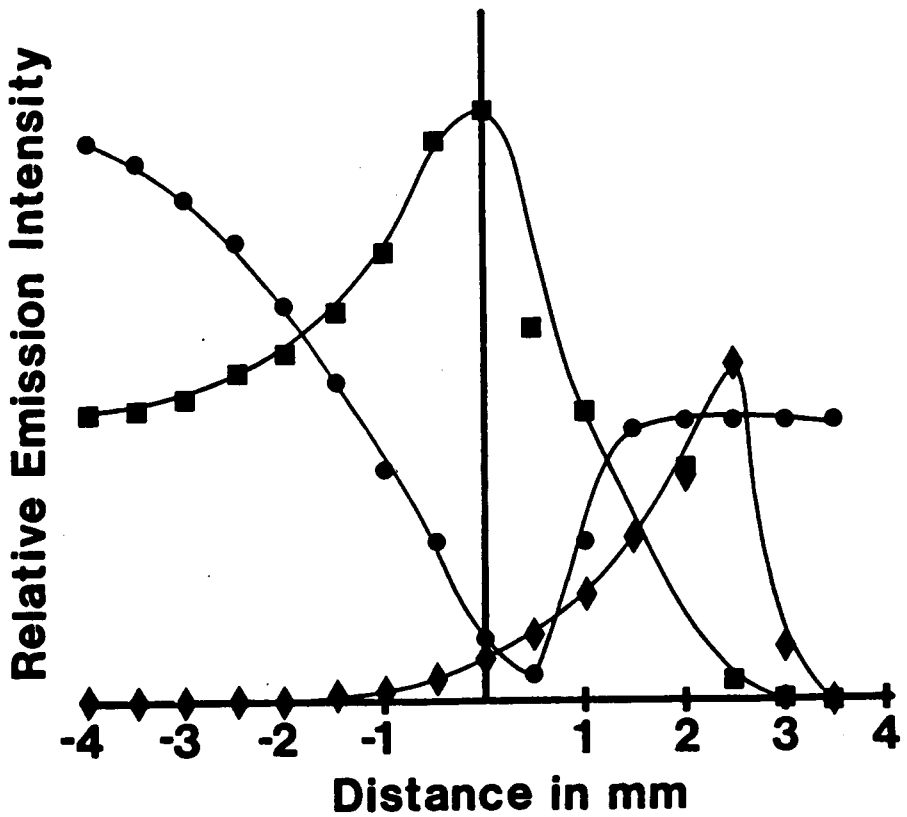

Figure 23: Vertical profiles of emission from atomic carbon (●), C_2, (♦), and CH (■) upon addition of propane

Emission from Oxide Slurries

Since the population of atomic carbon is greatest above the apex of the plasma, the logical place to observe this reduction would be in this upper region of the plasma. To more clearly observe carbon reduction reactions, emission profiles using slurries of magnesium, silicon, tungsten, and titanium were prepared [Figures 24 through 27] and compared to those of the corresponding metal solutions. To avoid differences in transport efficiency, the Babington nebulizer was used for both solutions and slurries in this study. It can be seen that, in the NVZ, tungsten and magnesium oxides show a smaller decrease in emission than do their corresponding solutions. Above the apex of the plasma tungsten, magnesium, and titanium oxides all exhibit a small but significant enhancement relative to their solutions; silicon dioxide shows a slight depression or no effect relative to its solution.

The enhancement of slurry signals relative to solution signals may be attributed to changes in one or more of the following: desolvation, vaporization, atomization, and excitation. If propane affected the desolvation step, we would expect no difference between emission from oxides and from solutions, since the same nebulizer was used and the same droplet formation characteristics can be inferred for the low slurry concentrations used [54]. If the step affected were the vaporization step, the solution would show an enhancement relative to the slurry when propane was added; the particle size from desolvation of a solution droplet is on the order of 100 nm [55], which is much smaller than the 1-10 um particle size of the slurry. The larger specific surface area of the desolvated solution particles would cause

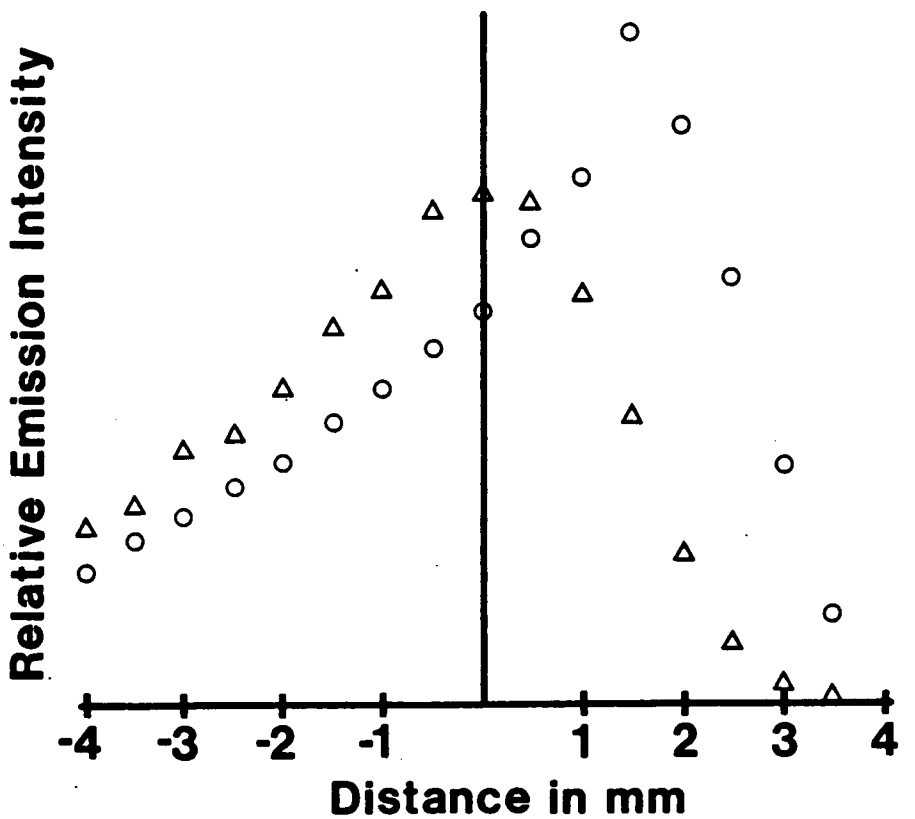

Figure 24: Vertical profile of emission from magnesium oxide slurry, with (△) and without (○) propane

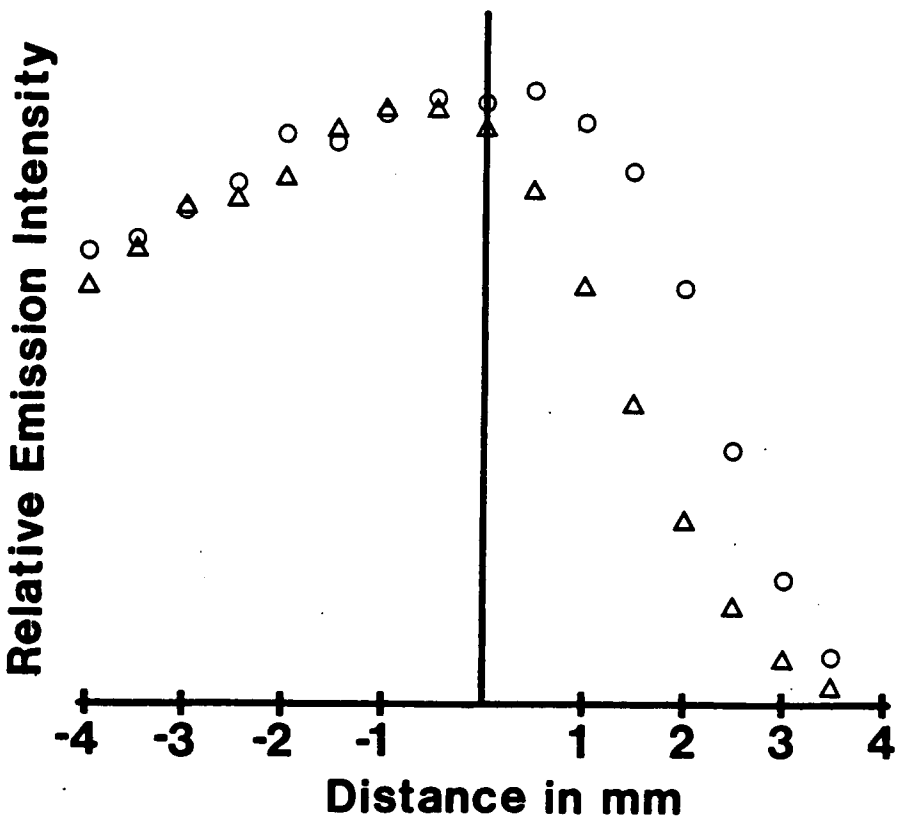

Figure 25: Vertical profile of emission from silicon dioxide slurry, with (△) and without (○) propane

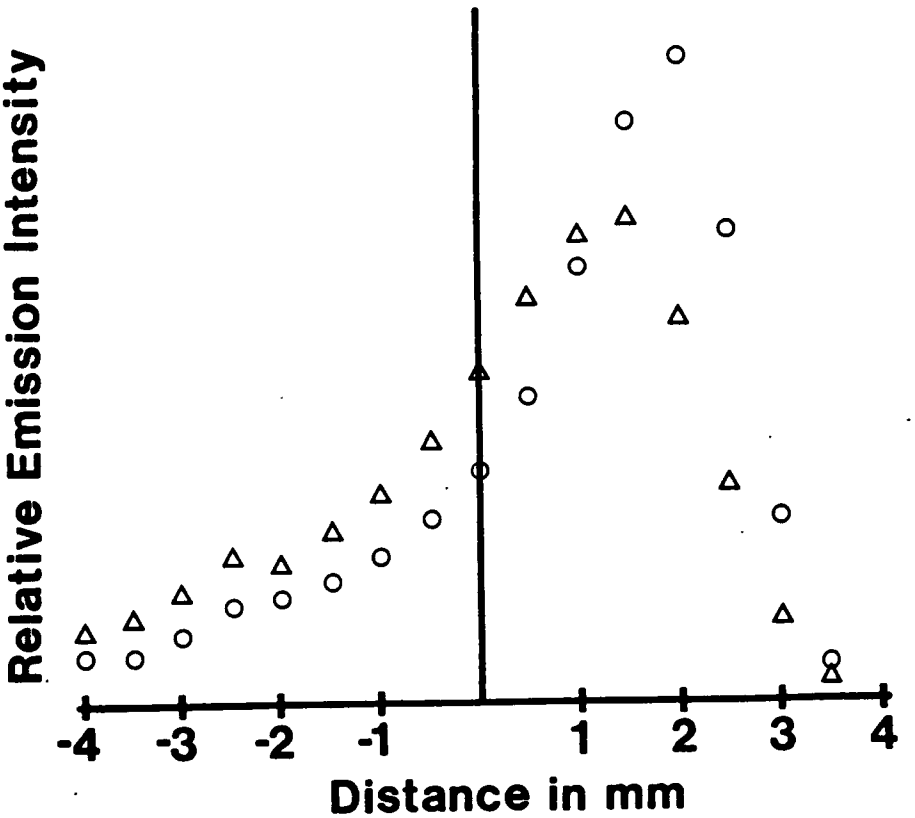

Figure 26: Vertical profile of emission from titanium dioxide slurry, with (Δ) and without (O) propane

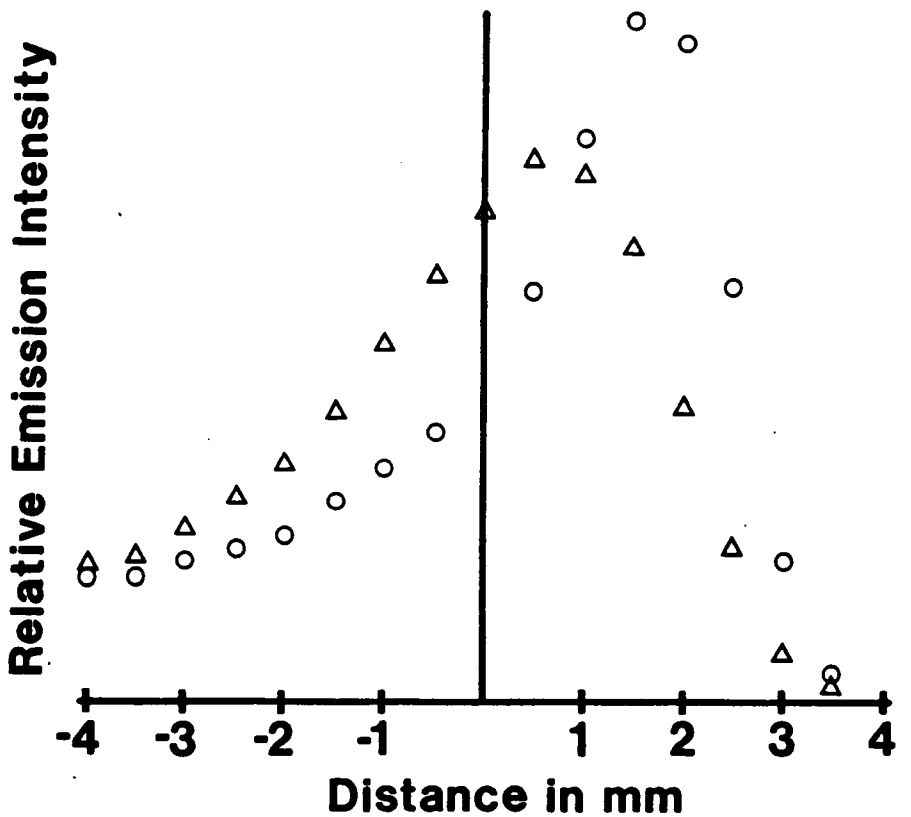

Figure 27: Vertical profile of emission from tungsten oxide slurry, with (△) and without (○) propane

them to vaporize faster. If excitation were the step affected, there should be no difference between the emission from the solution and the slurry, since just prior to excitation, analyte from both solutions and slurries is in the same atomic state. Thus, the step that must be affected when propane is added is the atomization step, indicating that the metal oxide is reacting with carbon or carbon-containing species to liberate the corresponding metal. Since a large reservoir of carbon exists in the region of the plasma which exhibits the most profound effect relative to propane, it is reasonable to conclude that the reacting species is atomic carbon.

Parallels Between DCP and ICP Carbon Reduction

In the ICP, studies with propane have been performed only above the induction coil, i.e., above the plasma toroid. The toroid is the region of the ICP that corresponds to the discharge core of the DCP, as a localized very-high-temperature region of the plasma. The region above the induction coil in the ICP then corresponds to the analyte residence region above the apex in the DCP. Propane added to the ICP has been found to dissociate nearly completely by the time it reaches the NVZ of the ICP, 15 mm or more above the load coil [56], in much the same way as it dissociates completely a few mm above the apex of the DCP. Effects of propane on the ICP toroid itself due to molecular species have not been examined to date, although it has been noted that the toroid does change, becoming slightly smaller and more violet upon addition of propane to the auxiliary flow [57]. Addition of propane to the analyte flow does not affect the plasma severely, presumably

because the delivery tube is situated in the middle of the toroid and the propane does not diffuse appreciably to the toroid.

Of those workers who have examined the effect of propane on the ICP, none have reported a temperature change in the NVZ with small amounts of propane. This concurs with the temperature effects above the apex in the DCP. Likewise, n_{e^-} has been found to remain unchanged in the NVZ of the ICP upon addition of propane; Ar_m has been found to decrease slightly in this region [56]. It might be instructive to examine the behavior of the region below the toroid of the ICP, to determine whether parallels can be drawn between this region of the ICP and the NVZ of the DCP. If the regions behave in a similar fashion, it might be possible to model the behavior of the DCP by using the region below the toroid of the ICP.

An interesting and elucidating parallel exists between results seen in ICP-AFS and results seen in this study. The effect of propane on emission from aluminum and barium under various conditions in the DCP were studied, and the results are shown in Figures 28 through 30. Above the apex of the plasma, where excitation temperature is unaffected, the elements studied show either no significant effect or an enhancement when propane is added. In hollow-cathode excited ICP-AFS, all elements exhibit either an enhancement or no effect upon addition of propane [33]. Contrariwise, in ICP-AES, some elements exhibit enhancements, and some exhibit depressions; to date, there is no clear explanation of this effect [57]. This data supports the idea that, above the apex of the plasma, excitation in the DCP is at least partially radiative rather than thermal in nature. This theory was

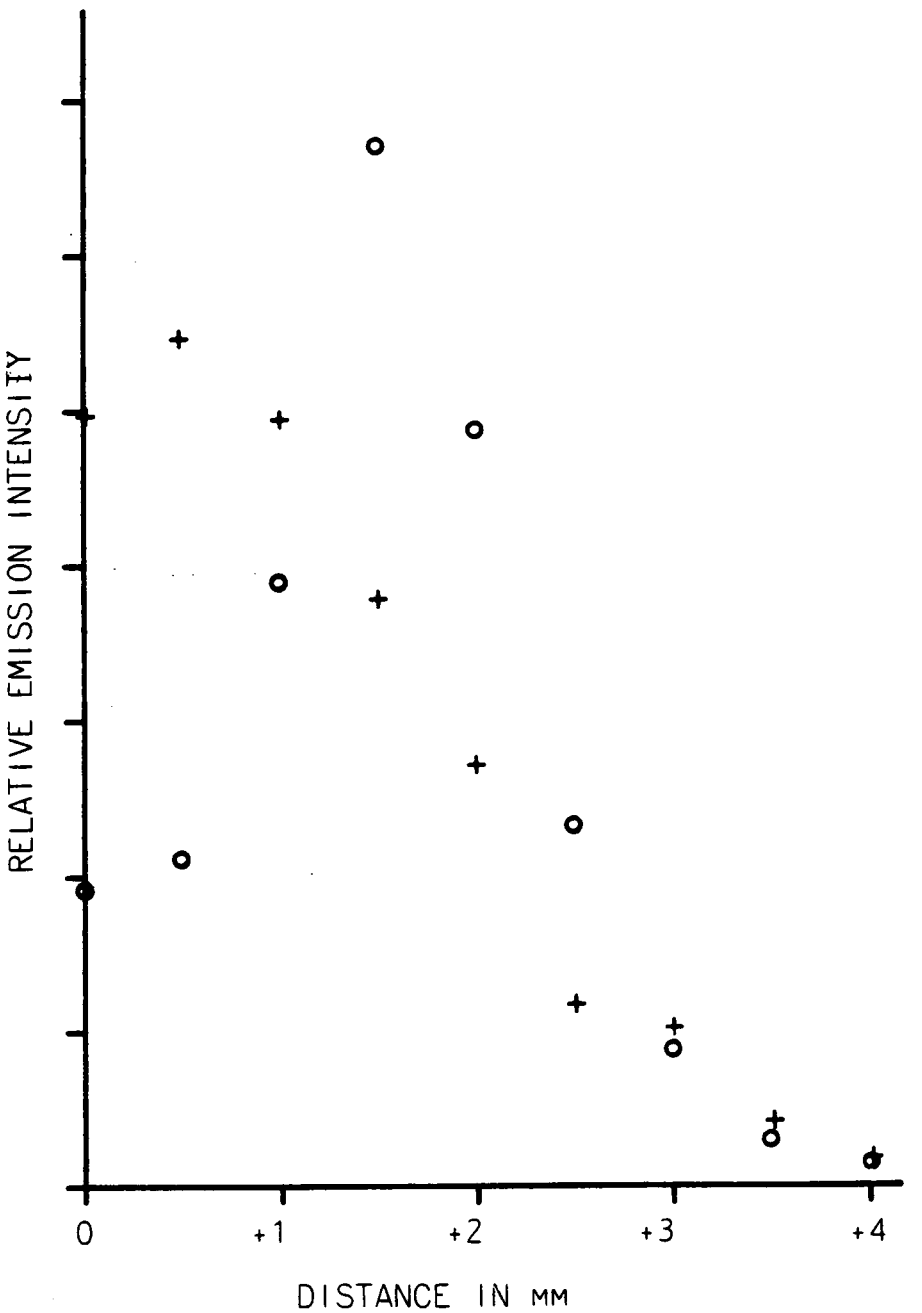

Figure 28: Vertical profile of emission from aluminum solution, with (+) and without (O) propane. Data farther above the normal viewing zone not obtainable due to excessively high background

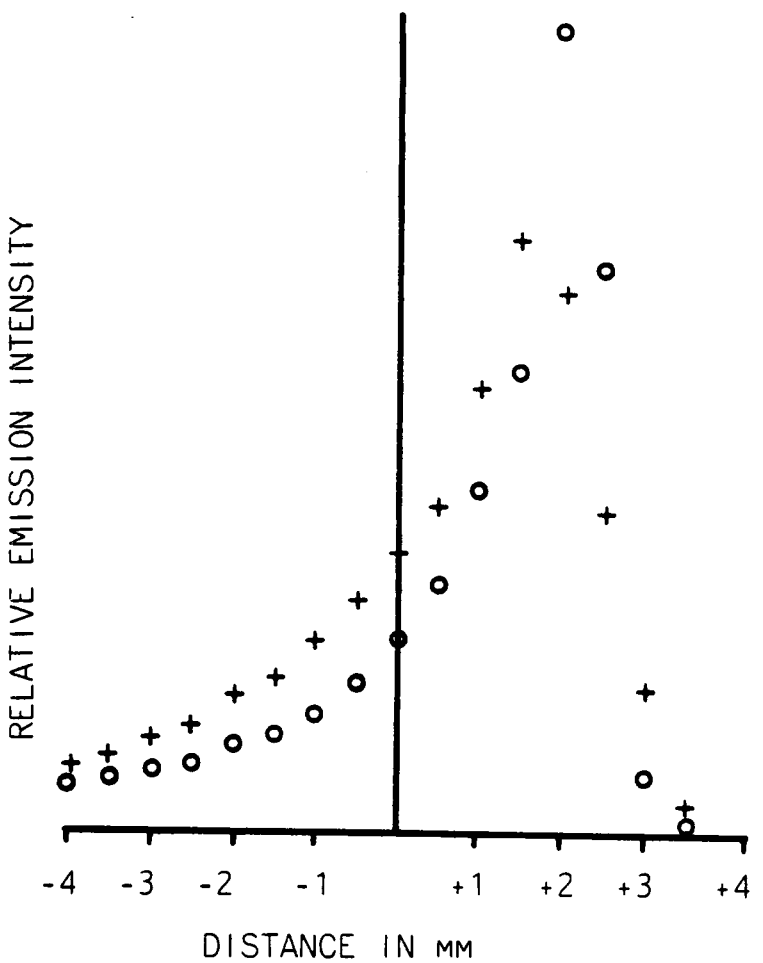

Figure 29: Vertical profile of emission from barium solution, with (+) and without (O) propane

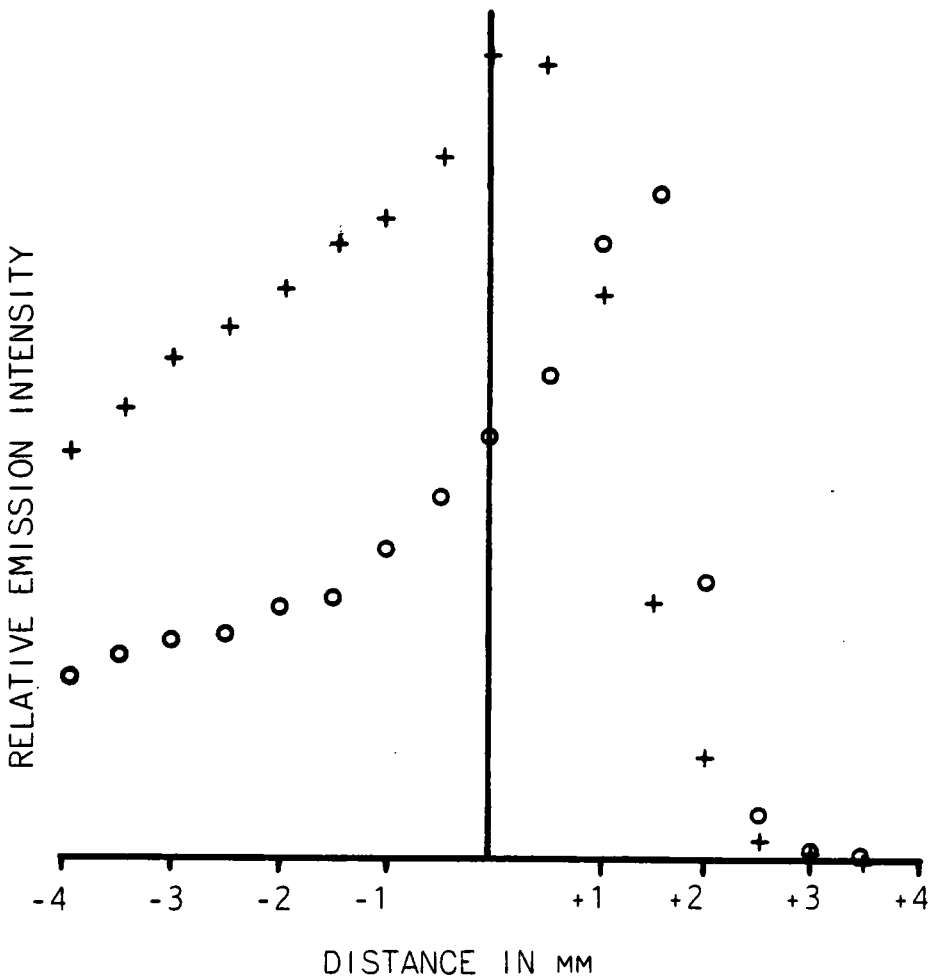

Figure 30: Vertical profile of emission from barium solution, with (+) and without (o) propane, at reduced (< 1 L/min) sleeve flow rates

proposed by Miller et al [43]; the current study provides supportive evidence for the theory.

CONCLUSIONS

Propane added to the nebulizing argon of the DCP effects a decrease in excitation temperature in the normal viewing zone and below it. This temperature reduction probably results from the consumption of energy required to atomize the propane. Propane also causes a reduction in the argon metastable population in all regions of the plasma, but does not appear to affect the electron number density. Carbon from atomization of propane appears to increase the atom population of metal analytes, due to reduction of metal oxides. This reduction may occurs in the NVZ, but the temperature and/or argon metastable decrease results in a net decrease in atom population in this zone. Above the NVZ, in the analyte residence region above the apex of the plasma, carbon can also reduce metal oxides and effect an enhancement in emission signals.

Results seem to indicate similarities in the effect of propane on the upper regions of the DCP when compared to the effect of propane on ICP-AFS. The data provides supportive evidence that excitation in some regions of the DCP is at least partly radiative in nature.

CHAPTER 4

DETERMINATION OF SULFUR IN COAL SLURRIES USING THE DIRECT CURRENT PLASMA

The sulfur content of coal is a parameter which is very important in industrial-scale combustion of coal, for reason of air pollution. Sulfur is a major element in most coals (ca 1% concentration), and combustion of the coal produces sulfur dioxide and to a lesser extent, sulfur trioxide. These oxides dissolve in water to produce acid rain, which is currently the subject of much controversy. Thus, the sulfur content of coal must be carefully monitored during industrial use.

Sulfur is considered a difficult element to determine by atomic spectrometric methods, in that the strongest sulfur emission and absorption lines exist primarily in the deep or "vacuum" ultraviolet region, below 190 nm. Thus, the spectrometer to be used for sulfur determinations must either be purged with an inert gas or evacuated, depending on the wavelength(s) to be used. Also, most monochromators have increasingly poor efficiency at shorter wavelengths; for example, the throughput of the echelle monochromator at 190 nm is about half that at 350 nm [58]. Finally, transmission optics for the deep UV region of the spectrum must be of unconventional and expensive materials, such as SupraSil or magnesium fluoride. As a result of these circumstances, methods for determination of sulfur by atomic

spectrometric techniques that are acceptable to the industrial community and/or ASTM do not exist.

Determination of sulfur by atomic spectrometric techniques is not a widely studied topic in the literature. Recently, Fry and McCurdy described a means by which sulfur could be determined in 1% coal slurries by ICP emission spectrometry [54]. However, as stated earlier, the ICP does not tolerate high levels of dissolved or suspended solids very well, and the ICP is rather expensive in its simultaneous multielement configuration. On the other hand, such samples are very well suited to the DCP with respect to sample introduction. Also, a simultaneous multielement DCP is about half the cost of an ICP of similar capabilities. Therefore, the DCP would appear to be a better analytical tool for determination of sulfur in such samples than would the ICP.

In this chapter, the utility of various sulfur emission lines and bands is examined. A simple, low-flow argon purge system designed to permit the use of shorter sulfur wavelengths has been designed and is discussed. Linear dynamic ranges, detection limits, and interferences for sulfur in the DCP are presented. Finally, the applicability of the technique for determination of sulfur in coal slurries is shown.

EXPERIMENTAL

The SpectraJet III plasma source was used as the excitation source, in conjunction with the Heath auxiliary monochromator as described in Chapter II. A laboratory-designed-and-constructed system

(described later in this chapter) was incorporated to purge the optical path between the plasma jet and the monochromator. All other experimental procedures were as described in Chapter 2.

RESULTS AND DISCUSSION

Sulfur Emission Lines.

Table 4 is a compilation of the strongest sulfur emission lines from 180-1000 nm that have been reported in the literature [59,60]. Unfortunately, the intensity data provided for these lines is characteristic of arc, spark, and/or glow discharge devices. All these devices have energetic and thermodynamic characteristics which are very different from analytical plasma sources. Thus, the relative intensities of these lines were expected to be somewhat different in the DCP. Careful examination of the entire emission spectrum from 180-960 nm in the DCP showed only four readily visible sulfur emission lines, at 180.7, 182.0, 182.6, and 393.3 nm.

There are two suspected reasons for this lack of useable lines. First, many sulfur lines are inherently weak, and the DCP spectrum is rich in argon emission lines and band spectra. This background can obscure the finer features of a spectrum. Many sulfur lines which should have been seen may not have been visible for this reason. Also, two of the four lines which could be seen result from a transition from the $3p^4(2,1,0)$ state [61]. It is suggested that this state is overpopulated relative to other states of sulfur in the DCP; thus, the other, underpopulated states in the DCP cannot produce emission of

Table 4: Prominent emission lines (nm) for sulfur in the UV-visible region

180.7	469.4	560.6	641.4
182.0	469.5	564.0	674.9
182.6	471.6	564.7	675.7
190.0	481.6	566.0	757.9
191.5	492.4	581.9	763.0
386.7	492.5	605.3	768.6
390.2	499.3	628.6	769.7
393.3	542.9	628.7	792.4
412.1	543.3	630.6	793.0
414.2	545.4	631.3	793.2
414.5	547.4	638.5	796.7
415.3	551.0	639.7	
416.2	556.5	639.8	

sufficient intensity to be analytically useful.

The 393.3 nm line was the first line tried for analysis, since it lies in the normal UV region of the spectrum and can be accessed using the echelle grating supplied with the instrument. Sodium sulfate was used as the standard, for when ammonium sulfate was tried, no signal for this line seen. It was found that the 393.3 nm line is very strongly affected by the sample matrix. At least 1000 ppm of Na had to be added to sulfur solutions for this line to be visible. Moreover, this line is within 0.05 nm of a very strong calcium ion emission line. An experiment to quantitate the spectral interference effect of calcium on sulfur showed a background equivalent concentration of over 100 ppm S for 1 ppm Ca; in other words, a 1 ppm Ca solution gave the same emission signal as a 100 ppm S solution. Since calcium is present in significant quantities in coal, this line was deemed useless for the purpose of sulfur determination in coal.

The Purge System.

In order to use the sulfur lines between 180-184 nm, the monochromator and optical path must either be evacuated or purged with an inert gas. Evacuation of the optical path was deemed impractical, since the DCP is operated at atmospheric pressure. One would require either a high-capacity vacuum pump with the optical path open to the plasma or a transparent, highly refractory window in contact with the plasma in conjunction with a closed optical path. Instead, purging with argon was selected for this work. Although nitrogen might be useful for this purpose, it was decided to use argon to minimize

possible changes in the nature of the plasma.

Carr and Blades described a purge system for the DCP in which a quartz chimney was used to enclose the plasma jet and a side tube on the chimney was helium-purged to view the plasma (helium was used because of its high transparency at very short wavelengths) [62]. Although useful, this system consumed a great deal of purge gas (>10 L/min), and was rather complex to build and to set up. It was decided merely to use a purge tube in near contact with the plasma; the tube had to be small enough so that a small volume of argon exiting the tube to the plasma would be sufficient to sweep all the air from the plasma-tube interface (it was decided that argon would be used as the purge gas to minimize possible alterations of plasma characteristics by helium; Braun has shown that helium can affect the stability and emission characteristics of the direct current plasma [63]). The tube also had to be large enough to accomodate a lens for imaging of the plasma on the monochromator entrance slit at an effective focal ratio of f/6.7 or greater, in order that the full capability of the monochromator would be utilized. Since the ultimate purpose of the system was the rapid simultaneous elemental analysis of coal, it would be desirable to use the echelle and the auxiliary monochromator simultaneously. Given this circumstance, the purge tube could not be allowed to affect the plasma significantly, or the determinations of other elements would suffer.

The purge system devised is shown in Figure 31. Basically, it consists of two aluminum tubes which are connected at the housing around the plasma jet. A threaded lens cell permits focusing of the

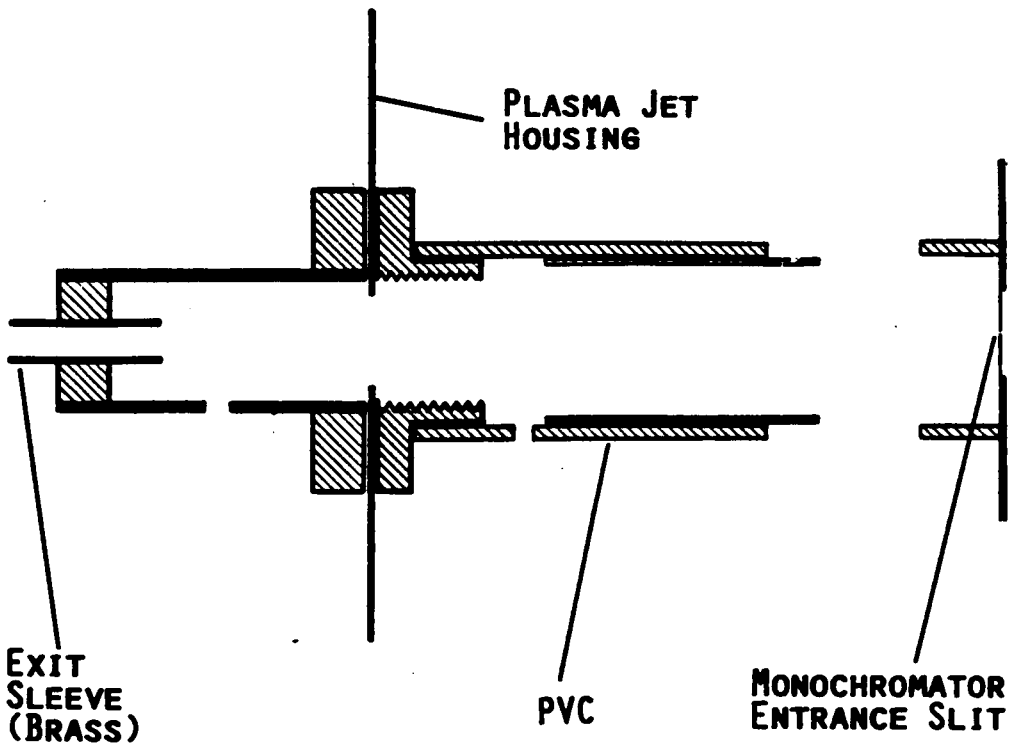

Figure 31: Purge system for the Spectraspan III direct current plasma. SpectraJet is used in place on the instrument with this purge system

optical system. Sliding tubes permit the system to be opened readily for focusing and for examination of the image; the fit between tubes was purposely not made airtight, to permit the incoming argon to sweep out the air. The tube in near contact with the plasma (the purge tube) is brass of 3/8" inside diameter. Argon is directed into each of the two aluminum tubes, and the argon passing out of the purge tube cools the brass sufficiently so as to avoid melting. A total argon flow of 2-3 L/min was required for the purge system, and another 2.5 L/min was required for the monochromator (the latter was purged through a fitting provided for this purpose).

A later version of this purge system was constructed when it was decided to demount the plasma jet from the instrument. This revised device (shown in Figure 32) uses two lenses that are independently focused, with slots milled on the outer edges of the lens cells to permit passage of the purge gas. The purge gas inlet is a fitting on the side of the PVC tube. This purge system was supported on a magnetic mount on an optical table. No significant difference in operation of the two purge systems was found.

When the purge gas was turned on, the plasma generally exhibited instability, flickering back and forth rather rapidly, until the purge tube was moved to within about 5 mm of the plasma, at which time the fluctuations disappeared and the plasma remained quite stable. If the plasma was not well centered in the purge tube, the plasma was distorted to one side and flickered excessively. It is thought that at large purge tube-plasma distances the argon flow from the purge tube is turbulent and disturbs the plasma. When the purge tube is brought in

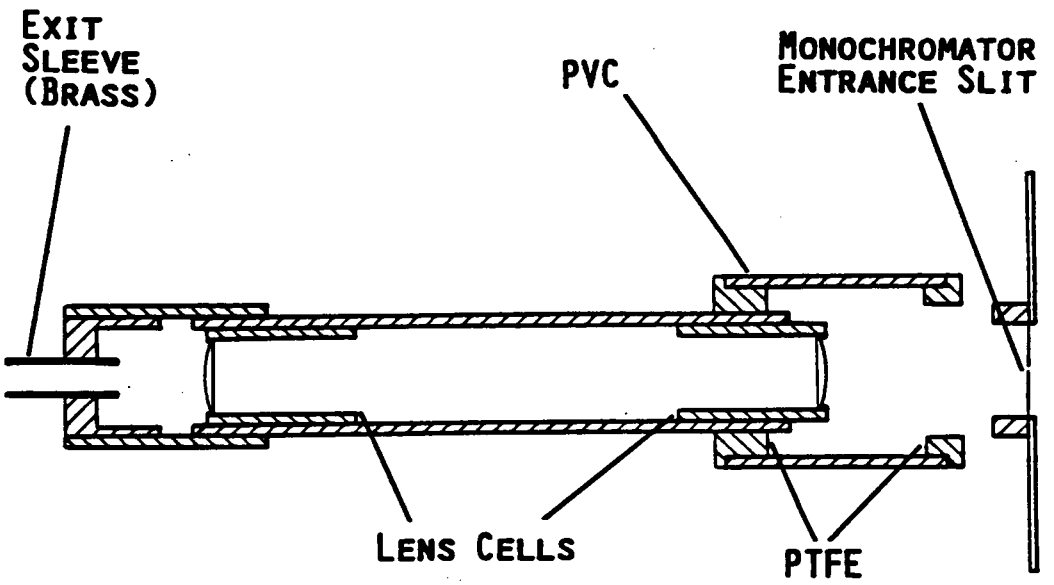

Figure 32: Purge system for the Spectraspan III direct current plasma. SpectraJet is demounted onto a separate optical bench with this purge system

immediate proximity to the plasma, the more laminar flow from the purge tube tends to stabilize the plasma in much the same way that the nebulizer flow has been found to stabilize the DCP [50]. The plasma did move slightly away from the purge tube, but this was not found to affect the analytical utility of the plasma. The instability of the plasma upon lateral movement of the purge tube precluded the obtaining of emission profiles for sulfur. However, best analytical results seemed to be obtained by using a viewing position very slightly to one side of the normal analytical zone.

Working Curves and Detection Limits.

All three of the vacuum UV lines were found to be intense enough for analytical use. A log-log working curve was prepared using ammonium sulfate standards (Figure 33). This curve shows linearity of signal over three orders of magnitude for the 182.0 nm line; for the other two lines, linearity was obtained up to 1000 mg/L. The detection limits were found to be 3 mg/L at 182.0 nm, 32 mg/L at 182.6 nm, and 7 mg/L at 180.7 nm. For comparison, the best wavelength for another nonmetal, phosphorus, by DCP (214 nm) provides a detection limit of about 0.3 ppm (k=3) with the much more efficient echelle grating [34]. Considering that the echelle grating could not be used for vacuum UV work (since it is not calibrated in this region and is not easily purged) the results obtained for sulfur were thought to be satisfactory. The coal in typical slurries is 0.5-2% sulfur, so that a 1% coal slurry is equivalent to 50-200 ppm S. This means that the lines at 180.7 nm and 182.0 nm would be more useful for coal analysis

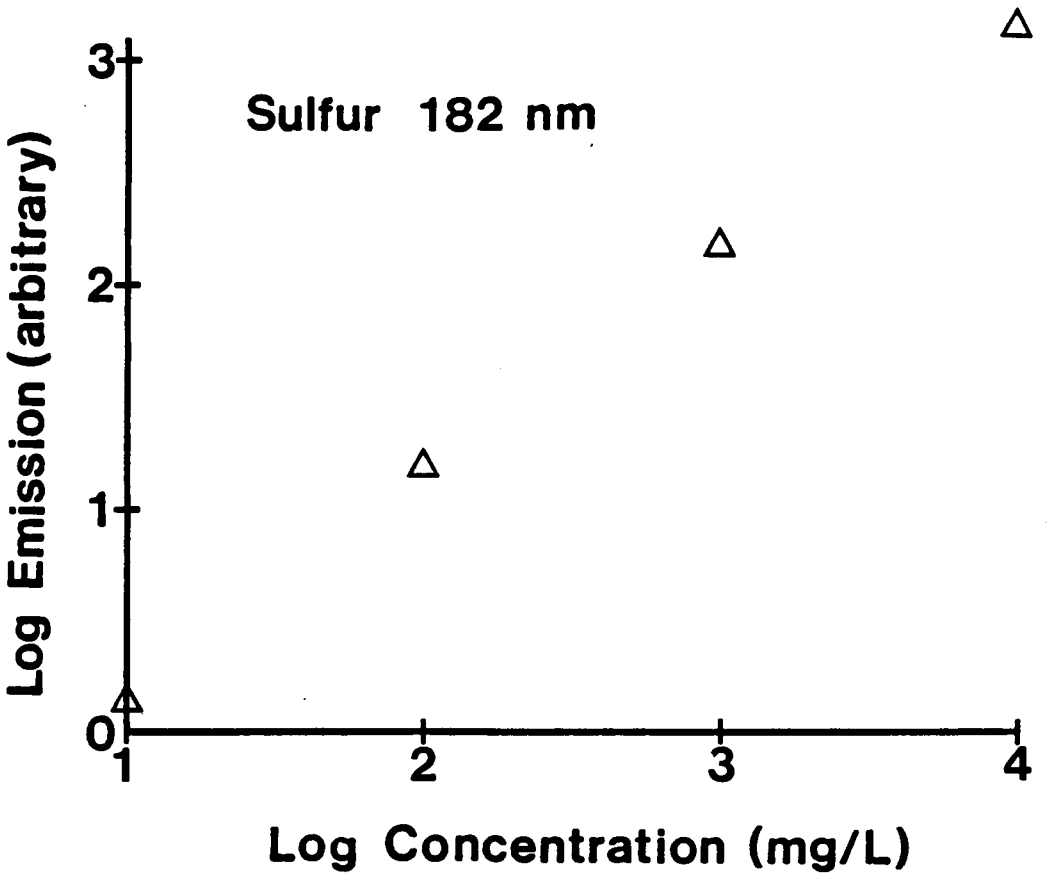

Figure 33: Plot of log of concentration of sulfur (in mg/L, as ammonium sulfate) versus log emission intensity at 182.0 nm

than the line at 182.6 nm.

Spectral and Chemical Interferences.

Potential spectral interferences with sulfur in the DCP include calcium, sodium, and boron [59,60]. It was expected that chemical interferences with sulfur would be negligible, since sulfur compounds are non-refractory. However, easily ionized element (EIE) interference is a potential problem for many emission lines in the DCP [64-66]. EIE interference was therefore investigated, using potassium added to the analyte. The results of this study are shown in Table 5. Surprisingly, no significant EIE interference was seen at any wavelength, and calcium and sodium showed no appreciable spectral interference. Boron was problematic in that 100 ppm of boron caused a 70% increase in the emission signal from a 1000 ppm sulfur solution. Although this is a significant interference, it is of little consequence in this work, since two other, more sensitive sulfur emission lines are available.

Effect of Different Chemical Forms of Sulfur.

Sulfur in coal exists in various forms, which are loosely categorized as pyritic or inorganic sulfur (ferrous sulfides) and organic sulfur (carbon-bound in the coal matrix itself). Thus, the effect of different forms of sulfur on emission is of some importance. The emission of sulfur at 182 nm was determined for four 1000 mg/L solutions of sulfur, using ammonium sulfate, ferrous ammonium sulfate, sulfamic acid, and thiourea. In the first three compounds named,

Table 5: Emission for 1000 mg/L sulfur solution with potential spectral/easily ionized element interferents added. Emission with no interference is arbitrarily equated to 100 units

	Wavelength, nm		
	180.7	182.0	182.6
No Interference	100	100	100
K, 500 mg/L	97.3	97.5	97.2
Na, 500 mg/L	99.9	97.3	99.1
Ca, 100 mg/L	100.0	101.8	99.5
B, 100 mg/L	102.2	100.0	169.2

sulfur is in an inorganic form; in thiourea, sulfur is in an organic form. The results are shown in Table 6. There was no statistically significant effect of the form of sulfur on emission, so that any of these compounds would suffice for standard solutions based on emission intensity alone. However, thiourea is an unsatisfactory primary standard, as aqueous solutions are subject to bacterial attack. Ferrous ammonium sulfate is satisfactory of itself, but would not be satisfactory for multielement standard solutions, as iron is a major element in most coals. For remaining work, ammonium sulfate was chosen as the standard for sulfur solutions, as it is less expensive than sulfamic acid; however, either of these named would be satisfactory as a standard.

Determination of Sulfur in Coal Slurries.

Slurries of several coals (Buller, Cedar Grove, Elkhorn #3) of mean particle size <10 um were prepared as described in Chapter II. The emission of sulfur from these slurries was compared to that of standard solutions of ammonium sulfate. Table 7 shows the results of this study. Recovery of the emission signal was rather poor, on the order of 50-60% in most cases, but seemed to be independent of the type of coal and of the slurry concentration. The recovery at 182.6 nm is somewhat higher than that at 180.7 nm and 182.0 nm; it is suggested that boron interference is significant for these coals. These results show recoveries similar to that seen for other slurry-type materials [67,68].

Another coal was obtained (R-coal) and ground to a mean particle

Table 6: Emission at 182.0 nm for 1000 mg/L sulfur solution using various standards

Standard	Emission
Ammonium sulfate	100
Thiourea	101.6
Ferrous ammonium sulfate	97.8
Sulfamic acid	98.7

Table 7: Sulfur Content of Coals as Determined by LECO SC-132 Infrared Sulfur Determinator and Slurry Injection in the Direct Current Plasma. Value in parenthesis is the error of the determination.

Coal	% sulfur with SC-132	% sulfur by Slurry Injection		
		180.7 nm	182.0 nm	182.6 nm
Cedar Grove	0.79 (0.01)	0.44 (0.02)	0.47 (0.03)	0.53 (0.03)
Elkhorn #3	0.82 (0.01)	0.42 (0.03)	0.45 (0.03)	0.55 (0.04)
Buller	1.63 (0.01)	0.94 (0.06)	1.08 (0.05)	1.14 (0.04)

diameter of 18 um. The recovery of this coal was even poorer, about 25% when compared to aqueous ammonium sulfate. It was therefore concluded that the grinding time was probably a factor in the poor recovery obtained. To test this idea, the recovery was determined for 1% slurries of R-coal, in which the coal had been ground for lengths of time varying from 10 minutes to 3 hours.

Figure 34 shows that grinding time and hence particle size is indeed a major factor in recovery. Furthermore, coal used must be ground for approximately 3 hr in order to obtain 100% recovery. However, an empirical correction factor for particle size could be used to avoid the time-consuming grinding.

It is worth noting that, if the 3 hour grinding time is assumed to give 100% recovery, nearly the same recovery is seen for aluminum and silicon as is seen for sulfur (see Figure 38, Chapter 5). These data show that the dependence of recovery on particle size should be the nearly the same for different elements. It can be inferred that physical factors which improve recovery of the slurry signal for sulfur should also be useful for improving recovery of other elements.

CONCLUSIONS

Sulfur in coal can be determined using the DCP, but the lines accessible to the echelle grating are not useful for coal analysis. A low-cost, medium resolution auxiliary monochromator coupled with a simple purge system provides sufficient sensitivity, precision, and linear dynamic range for the sulfur lines between 180-183 nm to be used

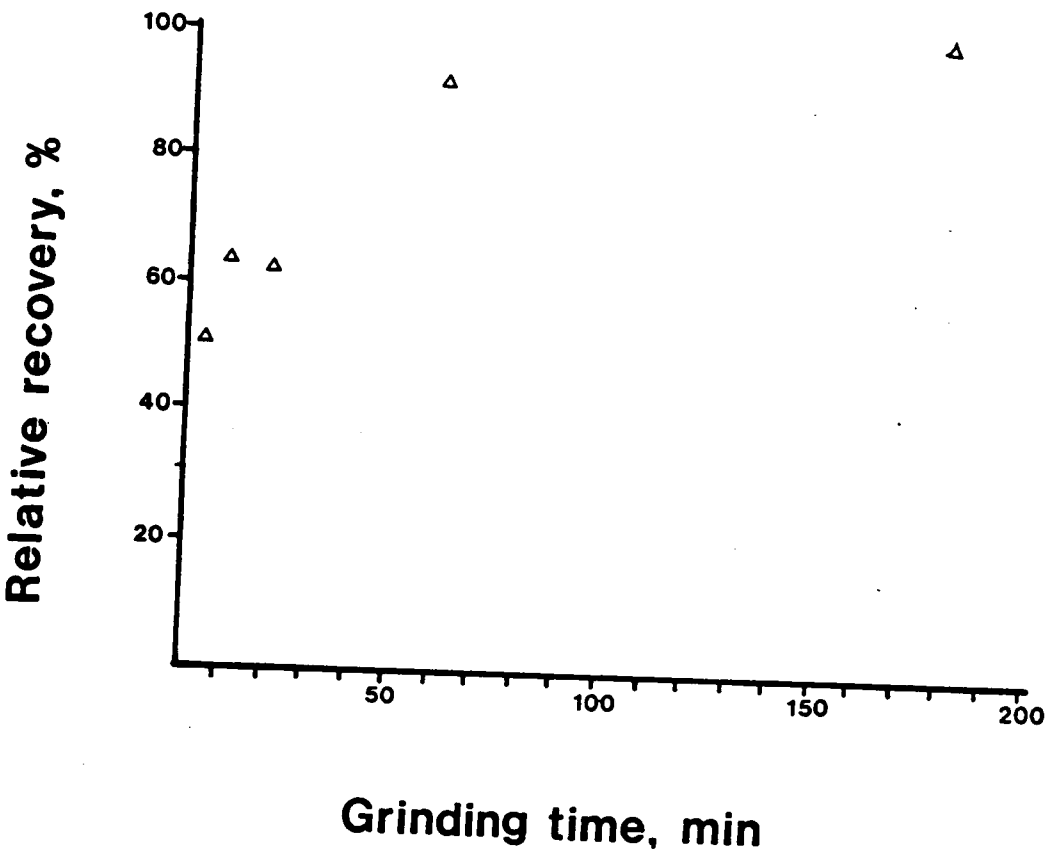

Figure 34: Percentage recovery of sulfur signal from R-coal versus grinding time in minutes

for sulfur determinations in coal slurries. Chemical and spectral interferences are negligible, with the exception of spectral interference from boron at 182.6 nm. Recovery of the sulfur signal from coal relative to that from aqueous solutions is less than unity for the coals tested, and is dependent on grinding time of the coal, with recovery decreasing as the mean particle size increases. An empirical correction factor can be used to compensate for large particle size, in order to avoid the time-consuming grinding of the coal to particle sizes that would effect 100% recovery.

CHAPTER 5

DETERMINATION OF IRON, SILICON, AND ALUMINUM IN COAL BY DIRECT CURRENT PLASMA EMISSION SPECTROMETRY

When coal is burned, the carbon, nitrogen, and hydrogen are converted to their gaseous oxides. The remainder of the coal is the ash, which consists primarily of oxide compounds of aluminum and silicon, and oxides and sulfides of iron. The elemental composition of the ash in coal is often useful in the total description of the quality of the coal. Knowledge of ash composition is also useful in predicting the behavior of the coal ash in combustion chambers. In coal, the aluminum and silicon oxides exist essentialy as a fireclay, and are highly refractory. A high iron concentration causes the ash to be less refractory, resulting in a "slagging" ash [2]. Such an ash is vitreous rather than powdery in nature, and a coal that has a high iron content should be utilized in a different sort of combustion chamber than one which has a low iron content. Of course, coal which has a low total ash content is more desirable than one which has a high ash content.

When coal is burned, a portion of the ash remains in the combustion vessel; the remainder is "fly ash". Fly ash consists of extremely fine particles of ash that are typically a tiny fraction of the size of the coal particle that produced them. Such small particles readily remain airborne, and are easily inhaled. Thus, dispersion of

fly ash is a type of pollution with serious consequences.

Clearly, it is important that the ash content of coal-water slurries be kept as low as practicable during combustion. It is consequently important that the metals content of coal be monitored in an on-line fashion during the combustion, to constantly determine the nature of and to provide a measure of the amount of the resulting ash.

Procedures for determination of metals in coal ash are described in ASTM publications [5]. The analysis requires conversion of a weighed quantity of the coal to ash at 750°C in the presence of air, which requires several hours. This step alone means that ASTM procedures will be far too time consuming for on-line analysis.

Several workers have examined the determination of metals in coal by direct slurry introduction. Fry et. al. found that unit recovery of several trace metals could be obtained by grinding the coal for 20 min in a McCrone Micronizing mill [36]. In similar work, Anigbogu and Coleman determined aluminum and several other elements in coal fly ash by grinding for 20 minutes in the presence of dilute nitric acid [35]. However, the analysis of coal slurries by DCP emission spectrometry with a view toward characterization of the ash has not been reported.

It is suggested in this work that the ash content of coal can be monitored by DCP emission spectrometry, by determining the concentrations of metals which cause the ash. The total metals content will give a measure of the ash in the coal. In this work, the determination of silicon, aluminum, and iron as the major elements in ash will be examined. Criteria for selection of the wavelengths will be noted, with a view toward simultaneous multielement analysis.

Problems with the analyses will be noted.

EXPERIMENTAL

Instrumentation

The Spectraspan IIIB DCP spectrometer was used for these studies as described in Chapter 2. The Babington nebulizer was used for all work except as noted otherwise.

RESULTS AND DISCUSSION

Selection of Emission Lines

Iron, silicon, and aluminum are all commonly determined by DCP emission spectrometry, so that a number of wavelengths for these elements have already been characterized for analytical use [34]. For multielement determination of metals in coal, it is not sufficient to arbitrarily select lines for analytical use. Several factors must be considered in selection of the line to be used for a particular element:

1. Linear dynamic ranges should be appropriate for the analysis of coal samples. The levels of iron, silicon, and aluminum in typical coals are listed in Table 8. Assuming that a 1% concentration of coal is to be used for analysis, the table shows the resulting elemental concentration ranges in the coal for various ash levels. The linear dynamic range for each element should extend

Table 8: Typical Levels of Silicon, Aluminum, and Iron in Coal (adapted from Reference [5])

Element	Reported as	typical % of ash	Elemental concentration range for 1% coal slurry that is: 2% ash	8% ash	15% ash
Si	SiO_2	10-60	9.3-56	37-224	70-420
Al	Al_2O_3	5-30	5.3-32	21-127	40-238
Fe	Fe_2O_3	5-50	7-70	28-280	53-525

to or beyond the limits of the elemental concentration ranges for the method to be fully versatile.

2. Chemical and spectral interferences should be avoided or minimized, especially interferences with elements that are common to coal.
3. Mechanical restrictions for multielement cassettes should be avoided. The type of multielement cassette used in the Spectrametrics DCP is illustrated in Figure 35. Holes 4 mm in diameter are drilled in the front of the cassette, and slits are positioned in these holes for the element to be determined. Two mirrors contained in the body of the cassette reflect the light from the slit to the appropriate PMT. The distance between the focal points of elemental lines must not be so small that these holes will overlap. It should be noted that all spectral interferences will result in a mechanical restriction, however, mechanical restrictions can arise from lines which are close together by virtue of closeness of two orders of radiation, and need not constitute a spectral interference. Fortunately, all the potential mechanical restrictions are cataloged in the manufacturer's literature [34].
4. All lines used should ideally result from a single state (atom or ion). The region of maximum emission in the DCP varies for different states; ionic emission maximizes about 1 mm above the maximum for atomic emission [49].

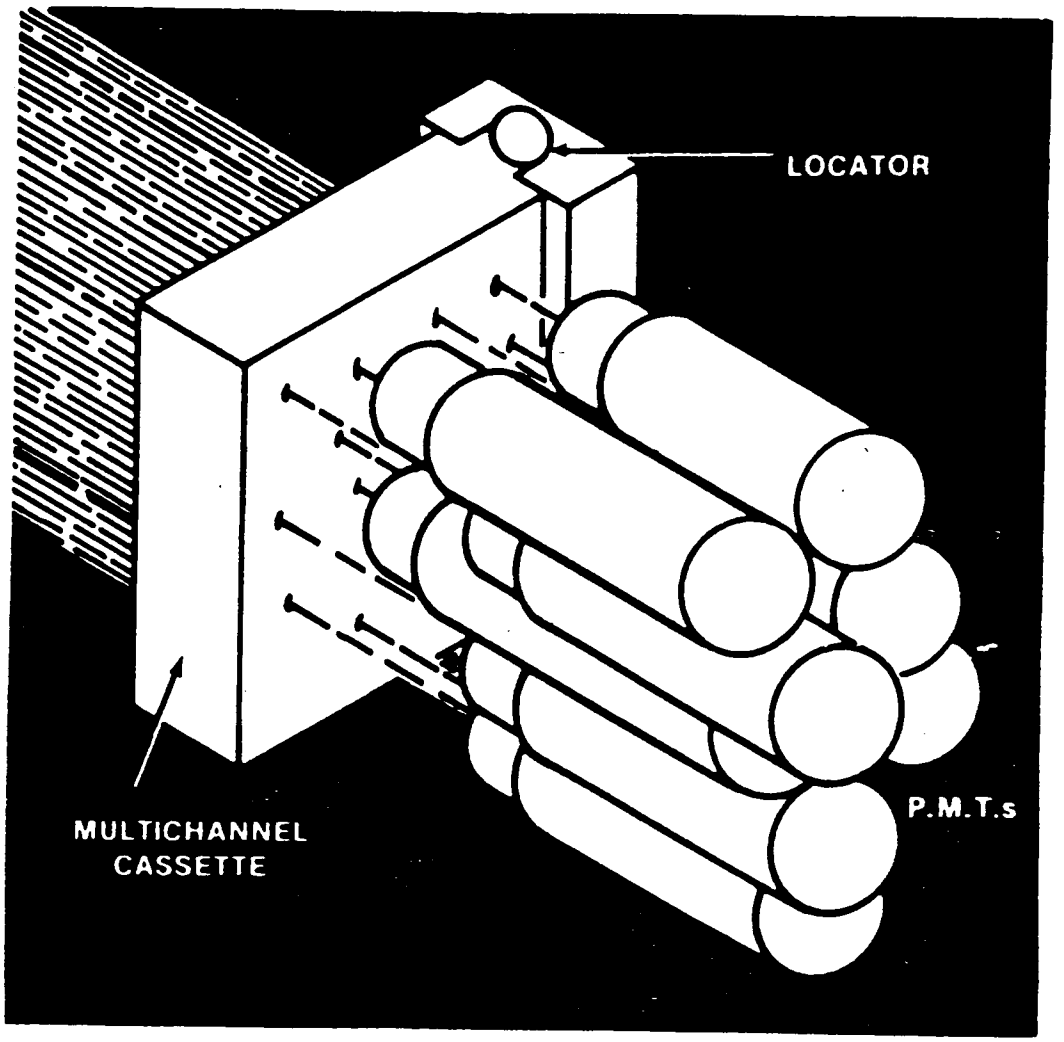

Figure 35: Multielement cassette for the Spectraspan III

However, only one physical position in the plasma can be imaged on the entrance slit and used for analysis. The use of an ion line in the observational position of maximum emission for an atom line would result in reduced sensitivity.

5. The lines should have the best possible detection limits concurrent with the first four factors.

Emission lines, and their established characteristics for the three elements selected are listed in Table 9. It can be seen that linear dynamic ranges for most of these lines extend up to 1000 mg/L and extend below 1 mg/L. All of these lines except the 396 nm line for aluminum have LDR that are sufficient for analysis of 1% slurries of typical coals; the 396 nm line would be adequate only if the ash content of the coal was known to be very low.

The DCP manufacturer's data lists those lines that are best employed for organic analysis. Since carbon is the major element in coal, it would be prudent to select lines that are recommended for organic analysis, to minimize potential matrix effects. Table 9 notes those lines which are considered most suitable for analysis of organic matrices. It is also apparent from the table that chemical interference from other elements is negligible for all the lines listed.

Mechanical restrictions are rarely a major difficulty, even with complex matrices. For most elements, one can select from alternative lines. In some cases, the same wavelength appears in two consecutive orders of radiation, and the alternative order can be used to eliminate

Table 9: Emission Lines for Aluminum, Iron, and Silicon in the DCP (from [34])

Wavelength	Atom/ Ion	LOD, mg/L	LDR, mg/L	Interferences BEC for 1000 mg/L interferent	Miscellaneous
Aluminum					
236.705	Atom	1	10-1000	Fe, 12 mg/L	No mechanical restrictions
308.215	Atom	0.08	0.8-1000	Ca, 0.04 mg/L	Best for organics
396.152	Atom	0.002	0.02-100	Ca, 1.1 mg/L Fe, 0.05 mg/L	Mechanical restriction Mn, 403.076 Bkg. too high for organics
Iron					
238.204	Ion	0.02	0.2-1000	Ca, 0.04 mg/L	
259.940	Ion	0.007	0.07-1000	Ca, 0.03 mg/L Ti, 0.05 mg/L	Best for organics
371.994	Atom	0.005	0.05-1000	Ca, 0.08 mg/L	
Silicon					
251.611	Atom	0.01	0.1-1000	Al, 0.1 mg/L Fe, 0.08 mg/L Mg, 0.06 mg/L	Best for organics Mechanical restriction Mn, 257.610
288.158	Atom	0.01	0.1-1000	Al, 0.1 mg/L Ca, 0.03 mg/L Fe, 0.08 mg/L Mg, 0.1 mg/L	

a mechanical restriction. In this work, the 251.6 nm line for silicon appears in both orders 89 and 90. The two lines are equal in analytical utility, but the line at order 89 has a mechanical restriction with manganese, as noted in Table 9; the line at order 90 has no such restriction, and that line was chosen for analysis. Thus, there are no significant mechanical restrictions for multielement analysis of coal by DCP emission.

The only lines that has been characterized for silicon analysis result from atomic excitation, and the sensitivity of these lines is only moderate. Thus, atomic lines for other elements would ordinarily be preferred over ionic lines. However, the use of ionic lines is not to be totally ignored. Figure 36 shows a ion line emission profile and an atom line emission profile, normalized to the same maximum emission. In the position of the atomic emission maximum, the ionic emission is about 65% of its own maximum. Thus, a corresponding decrease in sensitivity can be expected when using an ion line in the atom maximum position. Although this decrease may appear to cause a significant loss in sensitivity, the reduced sensitivity should not be a problem for iron and aluminum analysis. The ion lines for these elements have more than adequate sensitivity even when the signal magnitude is reduced by utilization of the atom position.

As regards selection of the lines to be used, the silicon line at 251.6 nm was selected over the one at 288 nm, because the former is recommended for organic analysis. The iron ion line at 259.9 nm was selected over the atom line at 371.99 nm, because the former is recommended for organic matrices (oil analysis), and has comparable

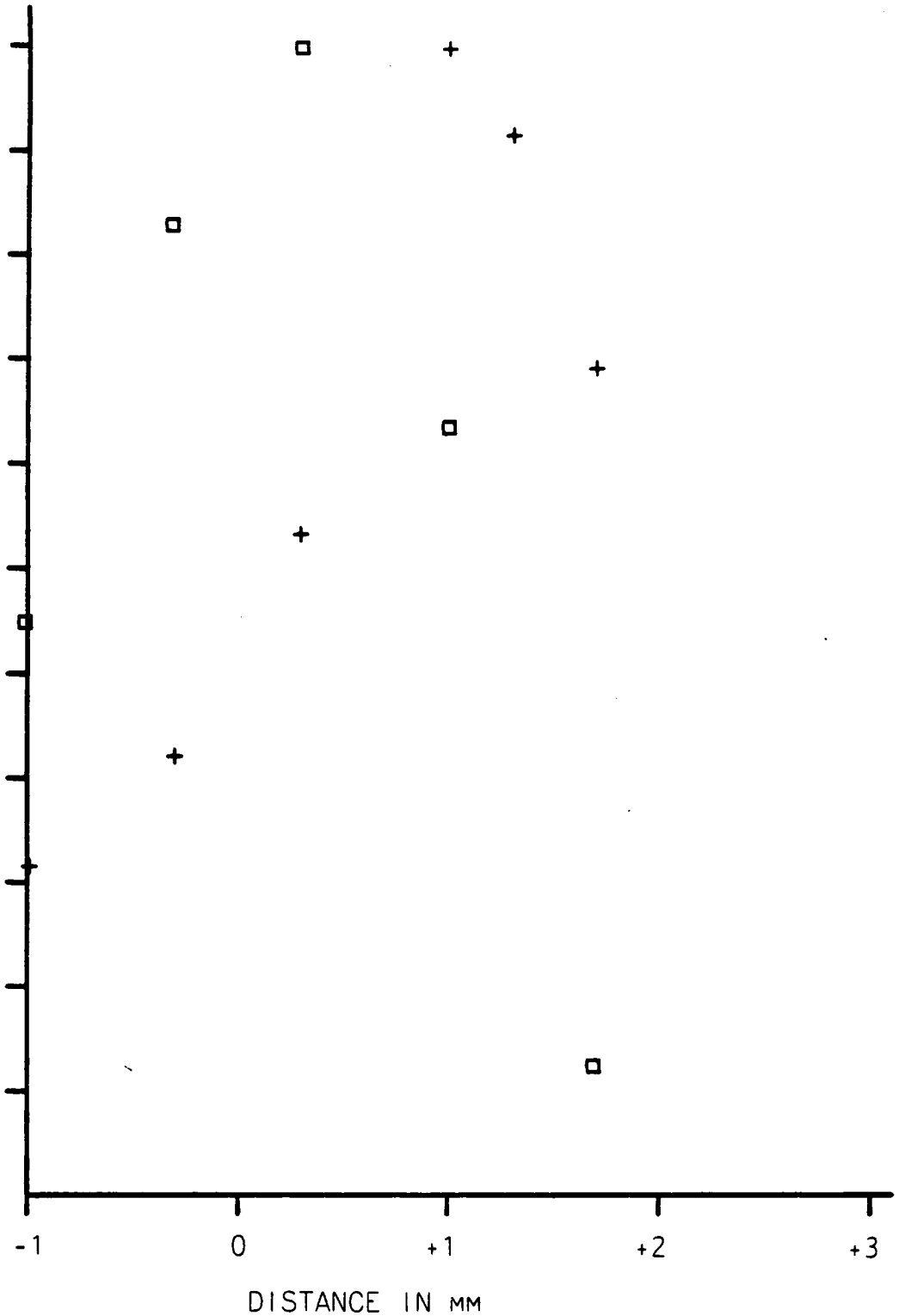

Figure 36: Vertical profile of normalized emission from Ca I (+) and Ca II (□), showing relative intensities in the normal viewing zone. From Reference [49]

detection limits. For aluminum, the limits of detection for the 308 nm line are significantly better than those for the 236.7 nm line, and the former is recommended for organic matrices.

Detection Limits and Linear Dynamic Ranges

The method of determination of the detection limits and linear dynamic ranges that have been reported for the lines selected are as follows:

"1. Detection Limit (DL): This is the analyte concentration which corresponds to a signal equal to three times the standard deviation of the background noise beneath the analyte line on a set of nine consecutive mearsurements of the background intensity. Each measurement is taken over a 10 sec integration period on the analyte line.

2. Linear Dynamic Range (LDR): The concentration range from 10 X DL to the highest concentration found which is within +- 10% of perfect linearity."[34]

The criterion for detection limits listed above is slightly different from that suggested by Long and Winefordner [38]; the latter suggest a minimum of twenty background readings to obtain an accurate value of the standard deviation of the blank. In fact, the detection limits obtained from the Long/Winefordner criterion should be about 1.2 times larger than for the Spectrametrics criteria, based on the difference in t-values between nine and twenty background readings

[69]. More significant is the fact that the Babington nebulizer was used for all the work in this chapter, and the detection limits and linear dynamic ranges reported in Table 9 are characteristic of the stock instrumental system (using the ceramic nebulizer, with optimal gas and liquid flow rates that are very different from those for the Babington nebulizer). A comparison of the Babington nebulizer and the ceramic nebulizer as used in the DCP has not been reported, however, the Babington nebulizer has been found to be somewhat less efficient than other pneumatic nebulizers [70]. It was therefore decided that determination of detection limits and linear dynamic ranges with the system as it was to be used for coal analysis would be prudent.

Detection limits and linear dynamic ranges with the Babington nebulizer were determined by aspiration of a blank and of several standard solutions of the elements. Concentrations ranging from 3 to 1000 mg/L of the elements were used. For comparison, the detection limits for the system with the ceramic nebulizer were also determined. Limits of detection are summarized in Table 10, and logarithmic working curves are shown in Figure 37.

There appears to be only a slight difference in performance of the Babington nebulizer when compared to the ceramic nebulizer, indicating that the two are about equal in their ability to produce analyticalaly useful aerosol. However, there is a fairly large difference of up to two orders of magnitude between detection limits determined and those reported in Table 9. This data is noted without any attempt to explain or justify the results. Fortunately, even the lower detection limits determined do not limit the utility of the DCP for analysis of

Table 10: Detection Limits (k=3) for Silicon, Aluminum, and Iron by DCP-OES, mg/L

		Determined (nebulizer)	
	From [34]	Ceramic	Babington
Silicon	0.01	0.4	0.3
Aluminum	0.08	0.5	0.6
Iron	0.005	0.4	0.3

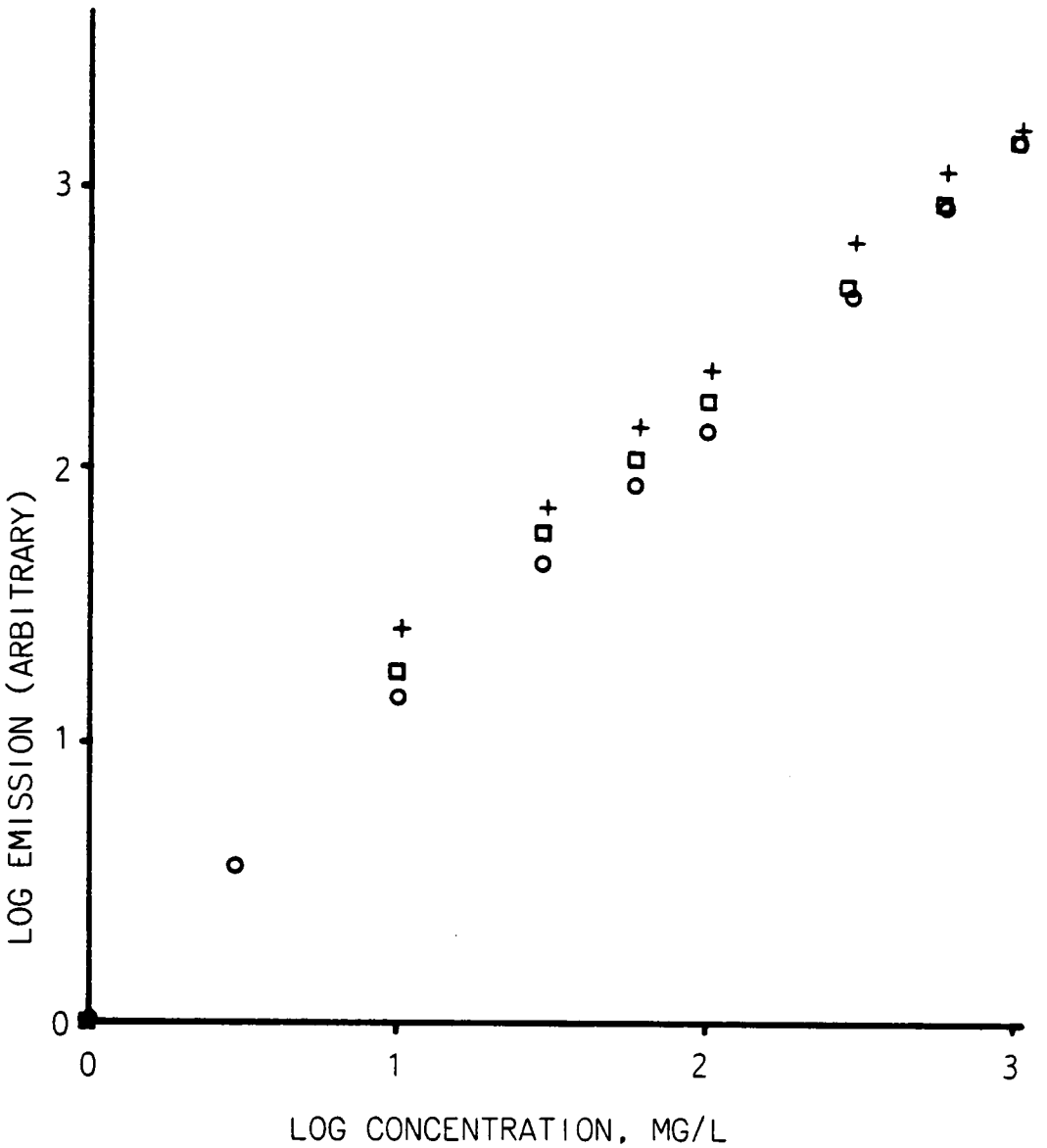

Figure 37: Plot of log concentration in mg/L versus log emission signal for iron (o), silicon (+), and aluminum (□)

aluminum, silicon, and iron in coal.

Metals Analysis

For comparison purposes, it was necessary to accurately determine the iron, aluminum, and silicon content of the coals to be used in this study. The four coals used in the studies of Chapter 4 (Buller, Elkhorn #3, Cedar Grove, and R-coal) were analyzed by the following procedure, which is derived from the procedure described in Reference [5]:

1. A weighed sample of the coal was ashed in the presence of air in a muffle furnace for 4 hrs. at 750°C.
2. An accurately weighed sample of the ash (0.1 g) was fused with 1 g of lithium tetraborate in a graphite crucible at 1000°C for 20 minutes. A blank consisting of lithium tetraborate was also prepared by fusion.
3. The melt was poured directly into 100 mL of 5% HCl, which was heated to boiling and stirred for 30 min. The resulting solution was diluted to 250 mL in a volumetric flask.
4. The concentrations of the metals were determined by DCP emission spectrometry, using the same lines as were selected for coal slurry analysis for verisimilitude.

Analysis of Coal Slurries

Slurries of the four coals listed above, prepared in 1% concentrations as described in Chapter 2, were analyzed by comparison

of the slurry emission signals to those of aqueous solution standards. The observational position was optimized for silicon, and this same position was used for all the analyses. The results are summarized in Table 11. It is immediately obvious that recovery of signal is not unity for any of the three elements. More important, recovery seems to vary more from coal to coal than it does from element to element. Cedar Grove and Elkhorn coals both show recoveries on the order of 50% for all three elements; Buller coal is slightly finer in particle size, and shows recovery that is correspondingly higher, from 60-85%; Buller coal also showed a higher recovery than the other coals in sulfur analysis. R-coal has a mean particle size of 18 um and shows a significantly lower recovery for all three elements than do the other coals.

These results parallel the results obtained from these coals for sulfur analysis (see Chapter 4), which suggests that a particle size interference is again the operative mechanism. The results also suggest a slight chemical interference with aluminum; the recovery for aluminum is lower than that of other elements, but not greatly so (Anigbogu and Coleman reported recovery of aluminum of 40-50%, as compared to 80-120% for other elements [39]). It is suggested that this reduced recovery may be due to the formation of aluminum oxides during the vaporization process.

To confirm the particle size effect, plots of emission signal magnitude for aluminum and for silicon vs. grinding time were prepared (Figure 38). These data show curves that nearly coincide with a similar plot for sulfur recovery (Figure 34), if the recovery at 3

Table 11: Silicon, aluminum, and iron content of coals as determined by ASTM procedure and by slurry injection into the Direct Current Plasma. Value in parenthesis is the error of the determination.

Coal	ASTM	Slurry Injection
Silicon, percent in coal		
Cedar Grove	1.53 (0.01)	0.92 (0.01)
Elkhorn #3	2.11 (0.01)	1.24 (0.02)
Buller	0.062 (0.001)	0.053 (0.001)
R-coal	1.03 (0.02)	0.15 (0.01)
Aluminum, percent in coal		
Cedar Grove	1.84 (0.03)	0.99 (0.01)
Elkhorn #3	2.12 (0.02)	1.03 (0.01)
Buller	0.175 (0.003)	0.108 (0.002)
R-coal	1.25 (0.01)	0.041 (0.002)
Iron, percent in coal		
Cedar Grove	1.25 (0.01)	0.68 (0.03)
Elkhorn #3	1.98 (0.02)	1.07 (0.02)
Buller	0.392 (0.003)	0.332 (0.008)
R-coal	0.99 (0.02)	0.33 (0.05)

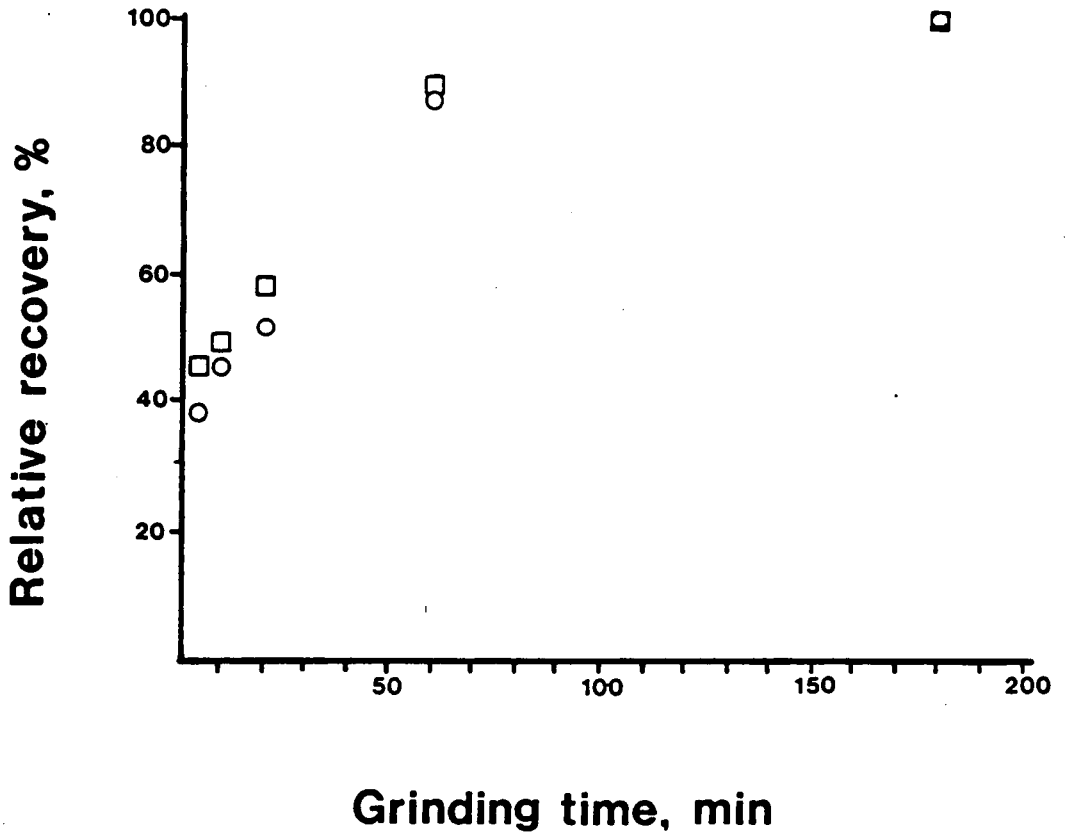

Figure 38: Relative percentage recovery of emission signal from aluminum (O) and silicon (□) versus grinding time. 180 minutes grinding time is equated to 100% recovery

hours grinding time is equated to unit recovery as was seen for sulfur. This coincidence indicates that the magnitude of dependence on particle size is independent of the element. It also indicates that the same empirical correction factor could be used to compensate for the particle size difference.

CONCLUSIONS

Iron, aluminum, and silicon can be determined in 1% coal slurries using direct current plasma emission spectrometry, by choosing the appropriate emission lines. The recovery of the slurry signal as compared to aqueous solutions is dependent on particle size of the slurry, in a fashion similar to that described in Chapter 4 for sulfur. Also, recovery of aluminum emission from slurries is significantly lower than that for iron, silicon, or sulfur. This reduced recovery may be due to formation of highly refractory aluminum oxides in the plasma.

CHAPTER 6

EFFECT OF POLY(ETHYLENE OXIDE) ON THE BEHAVIOR OF SLURRIES AND SOLUTIONS IN THE DIRECT CURRENT PLASMA

It has been shown in Chapters 4 and 5 that the recovery of DCP emission signals for coal slurries (signal from slurry/signal from equivalent aqueous solution) depends on the particle size of the coal. The particle size can be reduced and the recovery improved by grinding the slurry. This is in agreement with work performed by Fry and associates [31,36,71] and by Ebdon [72].

In the work by Fry and McCurdy, the amount of grinding that was required to obtain 100% signal recovery for solid samples in slurry form was determined. The droplet size distribution entering the plasma was determined and shown as an histogram. Particle size distribution histograms for solid samples (coal, cabbage) ground in a mill were also obtained. In order for particles to undergo desolvation and vaporization, they must fit within the droplets normally produced by the nebulizer, so the particles can be transported to the plasma. It was hypothesized by Fry that, for this condition to be satisfied, the mean droplet size from the nebulizer must exceed the mean particle size of the slurry; furthermore, the histogram for particle size should not exceed the histogram for droplet size at larger-than-mean droplet sizes. This concept is graphically represented in Figure 39. Part A

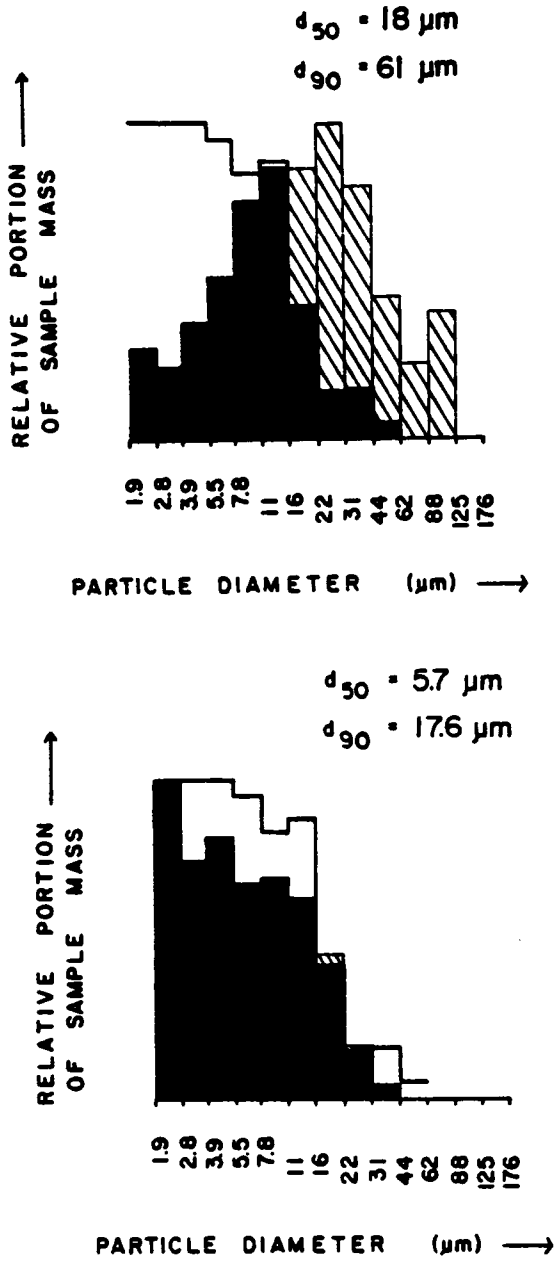

Figure 39: Size distributions for droplets (solid line) and particles (shaded region) produced by the DCP Babington nebulizer; (A) Cabbage leaves ground to d_o = 18 um; (B) Cabbage leaves ground to d_o = 5.7 um

shows the droplet size distribution of the nebulizer (solid line) and the particle size distribution of the sample (cabbage, shaded region). The darkened overlap of these regions indicates that sample which is aerodynamically transported into the plasma; in Part A, this corresponds to roughly 50% transport. In Part B of the figure, the particle size of the cabbage has been reduced so that almost all of the cabbage is transportable, and signal recovery was determined to be 94% for this case [71]. In effect, the particle size distribution should either match or fall within the droplet size distribution for total transportability of the solids. Fry also noted that the use of impact beads and torturous bends and baffles in the spray chamber caused particles to be preferentially removed from the analytically useful aerosol [73]. It was determined that solid samples must be ground for 20 minutes or longer in a McCrone Micronizing mill to meet the particle-size reduction criteria for this technique.

The work of Fry implies the possibility of improving transport of solids by attacking the problem from the opposite direction, that is, by changing the droplet-producing characteristics of the nebulizer. If the droplet size is increased, larger particles can be transported to the plasma, which would increase the recovery. The droplet size obtained from a pneumatic nebulizer can be described by the Nukijama-Tanasawa expression [74]:

$$do = \frac{585}{V}\left(\frac{\gamma}{\rho}\right)^{0.5} + 597\left[\frac{\eta}{(\gamma\rho)^{0.5}}\right]^{0.45} 1000\left[\frac{Q_L}{Q_G}\right]^{1.5}$$

d_o = mean droplet size (um)

V = gas velocity through orifice (m/s)

γ = surface tension of liquid (dyne/cm)

ρ = density of liquid (g/cm^3)

η = viscosity of liquid (poise)

Q_L = flow rate of liquid (cm^3/s)

Q_G = flow rate of gas (cm^3/s)

The Nukijama-Tanasawa expression has been shown to generally describe the dependence of droplet size on the physical parameters noted [75-77], although the size predicted by the equation may not correspond to the size obtained, depending on the type of nebulizer used. Browner et.al. have shown that the droplet size predicted with this equation is about twice the size actually obtained from a Meinhard nebulizer [75].

Not all of the parameters in the Nukijama-Tanasawa expression can be readily altered. Changing the gas velocity or flow rate would change the operational characteristics of the DCP, as the plasma is stabilized and thermally pinched by the nebulizer flow [50]. However, in Fry's work, a reduction in flow rate and velocity of the nebulizer gas could be realized without appreciably affecting the (inductively coupled) plasma, and did effect an increase in recovery.

Flow rate of the sample can be varied with the Babington nebulizer, but beyond a certain extent, the excess sample flow does not pass over the groove of the nebulizer orifice, but simply drains away without reaching the orifice. The density of aqueous solutions cannot readily be changed to any great extent. Although surface tension can be decreased easily by adding surfactants, no known reagent will

increase the surface tension of water sufficient to affect the drop size appreciably [78]. Thus, the only parameter that can readily be changed to increase droplet size from the DCP Babington nebulizer is the viscosity.

It is hypothesized here that the recovery of coal slurry signals relative to aqueous solutions can be improved by increasing the viscosity of the standards and the samples. In this chapter, the effect of a viscosity-increasing agent (poly(ethylene oxide) on solution and slurry signals is examined. The consequences of increased viscosity on analytical figures of merit is also discussed, and the effect of particle size in terms of transportation is examined.

EXPERIMENTAL

Reagents and instrumentation were as described in Chapter 2, with experimental procedures as described in Chapters 4 and 5.

RESULTS AND DISCUSSION

Characteristics of PEO solutions

PEO is a high molecular weight polymer of the formula $(-CH_2-CH_2-O-)_n$, where n is >2000. Lower molecular weight polymers of this formula are referred to as poly(ethylene glycol)s. For this work, the PEO used had an average molecular weight of 900,000. PEO has two effects that are of importance in droplet formation from aqueous solutions. First, it acts as a surface active agent, reducing the

surface tension; second, it increases the viscosity of the solution.

The mechanism by which droplets form in a pneumatic nebulizer involves the breakup of a low-velocity liquid stream by a high-velocity gas stream, usually moving at right angles to the liquid stream [27]. Surface tension (more properly, surface free energy) of the liquid is a measure of the amount of work required to form more surface [79], and the formation of droplets from a stream of liquid requires the formation of more surface area. The lower the surface tension, the more difficult it is to form this surface, and the larger will be the droplets that are formed, since large droplets will have a lower specific surface area than will an equal mass of small droplets.

Viscosity can be thought of as the force required to make a layer of unit area move with a unit velocity greater than that of another layer a unit distance away [80]. Formation of a droplet requires that the volume of the droplet be detached from the bulk of the liquid stream. The greater the viscosity, the more force required to detach the droplet, resulting in larger droplets. Thus, droplet size should vary directly both with viscosity and with surface tension.

Both terms appear in the Nukijama-Tanasawa expression, and Figures 40 and 41 quantitatively illustrate the effect of each term on droplet size. It is immediately obvious from these plots that a far larger change in viscosity than in surface tension is required to change the droplet size a given amount. Since PEO reduces the surface tension while increasing the viscosity, one might expect that the droplet size could not be increased by using PEO. However, surfactant activity is not a linear function of concentration, but reaches a plateau at the

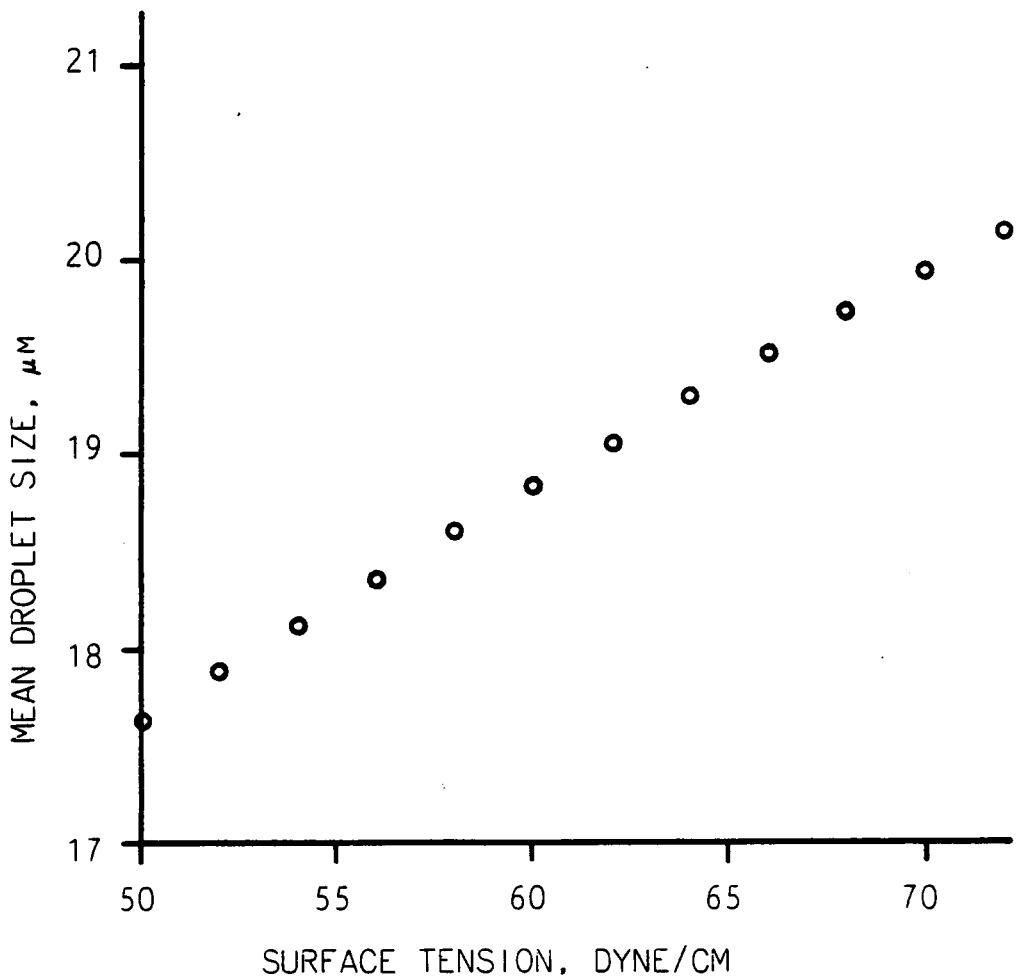

Figure 40: **Mean droplet size (calculated from the Nukijama-Tanasawa expression) as a function of surface tension at η = 10 centipoises**

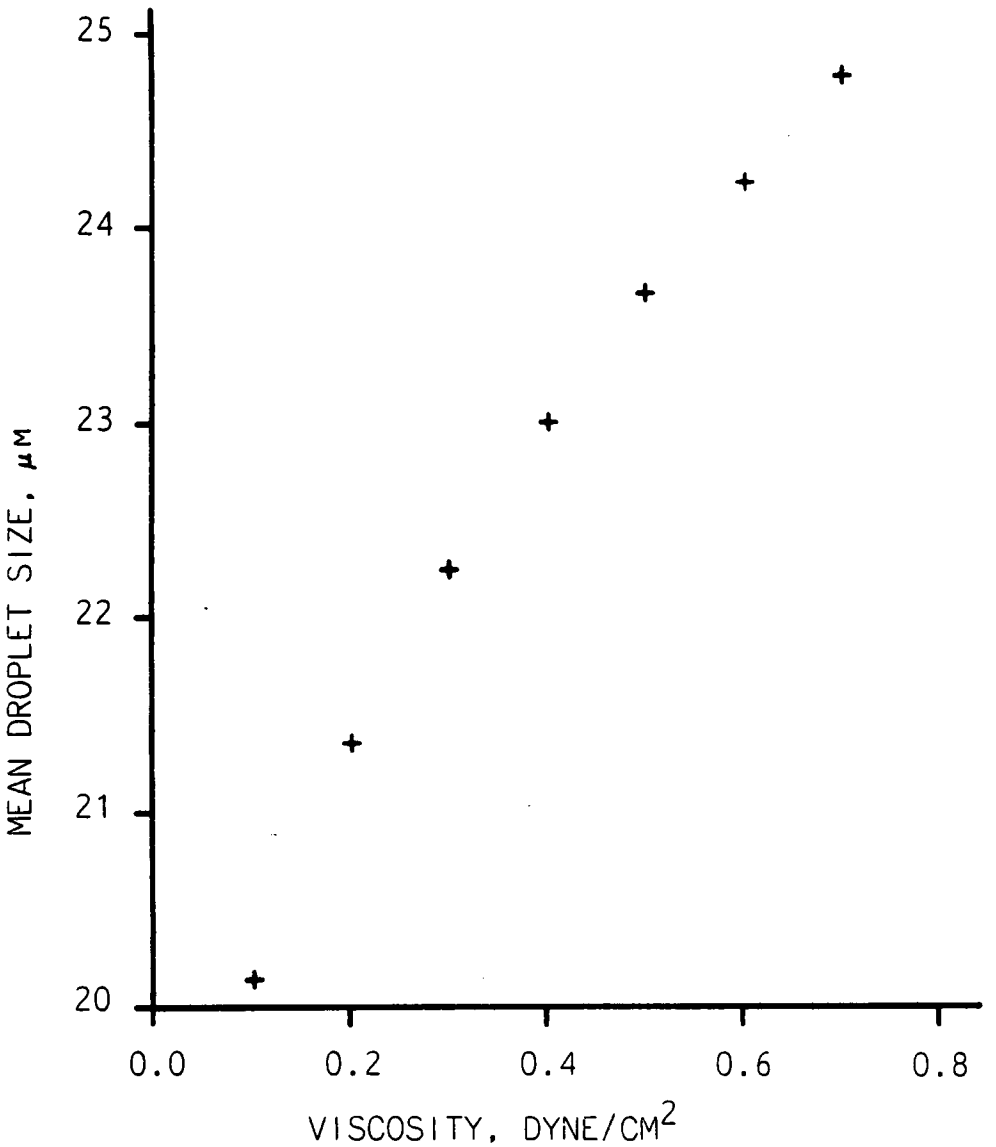

Figure 41: Mean droplet size (calculated from the Nukijama-Tanasawa expression) as a function of viscosity at $\gamma = 72$ dyne/cm

critical micellular concentration [79], whereas the viscosity should continue to increase with increasing concentration. Thus, relatively high concentrations of PEO should have a significant effect on viscosity without changing the surface tension from that of low concentrations. A study of viscosity and surface tension of PEO solutions should provide insight as to whether PEO can be employed for the purpose of increasing droplet size according to the Nukijama-Tanasawa expression.

The surface tension of solutions of PEO ranging from 1-10000 ppm concentration was determined by the capillary rise method [79]; viscosity of each solution was determined using the falling-ball method [81]. The results are shown in Figures 42 and 43. Low concentrations of PEO affect the surface tension significantly without appreciably affecting the viscosity. The critical micellar concentration of PEO apparently occurs around 3-10 ppm. At concentrations beyond this, the effect of increased PEO concentration on surface tension is negligible. Viscosity is not significantly affected until the concentration of PEO reaches about 1000 ppm, after which the viscosity increases rapidly. At 10000 ppm PEO, the viscosity has increased by a factor of approximately 300.

Figure 44 shows the mean droplet size predicted by the Nukijama-Tanasawa expression, as a function of PEO concentration, based on the viscosity and surface tension data collected above. Initially, a decrease in droplet size should be observed, corresponding to an increase in the population of small droplets. The droplet size should be unaffected from concentrations of PEO between about 3 ppm and 1000

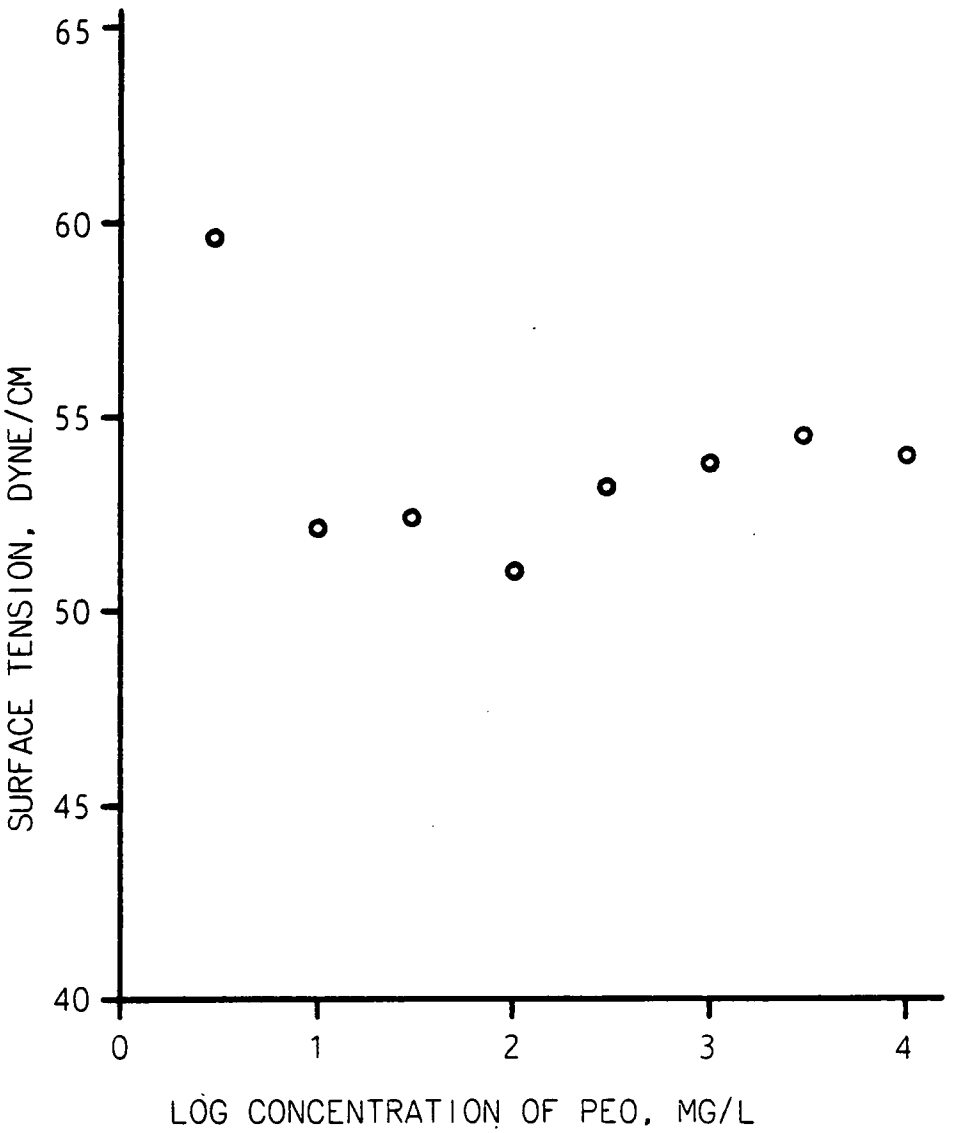

Figure 42: Surface tension versus log concentration of poly (ethylene oxide) in mg/L

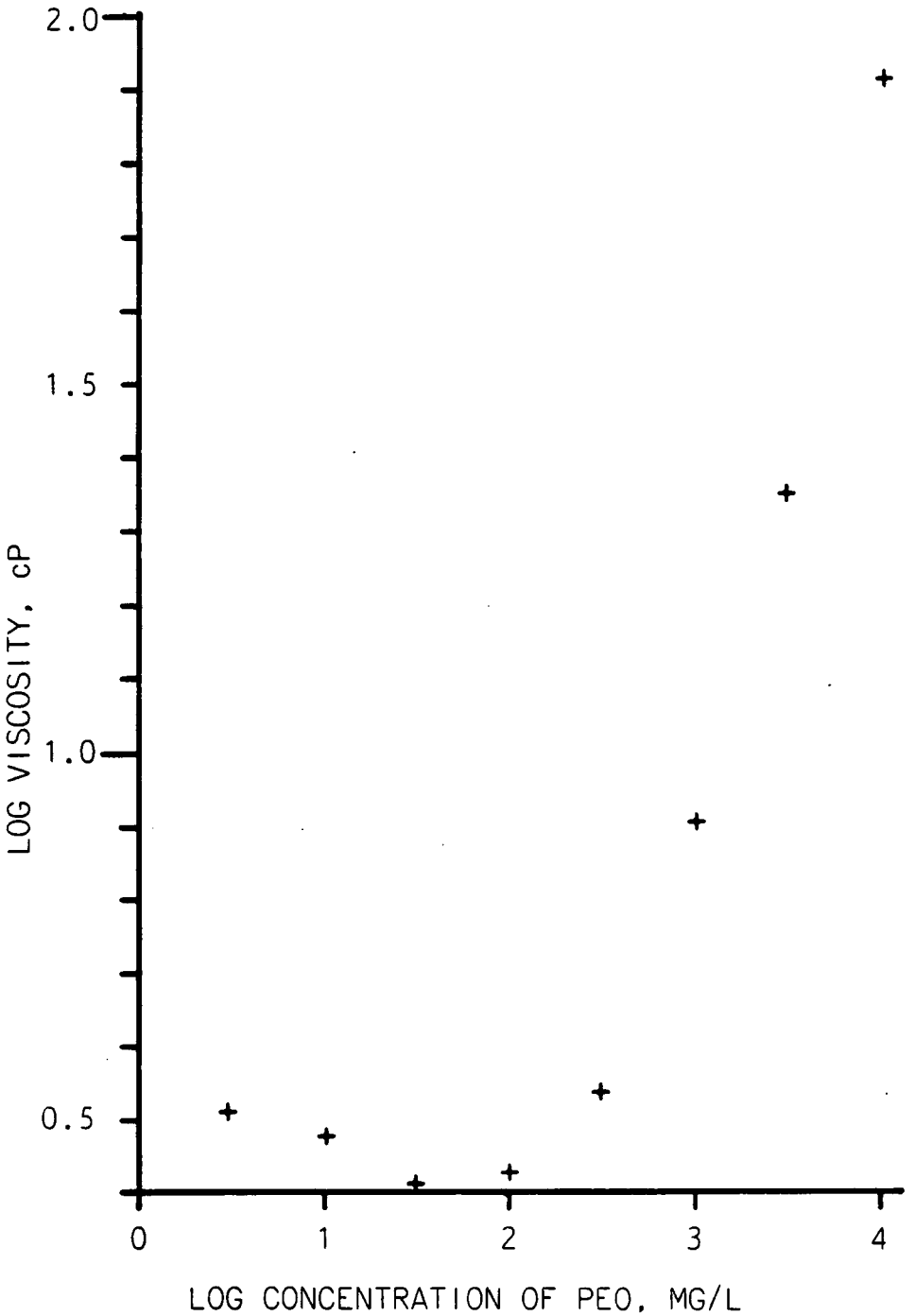

Figure 43: Log viscosity versus log concentration of poly (ethylene oxide) in mg/L

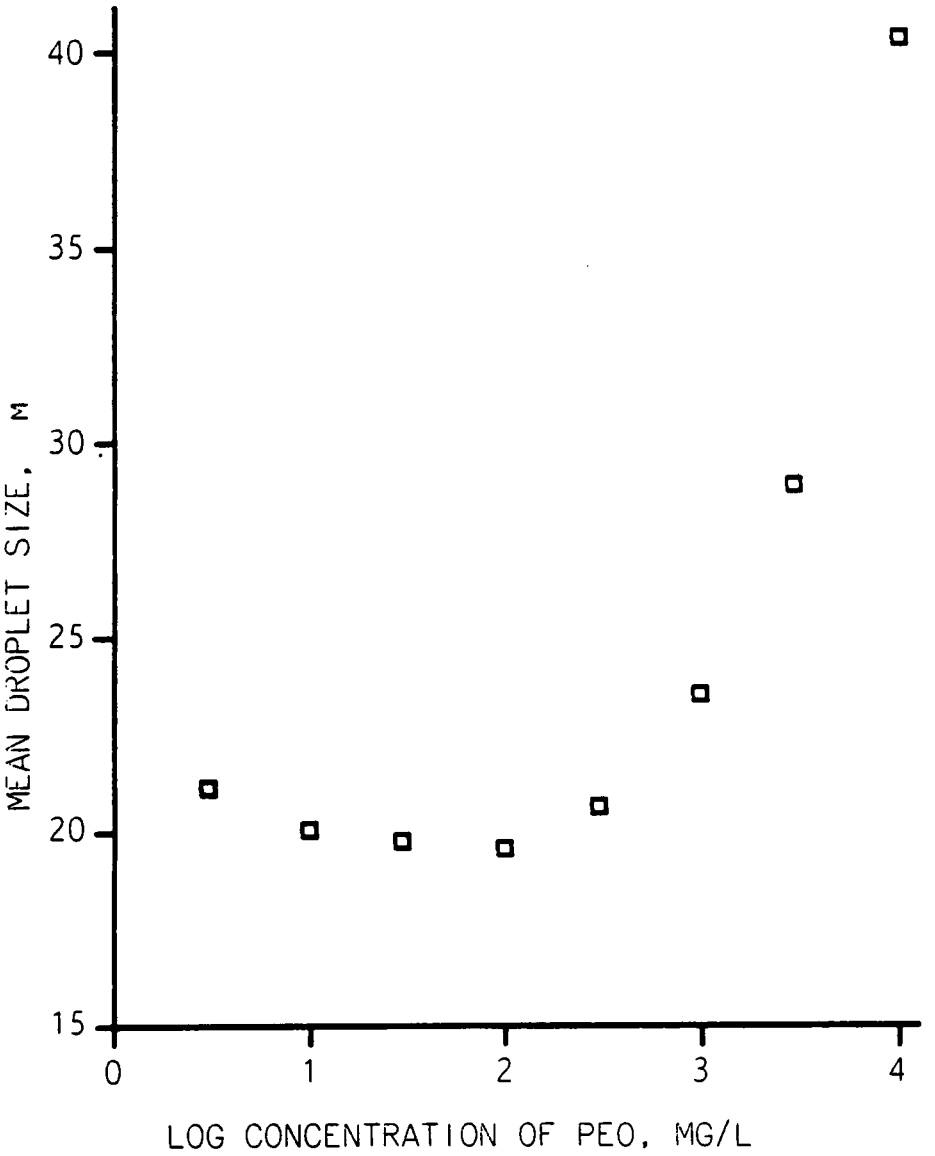

Figure 44: **Mean droplet size (calculated from the Nukijama-Tanasawa expression) versus log concentration of poly (ethylene oxide)**

ppm, after which the droplet size should increase. However,it should be noted that the Nukijama-Tanasawa expression has been shown to be valid only within the range of η = 0.01 to 0.3 [82]. The high-viscosity solutions used in this study may be expected to show deviations from the Nukijama-Tanasawa expression.

Effect of PEO on Emission from Solutions

Small droplets are more readily desolvated and the resulting particles are more readily vaporized than are large droplets. All other things being equal, a shift toward smaller droplets should cause an increase in the analytical signal, and a shift toward larger droplets should decrease the signal-to-noise ratio. In fact, the former proposition has been illustrated by a number of workers [27,75-77]; a reduction in surface tension is often used to improve the analytical sensitivity. Until now, the latter proposition has not been studied extensively.

Based on the varying concentrations of PEO, it was anticipated that the signal for aqueous solutions should increase at first, reaching a plateau at or near the critical micellular concentration of about 10 ppm of PEO. At concentrations of PEO greater than 1000 ppm, the signal magnitude from aqueous solutions should decrease.

To test this theory, solutions that were 50 ppm in iron with varying concentrations of PEO were prepared, and the iron emission signals were monitored. The results, shown in Figure 45, show that an increase in emission was seen at low concentrations of PEO, wherein the surface tension effect outweighed the viscosity effect. The emission

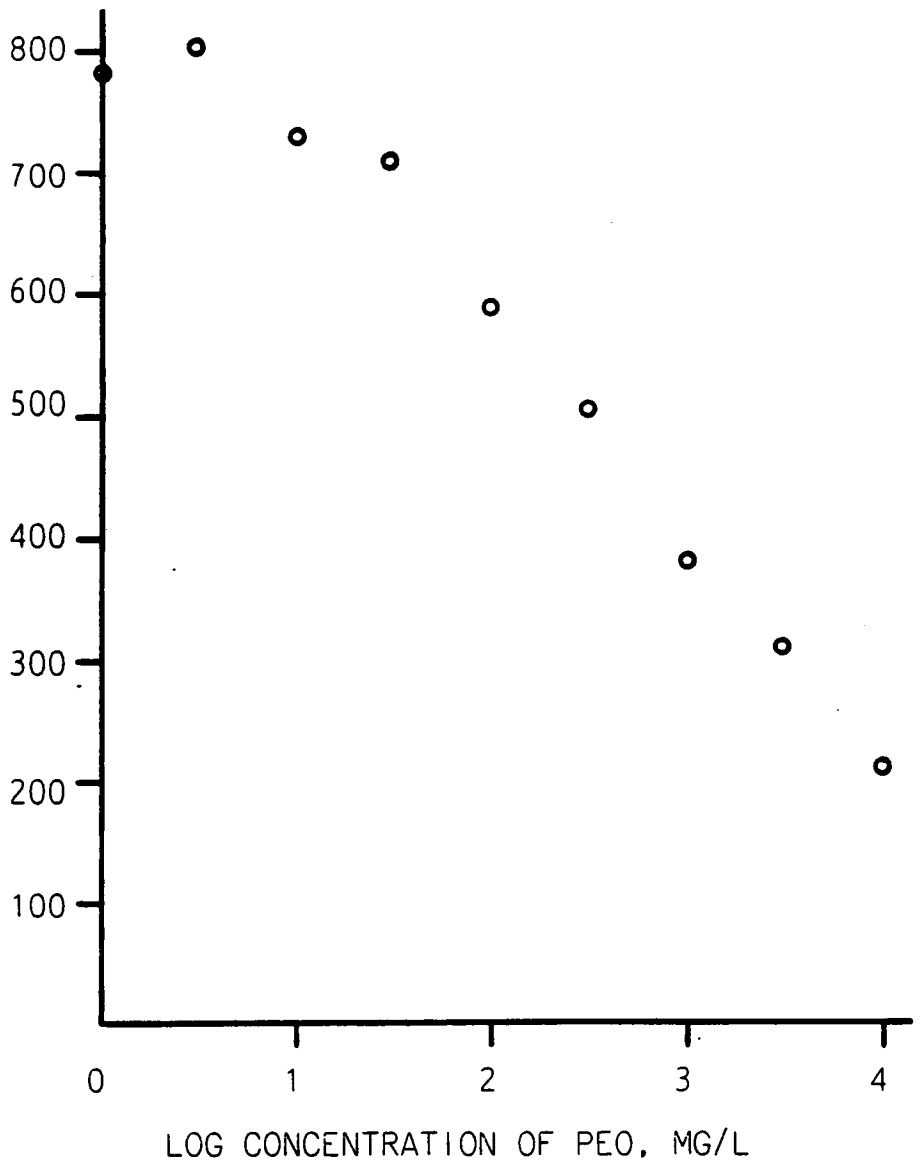

Figure 45: **Emission from 50 mg/L iron versus log concentration of poly (ethylene oxide). Emission intensity with no poly (ethylene oxide) added = 732**

was found to reach a maximum at 3 ppm PEO; at this concentration, a 9% increase in signal was seen. At 30 ppm PEO, the iron emission was about the same as for the solution which had no PEO. At concentrations of PEO greater than 30 ppm, the emission signal decreased; at 10000 ppm, the emission was less than one third of that for the solution without PEO. It is significant that the trend shown in this figure is nearly a mirror image of that shown in Figure 44.

Effect of PEO on Detection Limits and Working Curves

Two potential consequences of an increase in the mean size of droplets are an increase in noise and a decrease in signal magnitude. The former would arise from scatter of emission signal by large droplets and particles that do not completely desolvate and/or vaporize in the NVZ. The signal decrease would result from the reduced atomic, ionic, and/or excited state population(s) that arises from incomplete vaporization of the larger particles and droplets. The net result of these two factors should be a decrease in the analytical sensitivity with an increase in droplet size.

A comparison of signal and noise magnitude as a function of PEO concentration showed was a significant but not extreme increase in the noise, probably because of the high noise level already inherent in the data acquisition system. There was, as noted earlier, a reduction in signal magnitude for aqueous solutions to which large amounts of PEO had been added. Since the noise remained nearly constant and the signal varied, the signal-to-noise ratio paralleled the change in signal observed, and decreased with increasing concentration of PEO.

From these results, it can be surmised that PEO does not cause a dramatic shift toward much-larger-than-average droplets exiting the spray chamber; if it did, a considerable increase in noise would be apparent. This does not mean that larger-than-average droplets are not produced by the nebulizer, but merely that they do not exit the spray chamber. Fry has suggested that the cutoff diameter for the Babington nebulized/spray chamber designed by him is 23 um (90th percentile). Recent work by Coleman has shown that less than 0.05% of the droplets actually introduced into the plasma by the Fry-Babington nebulizer exceed 33 um diameter [83,84]. Apparently, the spray chamber has a significant effect on droplet transport. From these results, it can be concluded that the addition of PEO does not increase the number of large droplets introduced into the plasma so much as it increases the proportion of large to small droplets.

Figure 46 shows working curves of aqueous Fe, with and without 10000 ppm PEO. The slope for the PEO working curve is about one-fourth that of the ordinary working curve. This is to be expected, since the signal magnitude decreases at high PEO concentration. The relative standard deviation of the measurements is about 12%. This is not of major concern, since the concentration of coal can be increased to some extent to improve the error of measurement. Fry has shown that coal concentrations up to 10% do not significantly affect the nebulizing characteristics of the slurry [36].

Effect of PEO on Emission from Slurries

All solution droplets should contribute to signal magnitude, since

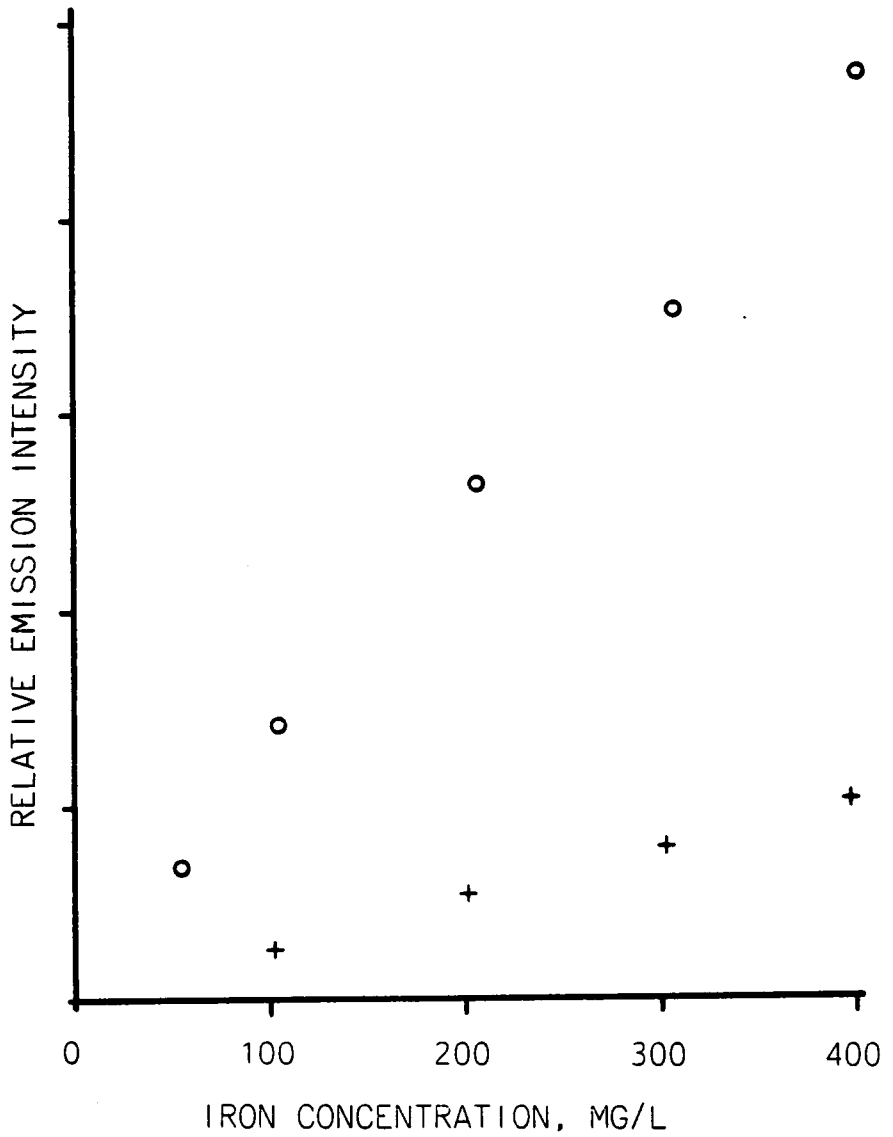

Figure 46: Emission from iron versus concentration in mg/L, with (+) and without (o) 1% poly (ethylene oxide)

all the droplets contain analyte. This is not true for slurries; only those droplets containing slurry particles can contribute to analyte signal. A decrease in the mean droplet size should either have no effect on slurry emission signals, or it should actually increase the emission from slurries. This is because the droplets which are being depleted are the smallest droplets, which do not carry an appreciable amount of the slurry and thus do not contribute to signal; an increase in emission signal would be expected if the droplet size were increased to such an extent that a greater fraction of the coal could be transported.

To test this hypothesis, emission from 1% slurries of Cedar Grove coal to which varying amounts of PEO had been added was monitored. The results, shown in Figure 47, confirm that the signal from slurries is only slightly affected by the increase in viscosity. Although the signal appears to vary slightly, the changes are not statistically significant.

Effect of PEO on Recovery of Slurry Emission Signals

It is theorized that PEO added to aqueous solutions can shift the droplet size distribution toward larger droplets, which then permits transport of larger particles to the plasma. Work by others in this area suggests that droplets, and thus particles, larger than 23-33 um will not be transported into the plasma to a significant degree, even though the nebulizer can produce droplets as large as 150 um [84]. Thus, even if the viscosity of the solution caused production of large droplets that could accomodate the large particles, these large

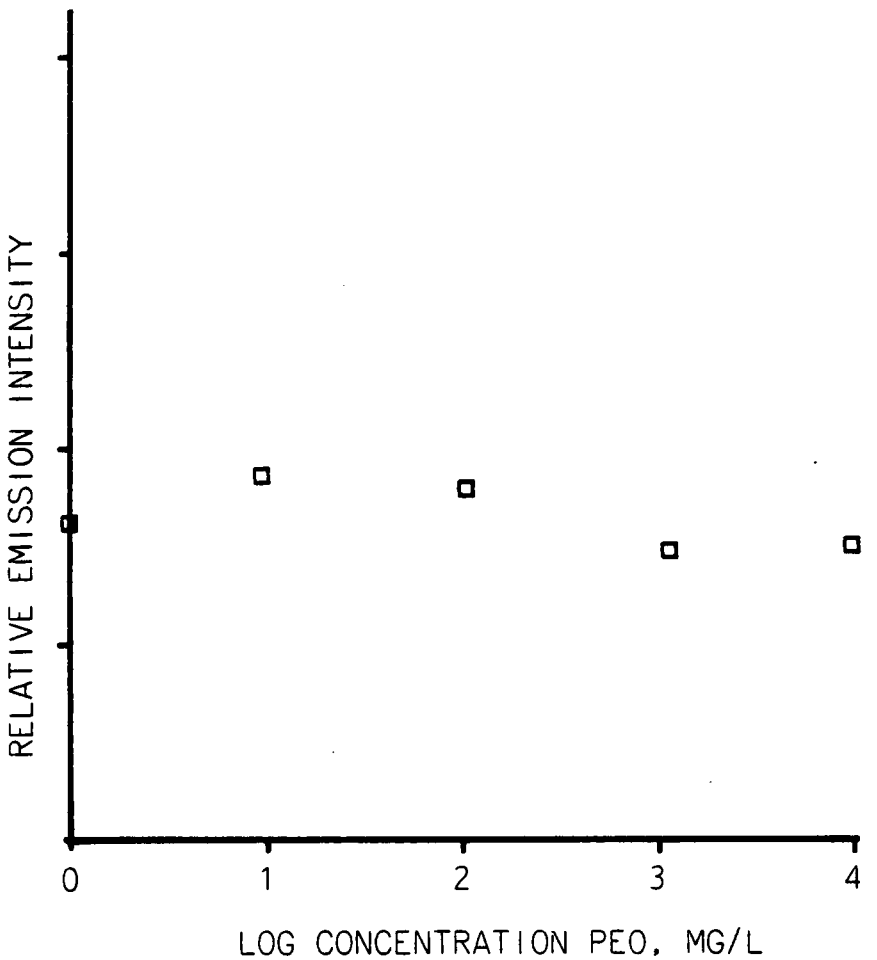

Figure 47: Emission from 1% slurry of Cedar Grove coal versus log concentration of poly (ethylene oxide)

particles would not be transported into the plasma. For unit recovery of emission from slurries, it should not be necessary to have total transport of the coal slurry, but should only be necessary to have total transport of that fraction of the coal which has a particle size below the cutoff size of the nebulizer/spray chamber combination. This concept is graphically illustrated in Figure 48.

The sulfur emission from 1% coal slurries with 0, 10, 100, 1000, 3000, and 10000 ppm PEO in the samples was determined and compared to equivalent concentrations of aqueous sulfur (ammonium sulfate) to which the corresponding amount of PEO had been added. The results for Cedar Grove coal are shown in Figure 49. As was found in the solution work earlier, the signal from the aqueous sulfur solution appears to increase slightly at about 10 ppm PEO (this increase is not statistically significant). As the fraction of PEO is increased, the solution signal magnitude decreases. The increased viscosity causes the fraction of tiny (ca 1 um) droplets to be depleted, and it is these droplets that produce the majority of the signal in atomic spectrometry [27,82]. By the time the PEO concentration reaches 10000 mg/L, the signal has reached a plateau. At the same time, the emission signal seen from the coal remains constant with changing PEO concentration; depletion of the smallest droplets does not significantly affect the amount of coal reaching the plasma. The two curves coincide at about 3000 mg/L PEO; at this point, there is no significant difference between the coal signal and the solution signal, and 100% recovery is attained.

The results suggest that a higher concentration of PEO would be

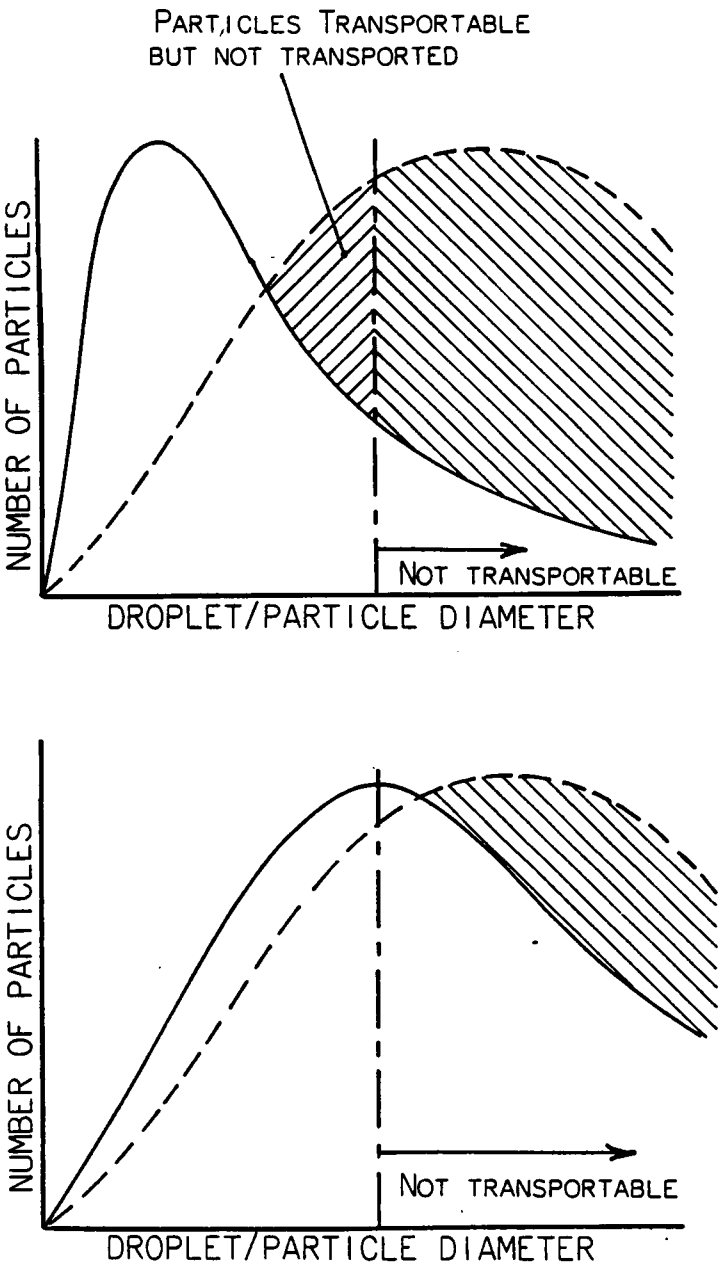

Figure 48: Illustration of relationship between droplet (——) size, particle (– – –) size, and transportability into plasma. Nebulizer cutoff diameter indicated by (—·—)

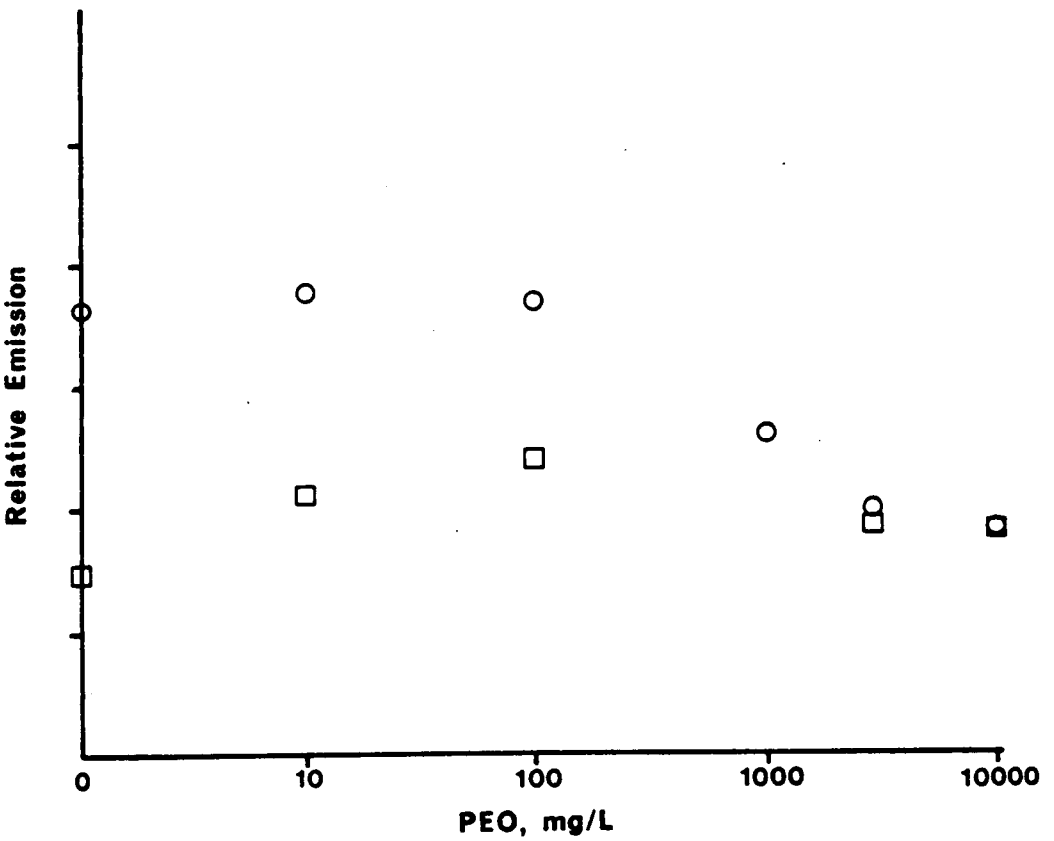

Figure 49: Sulfur emission as a function of poly (ethylene oxide) concentration for 1% Cedar Grove coal slurry (0.79% S, d_o = 8 um) (□) and 79 mg S/L aqueous solution (○)

required for 100% transport of coarser coals. A comparison of aqueous sulfur to R-coal (d_o=18 um) shows that the recovery at 3000 ppm PEO is less than unity. However, the recovery reaches unity at 10000 ppm PEO. The two other coals tested had particle sizes similar to that for the Cedar Grove coal, and also showed over 90% recovery at 3000 ppm PEO as shown in Figure 50; all coals provided 100% recovery at 10000 ppm PEO. Although there is a great deal of scatter of the data at lower concentrations of PEO, the general trend is toward increased recovery with increases in concentration of PEO. At these high concentrations of PEO, the signal-to-noise ratio is rather poor; the relative standard deviation of these results is on the order of 15%.

Comparison of these coal slurries to working curves for iron, silicon, and aluminum provided data on the recoveries of these elements. Iron and silicon showed the same behavior as did sulfur, as can be seen in Table 12. Silicon appears to have a recovery that is greater than unity, but this difference is within experimental error. Aluminum, however, paralleled its earlier behavior, providing less than 100% recovery. Since the physical parameters for incomplete recovery have been compensated for by the addition of PEO, it can be concluded that the poor recovery for aluminum is definitely chemical in nature.

CONCLUSIONS

Poly(ethylene oxide) acts as both a surfactant and a viscosity-increasing agent in aqueous solutions. When added to aqueous standards and to coal slurries, this agent can increase the recovery of

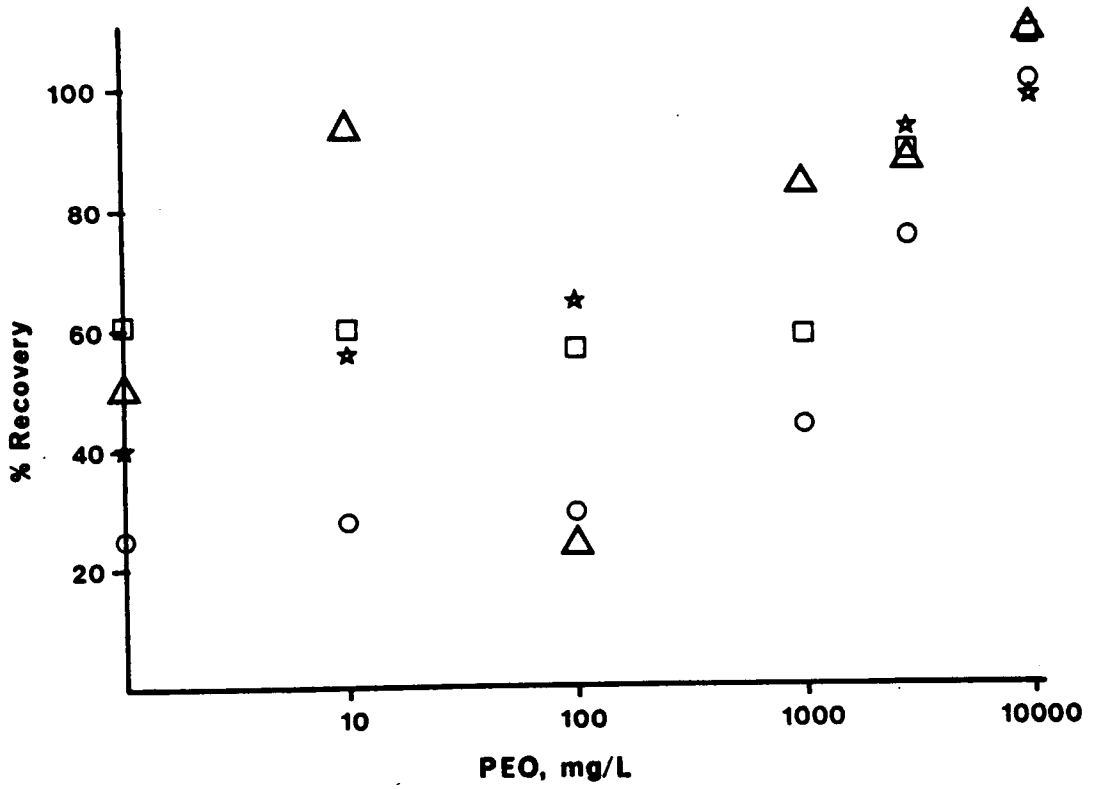

Figure 50: Percentage recovery of sulfur signal from Cedar Grove (★), Elkhorn #3 (△), Buller (□), and R-coal (○) as a function of poly (ethylene oxide) concentration

Table 12: Silicon, aluminum, and iron content of coals as determined by ASTM procedure and by slurry injection into the Direct Current Plasma, with 1% poly (ethylene oxide) added to all solutions. Value in parenthesis is the error of the determination.

Silicon, percent in coal

Coal	ASTM	Slurry Injection with PEO
Cedar Grove	1.53 (0.01)	1.57 (0.19)
Elkhorn #3	2.11 (0.01)	2.02 (0.23)
Buller	0.062 (0.001)	0.07 (0.02)
R-coal	1.03 (0.02)	1.15 (0.18)

Aluminum, percent in coal

Cedar Grove	1.84 (0.03)	1.44 (0.20)
Elkhorn #3	2.12 (0.02)	1.80 (0.27)
Buller	0.175 (0.003)	0.16 (0.03)
R-coal	1.25 (0.01)	0.97 (0.13)

Iron, percent in coal

Cedar Grove	1.25 (0.01)	1.13 (0.19)
Elkhorn #3	1.98 (0.02)	1.81 (0.27)
Buller	0.392 (0.003)	0.37 (0.04)
R-coal	0.99 (0.02)	1.02 (0.09)

emission signals such that no grinding is required for unit recovery of coals up to d_o = 18 um. The improved recovery is obtained at the cost of sensitivity; detection limits are poorer by at least a factor of four by addition of this agent. The sensitivity of DCP-OES is still sufficient for analysis of sulfur, iron, silicon, and aluminum with PEO added to 1% coal slurries.

CHAPTER 7

CONCLUSIONS

Coal slurries can be analyzed for sulfur, iron, aluminum, and silicon by direct current plasma emission spectrometry, using the lines at 182.0, 259.9, 308.2, and 251.6 nm, respectively. For sulfur analysis, an auxiliary monochromator and a purge system is required. A Babington-type nebulizer system is required to deliver the slurries to the plasma, which does not appreciably change the sensitivity of the technique when compared to the conventional ceramic nebulizer. The detection limits and linear dynamic ranges exhibited for these four elements with the Babington system are adequate for analysis of most 1% coal slurries. For very clean slurries (with very low ash levels and/or sulfur levels), more concentrated slurries would be required for precise results.

A particle size effect occurs with these coals such that the signal from the coal is less than that from an equivalent concentration of aqueous solution. This effect arises because large particles of coal cannot be transported into the plasma as readily as can smaller particles. This interference complicates the direct use of aqueous solutions as calibration standards for slurries that have been ground for only a short time. The particle size interference could be minimized in one of four ways: extended grinding of the coal samples;

application of an empirically derived correction factor; use of similar coal slurries as calibration standards; or addition of a viscosity-increasing agent to more closely match the behavior of solutions and slurries.

Addition of a viscosity-increasing agent causes an improvement in recovery for two reasons. First, it reduces the number of those smallest droplets which can carry solution (which contributes to signal) but which cannot carry slurry particles (in which case the droplets would not contribute to signal). Second, it shifts the mean droplet size toward larger droplets, so that larger coal particles can be transported to the plasma. The upper limit of particle size that must be transportable is the maximum droplet size that can be transported through the nebulizer, since larger droplets and particles alike will not reach the nebulizer and will not contribute to signal. For the nebulizer used, this corresponds to a required mean droplet size of 23-33 um.

Poly(ethylene oxide) can be used as a viscosity-increasing agent for coal slurries. Addition of 1% poly(ethylene oxide) to coal slurries and standard solutions increases the viscosity by over two orders of magnitude, causing an increase in droplet size to about 35-40 um. This permits unit recovery of signal for the elements mentioned at particle sizes up to d_o=18 um.

The improved recovery is obtained with a reduction in sensitivity of a factor of four or more. This reduction is seen because the smallest droplets, which would normally make the greatest contribution to signal magnitude, are depleted when the viscosity is increased.

Another effect of the improved recovery is a decrease in signal-to-noise ratio. These drawbacks should be minimizable by increasing the concentration of coal in the slurry.

A chemical interference is seen for aluminum analysis, presumably from formation of aluminum oxides. This interference results in recoveries for aluminum that are less than unity, even when poly(ethylene oxide) is used.

Addition of propane could conceivably improve the recovery of the emission signal from aluminum. Propane added to the nebulizing argon of the DCP atomizes and the resultant elemental carbon causes reduction of metal oxides, thereby increasing the population of the corresponding metal. However, this effect is accompainied by a reduction in signal magnitude; the atomization of the propane requires a significant fraction of the energy available in the plasma, resulting in a substantial temperature decrease in the normal viewing zone of the plasma. More important with respect to online analysis of coal is the fact that a large molecular and radical population in the form of a stoichiometric flame exists near the NVZ upon addition of propane. This flame would preclude the analysis of sulfur; lines below 190 nm are severely attenuated by product gases of carbon-fueled flames, which is why flame AAS is not performed for sulfur. Therefore, in practice, propane cannot be added to the nebulizing argon of the plasma to improve the recovery of the aluminum signal.

REFERENCES

1. J. N. Chakrabarti in "Analytical Methods for Coal and Coal Products", C. Karr, Ed., Academic Press, New York (1978).

2. D. W. Pacer and A. F. Duzy, Coal Mining & Processing, May 1982, p. 73.

3. G. E. Vaninetti and C. F. Busch, Journal of Coal Quality, Spring 1982, p. 22.

4. W. J. Montgomery in "Analytical Methods for Coal and Coal Products", C. Karr, Ed., Academic Press, New York (1978).

5. Annual Book of ASTM Standards, Vol. 5, Section 5, ASTM, Philadelphia (1987).

6. "Analytical Methods for Coal and Coal Products", C. Karr, Ed., Academic Press, New York (1978).

7. R. Dunk, R. A. Mostyn, and H.C. Hoare, Atomic Absorption Newsletter **8**, 79 (1969).

8. H. Willard, L. Merritt, J. Dean, and F. Settle, "Instrumental Methods of Analysis", 6th Ed., Wadsworth Publishing Co., Belmont (1981).

9. E. S. Gladney, R. Raymond, and N. W. Bower, Am. Lab **7**, 34 (1985).

10. D. R. Brown et al, FACSS XIII Meeting, St. Louis, 1986, Abstract #68.

11. J. E. O'Reilly and D. G. Hicks, Anal. Chem. **51**, 1905 (1979)

12. M. L. Parsons, S. Major, and A. R. Forster, Appl. Spectrosc. **37**, 411 (1983).

13. M. Margoshes and B. F. Scribner, Spectrochim. Acta **14**, 138 (1959).

14. V. V. Korolev and E. E. Vainshtein, J. Anal. Chem. USSR **14**, 731 (1959).

15. L. E. Owen, Appl. Spectrosc. **15**, 150 (1961).

16. F. A. Korolev and I. K. Kvaratskheli, Opt. Spectrosc. **10**, 200 (1961).

17. L. I. Greshikhin and V. D. Shimanovich, Opt. Spectrosc. **13**, 358 (1962).

18. L. I. Greshikhin, J. Anal. Chem. USSR **18**, 16 (1963).

19. M. Marinkovic and B. Dimitrijevic, Spectrochim. Acta **23B**, 257 (1968).

20. S. E. Valente and W. G. Schrenk, Appl. Spectrosc. **24**, 197 (1970).

21. W. G. Elliot, Am. Lab. **3**, 45 (1971).

22. Spectraspan IIIB Instruction Manual, Spectrametrics Inc., Andover, MA.

23. J. Babis, Pittsburgh Conference on Analytical Chemistry and Applied Spectroscopy, Atlantic City, 1987, Abstract #764

24. R. K. Skogerboe, I. T. Urasa, and G. N. Coleman, Appl. Spectrosc. **30**, 500 (1976).

25. R. J. Decker, Spectrochim. Acta **35B**, 19 (1980).

26. P. N. Keliher and C. C. Wohlers, Anal. Chem. **48**, 333A (1976).

27. R. F. Browner and A. W. Boorn, Anal. Chem. **56**, 787A (1984).

28. R. F. Browner and A. W. Boorn, Anal. Chem. **56**, 875A (1984).

29. H. Anderson, H. Kaiser, and B. Meddings in "Developments in Atomic Plasma Spectrochemical Analysis", R. Barnes, Ed., Heyden and Son, London (1981).

30. Popular Science, May 1973, p. 102.

31. N. Mohamed, R. M. Brown, Jr., and R. C. Fry, Appl. Spectrosc. **35**, 153 (1981).

32. G. L. Long and J. D. Winefordner, Appl. Spectrosc. **38**, 563 (1984).

33. D. R. Demers, Spectrochim. Acta **40B**, 93 (1985).

34. "Handbook of Spectral Line Characteristics for the DC Plasma/Echelle Systems", Spectrametrics Inc., Andover, MA

35. V. C. Anigbogu and G. N. Coleman, FACSS XIII Meeting, St. Louis, 1986, Abstract 695.

36. D. L. McCurdy, M. D. Wichman, and R. C. Fry, Appl. Spectrosc. **39**, 984 (1985).

37. "Analytical Methods for Atomic Absorption Spectrophotometry", Perkin-Elmer Co., Norwalk, (1982).

38. G. L. Long and J. D. Winefordner, Anal. Chem. **55**, 713A (1983)

39. S. Greenfield and M. Thomsen, Spectrochim. Acta **41B**, 677 (1986).

40. T. R. Gilbert and B. A. Penney, Spectrochim. Acta **38B**, 297 (1983).

41. R. H. Tourin, "Spectroscopic Gas Temperature Measurements", Elsevier, New York (1962).

42. A. Goldwasser and J. M. Mermet, Spectrochim. Acta **41B**, 725 (1986).

43. M. H. Miller, D. Eastwood, and M. S. Hendrick, Spectrochim. Acta **39B**, 13 (1984).

44. C. B. Boss and J. S. Gentry, FACSS XIII Meeting, St. Louis, 1986, Abstract #63.

45. P. E. Walters, G. L. Long, and J. D. Winefordner, Spectrochim. Acta **39B**, 69 (1984).

46. A. T. Zander, Anal. Chem. **58**, 1139A (1986).

47. C. E. Schmidt and R. D. Sacks, Spectrochim. Acta **38B**, 557 (1983).

48. H. R. Griem, "Plasma Spectroscopy", McGraw-Hill, New York (1964).

49. M. W. Blades and N. Lee, Spectrochim. Acta **39B**, 879 (1984).

50. A. T. Zander and M. H. Miller, Spectrochim. Acta **40B**, 1023 (1985).

51. G. W. Johnson, H. E. Taylor, and R. K. Skogerboe, Appl. Spectrosc. **34**, 19 (1980).

52. P. Merchant and C. Veillon, Anal. Chim Acta **70**, 17 (1974).

53. R. J. Decker, Spectrochim. Acta **35B**, 19 (1980).

54. D. L. McCurdy and R. C. Fry, Anal. Chem. **58**, 3126 (1986).

55. C. B. Boss and G. M. Hieftje, Anal. Chem. **51**, 895 (1979).

56. G. L. Long and J. S. Bolton, Spectrochim. Acta. **42B**, 581 (1987).

57. J. Bolton, personal communication.

58. A. T. Zander and P. N. Keliher, Appl. Spectrosc. **33**, 499 (1979).

59. "Wavelengths and Transition Probabilities for Atoms and Atomic Ions", National Bureau of Standards, Washington (1980).

60. F. M. Phelps, "MIT Wavelength Tables", Vol. 2, MIT Press, Cambridge (1982).

61. S. Bashkin and J. O. Stoner, "Atomic Energy Level & Grotrian Diagrams", Vol. 2, North-Holland, Amsterdam (1978).

62. J. W. Carr and M. W. Blades, Spectrochim. Acta **39B**, 667 (1984).

63. W. M. Braun, M. S. Thesis, University of Georgia, 1978.

64. G. W. Johnson, H. E. Taylor, and R. K. Skogerboe, Spectrochim. Acta **34B**, 197 (1979).

65. M. Miller, E. Keating, D. Eastwood, and M. S. Hedrick, Spectrochim. Acta **40B**, 593 (1985).

66. D. Eastwood, M. S. Hendrick, and G. Sogliero, Spectrochim. Acta **35B**, 421 (1980).

67. C. W. Fuller, R. C. Hutton, and B. Preston, Analyst **106**, 913 (1981).

68. W. A. Dick, J. R. Page, and K. E. Jewell, Soil Sci. **139**, 211 (1985).

69. "Fundamentals of Analytical Chemistry", D. A. Skoog and D. M. West, 4th ed., Saunders, Philadelphia (1982).

70. "Indcutively Coupled Plasma Emission Spectroscopy--Part I", P. W. J. M. Boumans, Ed., John Wiley & Sons (1987).

71. S. H. Vien and R. C. Fry, Appl. Spectrosc. **42**, 381 (1988).

72. L. Ebdon and J. R. Wilkinson, J. Anal. At. Spectrom. **2**, 39 (1987).

73. R. Fitkau, D. L. McCurdy, R. E. Clark, M. D. Wichman, and R. C. Fry, Pittsburgh Conference on Analytical Chemistry and Applied Spectroscopy, Atlantic City, 1987, Abstract #502.

74. S. Nukijama and Y. Tanasawa, Trans. Soc. Mech. Eng. (Japan) **4**, 86 (1938).

75. N. D. G. Msimanga and R. F. Browner, Pittsburgh Conference on Analytical Chemistry and Applied Spectroscopy, New Orleans, 1988, Abstract #723.

76. J. A. Dean and W. J. Carnes, Anal. Chem. **34**, 192 (1962).

77. J. A. C. Broekaert and F. Leis, Anal. Chim. Acta **109**, 73 (1979).

78. J. P. Wightman, personal communication.

79. "Physical Chemistry of Surfaces", 4th ed., A. W. Adamson, John Wiley & Sons, New York (1982).

80. "Physical Chemistry", 4th ed., G. M. Barrow, McGraw-Hill, New York (1979).

81. "Experimental Physical Chemistry", 7th ed., F. Daniels, J. W. Williams, P. Bender, R. A. Alberty, C. D. Cornwell, and J. E. Harriman, McGraw-Hill, New York (1970).

82. A. G. T. Gustavsson in "Inductively Coupled Plasmas in Analytical Atomic Spectrometry", A. Montaser and D. W. Golightly, Ed., VCH Publishers, New York (1987).

83. G. N. Coleman and N. J. Weeks, FACSS XIV Meeting, Detroit, 1987, Abstract #546.

84. N. J. Weeks and G. N. Coleman, Pittsburgh Conference on Analytical Chemistry and Applied Spectroscopy, New Orleans, 1988, Abstract #728.

85. N. Mohamed, R. M. Brown, Jr., and R. C. Fry, Appl. Spectrosc. **35**, 153 (1981).

APPENDIX A

COMPUTER PROGRAMS USED FOR DATA ACQUISITION/PROCESSION

The programs included here are "DCP", which was used to collect data for background-corrected emission profiles; "RAW DATA", which was used to collect individual (not background-corrected) profiles; "REAL WORK", which was used to collect data for analyses, providing a mean value and standard deviation; and "LR", a linear regression routine. All these programs are based on IMI QUICK I/O software, which uses the Applesoft "&" command for all data input and output. All programs are modifications of software originally written by Gary L. Long.

```
 100  CLEAR : HIMEM: 36095:D% = 0:: PRINT  CHR$ (4)"BRUN QUI
CKI/O,D1"
 110  POKE 36259,1: REM  this permits data acquisition witho
ut timing programming
 120  DIM D(50),B(50),S(50)
 130  PR# 0
 140  REM  The data acquisition rate will depend partly on
the size
 150  REM  of the signal.  Larger signals will take longer
to integrate
 160  REM  than will smaller signals.  Actual data acquisiti
on rates vary
 170  REM  in this program from about 20-50 points per secon
d.  The
 180  REM  number of points taken per integration time will
be the same;
 190  REM the actual time this takes to do will vary somewha
t.
 200  REM
 210  REM    If you wish to take more than 50 points per pro
file,
 220  REM   change the values in lines 120 and 390 as needed

 230  REM    This program was revised by Terry McCreary on
4/6/87
 240  REM
 250  REM
 260  HOME : HTAB (12): FLASH : PRINT "DCP PROFILE": NORMAL
: PRINT : PRINT
 270  PRINT : PRINT "  This program will collect data"
 280  PRINT "for DCP profiles (up to 50 points per"
 290  PRINT "profile).  A background profile will"
 300  PRINT "be taken first, followed by a signal"
 310  PRINT "profile."
 320  PRINT : PRINT "  Data will be saved on drive 2; be"
 330  PRINT "sure to place your data disk in"
 340  PRINT "that drive.": PRINT
 350  PRINT "  Two hard copies of the data will"
 360  PRINT "be printed for the lab notebook after"
 370  PRINT "the data is saved.": PRINT
 380  PRINT : PRINT : PRINT "One moment please..."
 390  FOR I = 0 TO 50:D(I) = 0::B(I) = 0:S(I) = 0: NEXT I:F$
= ""
 400  PRINT
 410  INPUT "File name for data";F$
 420  PRINT : PRINT "Date <";C$;">";: INPUT B$: IF B$ <  >
"" THEN C$ = B$
 425  PRINT "Analyte concentration <";M$;">";: INPUT B$: IF
B$ <  > "" THEN M$ = B$
```

```
 430  PRINT "Argon nebulizer flow <";R$;">";: INPUT B$: IF
B$ <  > "" THEN R$ = B$
 435  PRINT "Auxiliary gas <";X$;">";: INPUT B$: IF B$ <  >
"" THEN X$ = B$
 440  PRINT "Auxiliary gas flow <";H$;">";: INPUT B$: IF B$
<  > "" THEN H$ = B$
 445  PRINT "Position of profile start <";E$;">";: INPUT B$:
 IF B$ <  > "" THEN E$ = B$
 450  PRINT "Increment size <";I$;">";: INPUT B$: IF B$ <
> "" THEN I$ = B$
 460  PRINT : INPUT "Other comments";K$
 470  PRINT "Number of observations ";N
 480  PRINT "Length of integration in sec ";NN
 490  PRINT "Delay between observations in sec ";WT
 500 D(0) = N
 510  PRINT
 520  INPUT "HIT RETURN TO TAKE BACKGROUND";S$
 540  FOR I = 1 TO N
 550  & AIO
 560  GOSUB 1080
 570  PRINT I,( INT (IN / NN)) / 50
 580 B(I) = IN / (NN * 50)
 590  GOSUB 1140
 600  PRINT  CHR$ (7)
 610  PRINT "Hit any key to continue"
 620  GET G$: IF G$ = "" THEN 510
 630  NEXT I
 640  FOR I = 1 TO 5
 650  PRINT  CHR$ (7)
 660  NEXT I
 670  PRINT
 680  INPUT "HIT RETURN TO TAKE SIGNAL";S$
 690  PRINT
 700  FOR I = 1 TO N
 710  & AIO
 720  FOR I = 1 TO N
 730  GOSUB 1080
 740  PRINT I,( INT (IN / NN)) / 50
 750  GOSUB 1140
 760  PRINT  CHR$ (7)
 770  PRINT "Hit any key to continue"
 780  GET G$: IF G$ = "" THEN 780
 790 S(I) = ( INT (IN / NN)) / 50
 800 D(I) = S(I) - B(I)
 810  NEXT I
 820  FOR I = 1 TO 5: PRINT  CHR$ (7): NEXT I
 830  PRINT "SIGNAL MINUS BACKGROUND"
 840  FOR I = 1 TO N
 850  GOSUB 1190
 860  PRINT I,D(I)
 870  NEXT I
 880  PR# 3: HOME : PRINT "Data printout"
```

```
 890  PR# 1: PRINT  CHR$ (27);"!" CHR$ (5): FOR J = 1 TO 2
 900  PRINT F$;"     Date ";C$;"     Analyte ppm ";M$
 910  PRINT "Argon nebulizer flow  ";R$: PRINT "Auxiliary ga
s  ";X$;"     Auxiliary gas flow  ";H$
 920  PRINT "Profile start at ";E$;"     Increment size  ";I
$
 930  PRINT F$;"   Integration time ";NN;" sec";"   Delay ti
me ";WT;" sec"
 940  PRINT K$: PRINT
 950  PRINT  TAB( 15);"SIGNAL","BACKGROUND","S-B"
 960  FOR I = 1 TO N: PRINT I,S(I),B(I),D(I): NEXT I
 970  PRINT : PRINT : NEXT J: PRINT  CHR$ (12); CHR$ (27);"@
": PR# 0
 980  PRINT "DATA STORAGE ROUTINE "
 990  PRINT "Saving ";F$
 1000 CD$ =  CHR$ (4)
 1010  CALL 1002: PRINT  CHR$ (13) CHR$ (4)"OPEN "F$",D2":
PRINT  CHR$ (4)"WRITE"F$
 1020  FOR I = 0 TO N: PRINT D(I): NEXT I
 1030  PRINT CD$"LOCK "F$
 1040  PRINT CD$"CLOSE "F$
 1050  HOME : VTAB (6): HTAB (12): PRINT "Re-initializing pr
ogram"
 1060  CALL 1002: GOTO 380
 1070  END
 1080  REM   routine for integration of signal
 1090 IN = 0
 1100  FOR L = 1 TO (NN * 50)
 1110  & AI0:IN = IN + D%
 1120  NEXT L
 1130  RETURN
 1140  REM  WAIT
 1150 D% = WT * 10: &  TO 1
 1160  & TI1:T = D%
 1170  IF T <  > 0 THEN 1160
 1180  RETURN
 1190  REM  routine for rounding off values
 1200 LS = D(I) -  INT (D(I))
 1210 US =  INT (D(I)) + 1 - D(I)
 1220  IF LS >  = US THEN D(I) =  INT (D(I) + 1)
 1230  IF LS < US THEN D(I) =  INT (D(I))
 1240  RETURN

]
```

```
 100  CLEAR : HIMEM: 36095:D% = 0: DIM D%(300): PRINT  CHR$
(4)"BRUN QUICKI/O,D1"
 110  DIM D(50),B(50),S(50)
 120  REM    The data acquisition rate will depend partly on
 the size
 130  REM of the signal.  Larger signals will take longer to
 integrate
 140  REM than will smaller signals.  Actual data acquisitio
n rates vary
 150  REM in this program from about 20-50 points per second
.  The
 160  REM number of points taken per integration time will
be the same;
 170  REM the actual time this takes to do will vary somewha
t.
 180  REM
 190  REM      If you wish to take more than 50 points per pr
ofile,
 200  REM      change the values in lines 110 and 410 as need
ed.
 210  REM      This program was revised by Terry McCreary on
6/25/87
 220  REM
 230  PR# 0
 240  HOME : HTAB (12): FLASH : PRINT "RAW DATA2": NORMAL :
PRINT
 250  PRINT : PRINT "The program will only collect signal"
 260  PRINT "data for a profile of up to 50 points."
 270  PRINT "If you need to collect background"
 280  PRINT "corrected data, use DCP, ICP, or MIP."
 290  PRINT "Space will be provided for up to four"
 300  PRINT "lines (80 columns each) of comments."
 310  PRINT "Data is collected with a 'hit-any-key'"
 320  PRINT "prompt between points. If you do not"
 330  PRINT "wish this prompt, run RAW DATA."
 340  PRINT : PRINT "  Data will be saved on drive 2; be"
 350  PRINT "sure to place your data disk in"
 360  PRINT "that drive.": PRINT
 370  PRINT "  Two hard copies of the data will"
 380  PRINT "be printed for the lab notebook after"
 390  PRINT "the data is saved."
 400  PRINT : PRINT "One moment please..."
 410  FOR I = 0 TO 50:D(I) = 0:D%(I) = 0:B(I) = 0:S(I) = 0:
NEXT I:F$ = ""
 420  INPUT "File name for data";F$
 430  PRINT : INPUT "Date ";C$: INPUT "Analyte concentration
 ";M$
 440  INPUT "Argon nebulizer flow ";R$: INPUT "Auxiliary gas
 ";X$: INPUT "Auxiliary gas flow ";H$: PRINT
```

```
 450  PRINT : INPUT "Comments";K$: INPUT "More comments";W$:
 INPUT "More comments";U$: INPUT "More comments";V$
 460  PRINT : INPUT "Number of observations = ";N
 470  PRINT : INPUT "Length of integration in sec = ";NN
 480  PRINT : INPUT "Delay between observations in sec = ";W
T
 490 D(0) = N
 500  PRINT
 510  INPUT "HIT RETURN TO TAKE SIGNAL";S$
 520  PRINT
 530  & AIO
 540  FOR I = 1 TO N
 550  GOSUB 910
 560  PRINT I,( INT (IN / NN)) / 50
 570  PRINT  CHR$ (7)
 580  GOSUB 940
 590 S(I) = ( INT (IN / NN)) / 50
 600 D(I) = S(I)
 610  PRINT "Hit any key to continue"
 620  GET G$: IF G$ = "" THEN 620
 630  NEXT I
 640  FOR I = 1 TO 5: PRINT  CHR$ (7): NEXT I
 650  PRINT "POINT #/SIGNAL"
 660  FOR I = 1 TO N
 670  GOSUB 990
 680  PRINT I,D(I)
 690  NEXT I
 700  PRINT CD$"LOCK "F$
 710  PR# 3
 720  PRINT "Hit any key for hard copies of data"
 730  GET G$: IF G$ = "" THEN 730
 740  PR# 1: PRINT  CHR$ (27);"!" CHR$ (5): FOR J = 1 TO 2
 750  PRINT F$;"     Date ";C$;"   Analyte ppm ";M$
 760  PRINT "Argon nebulizer flow  ";R$: PRINT "Auxiliary ga
s  ";X$;"     Auxiliary gas flow  ";H$
 770  PRINT "Integration time ";NN;" sec";"  Delay time ";WT
;" sec"
 780  PRINT K$: PRINT W$: PRINT U$: PRINT V$: PRINT
 790  PRINT "POINT #","SIGNAL"
 800  FOR I = 1 TO N: PRINT I,S(I): NEXT I
 810  PRINT : PRINT : NEXT J: PRINT  CHR$ (12); CHR$ (27);"@
": PR# 0
 820  PRINT "DATA STORAGE ROUTINE"
 830  PRINT "Saving ";F$
 840 CD$ =  CHR$ (4)
 850  CALL 1002: PRINT  CHR$ (13) CHR$ (4)"OPEN"F$",D2": PRI
NT  CHR$ (4)"WRITE"F$
 860  FOR I = 0 TO N: PRINT D(I): NEXT I
 870  PRINT CD$"LOCK"F$: PRINT CD$"CLOSE"F$
 880  HOME : VTAB (6): HTAB (12): PRINT "Re-initializing pro
gram"
 890  CALL 1002: GOTO 400
```

```
 900  END
 910  REM   data collection and integration
 920 IN = 0: FOR L = 1 TO (NN * 50): & AIO:IN = IN + D%: NEX
T L
 930  RETURN
 940  REM   routine for wait between readings
 950 D% = WT * 10: &  TO 1
 960  & TI1:T = D%
 970  IF T <  > 0 THEN 960
 980  RETURN
 990  REM  routine for rounding off values
 1000 LS = D(I) -  INT (D(I))
 1010 US =  INT (D(I)) + 1 - D(I)
 1020  IF LS >  = US THEN D(I) =  INT (D(I) + 1)
 1030  IF LS < US THEN D(I) =  INT (D(I))
 1040  RETURN
```

```
 10  CLEAR : HIMEM: 36095:D% = 0: DIM D%(300): PRINT  CHR$
(4)"BRUN QUICKI/O,D1"
 20  DIM D(30),S(30): POKE 36259,1
 21  REM  The poke command in line 20 permits maximum data
acquisition rate
 22  REM  The number of data points collected will be 50X th
e time in
 23  REM  seconds
 30  PR# 0
 40  HOME : HTAB (12): INVERSE : PRINT "REAL WORK2": PRINT
: NORMAL
 50  PRINT "  This program will collect signal data"
 60  PRINT "only, at approximately 50 points per"
 70  PRINT "second, with a minimum delay"
 80  PRINT "between readings.  Data will not be"
 90  PRINT "saved to disk, but will be printed"
 100  PRINT "once on the printer, along with the"
 102  PRINT "average value and standard deviation.": PRINT
: PRINT
 110  FOR I = 0 TO 30:D(I) = 0:S(I) = 0: NEXT I:F$ = ""
 120  INPUT "Name for data set";F$
 130  PRINT : INPUT "Number of observations = ";N
 140  PRINT : INPUT "Length of integration in sec = ";NN
 150 WT = .1
 160 D(0) = N
 170  PRINT
 180  INPUT "HIT RETURN TO TAKE SIGNAL";S$
 190  PRINT
 200  & AIO
 210  FOR I = 1 TO N
 220  GOSUB 470
 230  PRINT I,( INT (IN / NN)) / 50
 240  PRINT  CHR$(7)
 250  GOSUB 540
 260 S(I) = ( INT (IN / NN)) / 50
 270 D(I) = S(I)
 280  NEXT I
 290  FOR I = 1 TO 5: PRINT  CHR$ (7): NEXT I
 300  PRINT "POINT #/SIGNAL"
 310  FOR I = 1 TO N
 320  GOSUB 590
 330  PRINT I,D(I)
 340  NEXT I
 350  PR# 1
 360  PRINT F$
 370  PRINT "Integration time ";NN;" sec";"  Delay time ";WT
;" sec"
 380  PRINT
 390  PRINT "POINT #","SIGNAL"
```

```
 400  FOR I = 1 TO N: PRINT I,S(I): NEXT I
 410 SUM = 0: FOR I = 1 TO N:SUM = SUM + S(I): NEXT I:VE =
SUM / N:AV =  INT (VE * 10) / 10
 415  GOSUB 1000
 420  PRINT "     Average signal = ";AV;"     Std. dev = ";S
DV: PRINT : PRINT
 430  PR# 0
 440  HOME : CALL 1002: GOTO 110
 450  CALL 1002: GOTO 110
 460  END
 470  REM  INTEGRATION
 480 IN = 0
 490  FOR L = 1 TO (NN * 50)
 500  & AIO:IN = IN + D%
 510 IN = IN + DTA
 520  NEXT L
 530  RETURN
 540  REM  WAIT
 550 D% = WT * 10: &  TO 1
 560  & TI1:T = D%
 570  IF T <  > 0 THEN 560
 580  RETURN
 590  REM  routine for rounding off values to whole numbers
 595 LS = D(I) -  INT (D(I))
 600 US =  INT (D(I)) + 1 - D(I)
 610  IF LS >  = US THEN D(I) =  INT (D(I) + 1)
 620  IF LS < US THEN D(I) =  INT (D(I))
 630  RETURN
 1000  REM  routine for calculating standard deviation
 1005 TT = 0: FOR I = 1 TO N
 1010 TT = TT + ((S(I) - VE) ^ 2): NEXT I
 1020 SDV =  SQR (TT / (N - 1))
 1030 SDV = ( INT (SDV * 1000)) / 1000: REM  this rounds off
 std dev to 3 decimal places
 1040  RETURN

]
```

```
 100  REM  LINEAR REGRESSION GLL 9/21/82 UF
 110  REM  modified by T. McCreary on 8/5/87
 120  PR# 0: HOME : PRINT "Linear Regression": PRINT
 130  PRINT : PRINT "This program will perform a linear"
 140  PRINT "regression analysis on up to 50"
 150  PRINT "pairs of data points."
 160  DIM X(50),Y(50),XX(50),XY(50),YY(50)
 170  PRINT : INPUT "TITLE OF DATA ";T$
 180  PRINT : INPUT "NUMBER OF DATA POINTS ";N
 190  PRINT : PRINT "ENTER DATA AS X,Y PAIRS"
 200  PRINT : FOR I = 1 TO N: PRINT "DATA PAIR "I: INPUT X(I
),Y(I): NEXT I
 210  PRINT : INPUT "CHECK THE DATA (Y/N) ";A$: IF A$ = "N"
OR A$ = "n" THEN 310
 220  PRINT : PRINT : PRINT "I                X
  Y"
 230  PRINT "-----------------------------------"
 240  FOR I = 1 TO N: PRINT I,X(I),Y(I): NEXT I
 250  PRINT : INPUT "CORRECT ANY DATA PAIRS (Y/N) ";C$: IF
C$ = "N" THEN 310
 260  PRINT : INPUT "BAD DATA PAIR NUMBER";BD
 270 I = BD
 280  PRINT : PRINT "DATA PAIR "I"  "X(I)","Y(I)
 290  PRINT : INPUT "CORRECT DATA X,Y ";X(I),Y(I)
 300  GOTO 210
 310  REM  SUM OF VARIABLES
 320 X = 0:Y = 0:XX = 0:XY = 0:YY = 0
 330  FOR I = 1 TO N
 340 X = X + X(I)
 350 Y = Y + Y(I)
 360 XX = XX + (X(I) * X(I))
 370 XY = XY + (X(I) * Y(I))
 380 YY = YY + (Y(I) * Y(I))
 390  NEXT I
 400  REM  CALCULATION OF SLOPE
 410 M = (((N * XY) - (X * Y)) / ((N * XX) - (X * X)))
 420  REM  CALCULATION OF INTERCEPT
 430 B = (Y / N) - (M * (X / N))
 440 XO =  - 1 * (B / M)
 450  REM  CALC. OF SUM SQUARE OF ERRORS
 460 SX = XX - ((X * X) / N)
 470 SY = YY - ((Y * Y) / N)
 480 SZ = XY - ((X * Y) / N)
 490 ER = SY - (M * SZ)
 500  REM  CALC OF ERROR
 510 S =  SQR ((SY - (M * SZ)) / (N - 2))
 520  REM  CALC OF SLOPE ERROR
 530 SM = S / ( SQR (SX))
 540  REM  CALC OF INTCPT ERROR
```

```
 550 SB = (S * ( SQR (XX)) / ( SQR (N * SX)))
 560  REM  CALCULATION OF COEF. OF CORR.
 570 R = SZ / ( SQR (SX * SY))
 580  REM  DATA OUTPUT
 590  PR# 1
 600  PRINT "====================================": PRINT
T$
 610  PRINT : PRINT "I                  X                  Y"
 620  PRINT "------------------------------------"
 630  FOR I = 1 TO N: PRINT I,X(I),Y(I): NEXT I
 640  PRINT "------------------------------------"
 650  PRINT : PRINT "Slope = ";M: PRINT "Y-intercept = ";B
 660  PRINT "X-intercept = ";XO
 670  PRINT "Coeff. of correlation = ";R
 680  PRINT : PRINT "Std dev of slope = ";SM
 690  PRINT "Std dev of intercept = ";SB
 700  PRINT : PRINT "SSE = ";ER
 710  PRINT : PRINT "SXX = "SX
 720  PRINT "SXY = "SZ
 730  PRINT "SYY = "SY
 740  PRINT "S   = "S
 750  PRINT "===================================="
 760  PR# 0
 770  HOME
 780  PRINT : INPUT "CALCULATE NEW X OR Y (X/Y/N) ";C$
 790  IF C$ = "N" THEN 1240
 800  REM  STD DEV ROUTINE
 810  HOME : PRINT : INPUT "TITLE ";X$
 820  PRINT : INPUT "NUMBER OF OBSERVATIONS ";NO
 830  PRINT
 840  FOR I = 1 TO NO
 850  PRINT "ENTER DATA POINT ("I")": INPUT NP(I)
 860  PRINT : NEXT I
 870  PRINT : INPUT "CHECK THE DATA (Y/N) ";CD$
 880  IF CD$ = "N" THEN 930
 890  HOME : PRINT : PRINT X$: PRINT : PRINT "#         DATA"

 900  PRINT "--------------------------------"
 910  FOR I = 1 TO NO: PRINT I"          "NP(I)
 920  NEXT I
 930  REM  CALCULATION
 940 P = 0:PP = 0
 950  FOR I = 0 TO NO
 960 P = P + NP(I)
 970 PP = PP + (NP(I)) ^ 2
 980  NEXT I
 990  IF NO = 1 THEN  PRINT "NOTE:  STANDARD DEVIATION CANNO
T BE"
1000  PRINT "PERFORMED ON ONE POINT..."
1010  IF NO = 1 THEN 1030
1020 SD =  SQR ((PP - ((P ^ 2) / NO)) / (NO - 1))
1030 MP = P / NO
```

```
 1040  IF C$ = "Y" THEN 1150
 1050  REM  NEW X
 1060 XN = (MP - B) / M
 1070 SXN = SD / M
 1080  PR# 1
 1090  PRINT : PRINT "++++++++++++++++++++"
 1100  PRINT : PRINT X$: PRINT "IF YN = "MP
 1110  PRINT "XN = "XN
 1120  PRINT "SXN = "SXN: PRINT : PRINT "++++++++++++++++++++
+"
 1130  PR# 0
 1140  IF C$ = "X" THEN 1220
 1150  REM  NEW YN
 1160 YN = (M * MP) + B
 1170 SYN = SD / M
 1180  PR# 1
 1190  PRINT : PRINT "####################": PRINT : PRINT
X$: PRINT "IF XN = ";MP
 1200  PRINT "YN = ";YN: PRINT "SYN = ";SYN: PRINT : PRINT
"####################"
 1210  PR# 0
 1220  PRINT : INPUT "ANOTHER POINT (Y/N)";AP$
 1230  IF AP$ = "Y" THEN 770
 1240  HOME : VTAB (12): HTAB (15): PRINT "Goodbye !": VTAB
(22): END

]
```

APPENDIX B

FUTURE WORK

Future investigations in the area of rapid coal analysis by DCP-OES could be approached in several directions. First, a different agent to be used for increasing the viscosity should be investigated. Poly(ethylene oxide) was found to be unstable in the acid solutions that are required to minimize hydrolysis of metal ions in atomic spectrometric standards, so that frequent preparation of fresh poly(ethylene oxide) stock solution is required. The preparation of this solution is not trivial, as was related in Chapter 2. Also, poly(ethylene oxide) causes a significant decrease in surface tension at all concentrations, so that the viscosity must be increased by some greater amount than would be otherwise required, to effect the increase in droplet size.

The ideal thickening agent would increase the viscosity significantly with very little change in surface tension, and with very little agent required for this purpose. One thickening agent which has been shown to be useful for graphite furnace atomic spectrometric work is Viscalex. Stephen, Littlejohn, and Ottaway have shown that this agent, added to aqueous slurries in low concentrations, is useful for keeping slurry particles suspended in graphite furnace AAS. However, Viscalex may not be entirely satisfactory, since it apparently requires

a neutral or slightly basic pH for its thickening effect to occur.

Second, an extensive comparison should be done to determine whether the fraction of particles in coal-water slurries that are greater than 33 um in diameter has a significantly different composition than that fraction which is smaller than 33 um. The only particles that are actually introduced into the plasma are those which are less than 33 um in diameter, and in fact the very smallest of these particles may provide the majority of signal. This means that the analysis is being performed on a small fraction of the sample which has very small particle sizes. Ebdon has shown that such segregation of particles does not affect the analytical results for determination of manganese in coal.

Finally, the detection electronics of the Spectraspan III DCP should be "overhauled". For online analysis, a chronologically stable signal is required, and the signal from the Spectraspan III is subject to considerable drift with time. A desirable alternative system would bypass the amplification/readout electronics of the DCP entirely, directing the twenty photomultiplier tube outputs to separate current-to-voltage converters, which could then be directed toward a twenty-channel multiplexer. Such a system would allow for individual gain adjustment for the current-to-voltage converters, which would permit "tailoring" of each channel to its particular element.

The vita has been removed from the scanned document